Dynamics in endovascular surgery

Vos, A.W.F.

2005

document version
Publisher's PDF, also known as Version of record

Dynamics in Endovascular Surgery

"Eppur si Muove"

Galileo Galilei (1564 -1642)

Galileo Galilei ontdekte dat de aarde om de zon draait. Hij schreef hierover een boek, getiteld: "De Motu", "over de beweging". Doordat dit tegen de uitgedragen opvatting van de katholieke kerk inging werd hij gevangen gezet. Uiteindelijk werd hij, hij was toen al oud en bijna blind, gedwongen in het openbaar te bekennen dat hij het fout had en dat de aarde niet bewoog. Men zegt dat iemand hem bij het verlaten van de rechtszaal hoorde mompelen: "Eppur si Muove", "en toch beweegt ze". Pas in 1992 sprak paus Johannes Paulus II een excuus uit, waarmee Galilei's naam eindelijk werd gezuiverd.

VRIJE UNIVERSITEIT

Dynamics in Endovascular Surgery

ACADEMISCH PROEFSCHRIFT

ter verkrijging van de graad Doctor aan
de Vrije Universiteit Amsterdam,
op gezag van de rector magnificus
prof.dr. T. Sminia,
in het openbaar te verdedigen
ten overstaan van de promotiecommissie
van de faculteit der Geneeskunde
op woensdag 7 september 2005 om 13.45 uur
in de aula van de universiteit,
De Boelelaan 1105

door

Adriaan Willem Floris Vos

geboren te Boston,
Massachusetts, Verenigde Staten

promotoren:	prof.dr. J.A. Rauwerda
	prof.dr. W. Wisselink
copromotor:	dr. J.T. Marcus

Voor de toekomst

CONTENTS

INTRODUCTION

Dilating and obliterative disease of the aorta and its branches accounts for a major part of the interventions in the vascular surgical field. Endovascular surgery is increasingly applied in both disease entities and consists of a minimally invasive procedure using an intraluminal approach from a remote artery access site to treat the diseased vessel with either a constraining stent-graft in case of dilation or a dilating stent in case of obliteration. In current vascular surgery practice, the opinion whether to perform an open conventional, often time proven, operation or an endovascular intervention is subject to continuous change. In short, an overview is provided describing the current treatment modalities. Subsequently this thesis focuses on the question whether and if so, which dynamic consequences are associated with endovascular treatment of abdominal aortic aneurysm as well as carotid artery stenosis.

TREATMENT MODALITIES

a. Open repair for abdominal aortic aneurysm

Open treatment of an abdominal aortic aneurysm requires direct surgical exposure of the aorta through a transperitoneal or left retroperitoneal approach. The aorta is cross clamped, the aneurysm opened and replaced by a tubular or bifurcated graft. Introduced in 1951 by Dubost, the open technique has evolved and nowadays is a time proven operation.[1] Overall, in elective open infrarenal AAA repair, early complication and mortality rates average 15% and 5% respectively.[2-4] Late graft related complications are uncommon with an overall incidence of 0-3% after more than 10 year follow-up.[4] Long term aneurysm-associated mortality is also rare (0-0.34% per year).[4] Overall, once the aneurysm is repaired with an open procedure, it is distinctly unusual for a patient to develop a subsequent problem related with the reconstruction, even at very long follow-up intervals. A history of congestive heart failure, chronic pulmonary disease, renal insufficiency, and age over 75 years are accountable for the major part of postoperative complications and long-term mortality.[5] This makes the procedure especially suitable for relatively healthy individuals with an otherwise normal life expectancy.

b. Endovascular Abdominal Aortic Aneurysm Repair (EVAR)

EVAR was first introduced, in 1991, by Parodi.[6] He inserted a tubular graft with a balloon expandable stent in the abdominal aorta via the femoral artery. The graft excluded the aneurysm from the circulation and allowed normal flow through the graft lumen. By doing this, the need for aortic exposure and cross clamping was avoided. Short term results were encouraging. However, the device and methodology needed further refinement and since this first report many lessons have been learned. The main worrying complications are stent-graft migration and material disintegration both inducing endoleak: e.g. persistent blood flow outside the lumen of the stent-graft within the aneurysmal sac. All are signs of a weakening construction causing possible aneurysmal sac enlargement, leading to reintervention or even aneurysm rupture. Factors associated with migration and material disintegration are: aortic neck dilatation due to progressive aneurysmatic disease, persisting repetitive displacement forces caused by the pulsatile blood flow, lack of support caused by inadequate biological incorporation of the stent-graft and in certain cases unfavorable aneurysm anatomy. In an effort to overcome these problems various fixation techniques were introduced. Stents with hooks, suprarenal bare stent fixation and stent-grafts with column strength, e.g. armored grafts with stents or longitudinal bars became available. After various revisions, this resulted in the commercial production of several endovascular grafts.[6-12] With these grafts, excellent short-term clinical successes were obtained: decreased blood loss, a reduced ICU period, shortened hospital stay and a 30-day mortality of 1-2%.[2,3,13] However, mid-term follow-up results showed stent- migration rates up to 13% with increasing incidence of migration along with length of follow-up.[8,9,11,14] Stent fractures or fabric disruption after the latest design modifications are rare although the limited follow-up period might be partially responsible for this. Endoleak is still present with average rates of 10-20% at one year follow-up.[7-9,11] This implicates the need for vigorous follow-up with annual reintervention rates up to 7% and annual conversion up to 2%.[7-9,12] The latest reports show a declining aneurysm related late mortality of less than 1% per year but still patients die of aneurysm rupture after EVAR. Although results improve, EVAR is still most appropriate only for high risk patients because of the uncertain long term durability as well as the burden of the surveillance as such.[4,15]

c. Open treatment for carotid artery stenosis, Carotid Endarterectomy (CEA)

There is unequivocal evidence that patients with symptomatic 70-99% stenosis benefit from CEA in terms of risk reduction of ipsilateral stroke.[4,15-17] CEA requires direct surgical exposure of the carotid bifurcation with access to the distal healthy part of the internal carotid artery at the level of the digastric muscle and hypoglossal nerve. The carotid artery is opened by a longitudinal arteriotomy and endarterectomy is performed. Subsequently the artery is closed primarily or with a patch. The operative risk of stroke and death defined as any stroke or death that occurred within 30 days is 5-7%.[18] In CEA with patch closure, recurrent stenosis (>50%) is below 10% after 1 year and gradually diminishes further until 1% per year in the long run.[19] Recurrent stenosis after CEA seems to follow a benign course, since there is no association between late stroke and recurrent stenosis.[20]

d. Endovascular treatment for carotid artery stenosis, Carotid Angioplasty and Stenting (CAS)

CAS has emerged as an alternative, less invasive treatment obviating the need of a direct surgical approach of the neck.[21,22] Through a remote, often femoral, approach a guidewire and catheter is manoeuvred in the aorta and subsequently into the common carotid artery. The stenosis is crossed by a guidewire and angioplasty and stenting is performed similarly to peripheral arterial stenting. Hereby the risk related to the incision in the neck is avoided. The main complication in CAS is the risk of stroke. During this procedure dislodgement of atherosclerotic debris by manipulation of catheters, guidewires or stents is a concern. To prevent these adverse effects there have been substantial technical innovations such as refinements in wires, catheters, balloons, stents and the development of cerebral protection devices. Results improved with those innovations and enhanced skills in endovascular navigation. In centers with large experience, rates of major adverse outcome (disabling stroke or death) within 30 days do not differ significantly between CAS and CEA.[23] Recurrent stenosis (>50%) averages 6% (1% - 21%).[24] Similar to CEA, the risk of recurrent stenosis seems to be greatest in the first year after the procedure and then decreases over time. However, currently available results are limited to an utmost 3 year follow-up.[24] Long-term durability of CAS in preventing stroke and maintaining patency is therefore unknown but will most likely depend on the stent and its interaction with the vessel wall.[25]

CONVENTIONAL (OPEN) VERSUS ENDOVASCULAR TREATMENT

Both conventional and endovascular treatment modalities currently compete for their position in the patient cohorts as convincing evidence is still lacking concerning the overall benefits of one above another. However, endovascular methods are increasingly used partly due to their elegant and innovative technique, but also unequivocally by manufacturer driven promotion. Along with this dynamic endovascular evolution in the last ten years, the urge of exploring a new field in the clinical setting prompted important computational, in vitro and in vivo (animal) experiments. The drive to minimize operative trauma to the patient, broaden indications and increase the volume of procedures is immense. Nowadays, migration and endoleak in EVAR and restenosis in CAS have become apparent and potentially threaten long term outcome. The interaction between vessel wall and stent, its combined geometry and the impact of the pulsatile blood flow is believed to be responsible for those weaknesses. Therefore, due to the various complex forces and interactions present, the importance of insight into the dynamics in endovascular therapies becomes increasingly apparent.

DYNAMICS IN ENDOVASCULAR THERAPY

a. Dynamics in EVAR

Several studies have focused on aneurysm and stent-graft motions. For one of the first reports focusing on diameter changes during the cardiac cycle e.g. Pulsatile Wall Motion (PWM) of the aneurysm before and after EVAR a uni-dimensional ultrasound based technique was used.[26] Reduced PWM after EVAR implies a lowered intra aneurysm pressure and subsequent successful aneurysm exclusion. Persistent aneurysm pulsatility after EVAR is related with the presence of endoleak.[26,27] Nevertheless PWM after EVAR did not show to be of substantial clinical value due to the overlap of data between groups.[28] Similar correlations between diameter change and aneurysm exclusion were observed using Cine Magnetic Resonance Imaging (Cine MRI).[29] Cine MRI consists of rapid ECG gated images that can be built up over a cardiac cycle and be replayed as a continuous movie loop. In case of quantifying uni-dimensional aneurysm pulsatility its clinical significance is to be awaited. With the use of computational techniques a downward pulling force on the

stent-graft related with diameter and tapering of the graft is described.[30] Recently a computational simulation was performed using fluid-structure interaction dynamics calculating the pulsatile 3 D hemodynamics combining blood flow, stent-graft and aneurysm wall characteristics.[31] The presence of stent-graft movements was confirmed with a low but still present transmission of pressure via the aneurysm thrombus to the aneurysm wall. Stress distribution showed a maximum of wall stress at the bifurcation of the stent-graft creating a longitudinal repetitive drag force of almost 2 Newton. In vivo, complex aneurysm neck motions were observed in patients during open surgery using close-range photogrammetry.[32] Besides radial and rotational motions, a 0.6-1mm longitudinal displacement was present. Pulsatile blood flow and motions of the aorta lead to micromovements of the stent-graft. Due to chronic wear of the woven stent-graft material against metallic stents or calcified aortic plaque, fabric abrasions and holes become apparent.[33,34] With increasing insights in these dynamic mechanisms, stent-graft manufacturers can improve the next generation of endoluminal grafts. Ultimately, analysis of the adjusted stent-grafts ought to be performed before they become available for clinical use.

b. Dynamics in CAS

Studies concerning carotid artery mobility after CAS are limited. However, movements of the carotid artery tree have been studied widely. Transitory neurologic deficits are described due to a reduction in hemispheric perfusion pressure while the patient attained a certain head position.[35,36] In other mobile arteries like the femoropopliteal segment, stents revealed to be exposed to extreme repetitive mechanical stress.[37] During knee flexion, extensive kinking and functional stenosis may occur. Increasingly, strut fractures and eventually stent destruction in this region have been observed. Unfortunately, however, all experience with popliteal artery stenting has been collected from 'do and see´ procedures.[37] Although stent fractures have not been described in CAS yet, the carotid artery is believed to be highly sensitive to the mechanical aspects of stenting. Regardless the morphological changes during head movements, a fluid dynamics study of the carotid artery after stent placement confirmed the essence of careful anatomical stent positioning. Disproportion of stent and vessel geometry induces flow disturbances which can promote intimal hyperplasia.[38] With this in mind, the stent might need flexible capacities to attain the ideal anatomical position during movements of the head. Several studies have assessed the mechanical properties of bare expanded stents.[39-41] However, their mechanical properties were not evaluated after insertion

in an artery. Whether flexibility is to be preferred, is controversial, as earlier reports conflict on this matter. The pulsatile nature of a flexible stent may induce platelet sloughing, embolization, and reaccumulation, thus leading to an irregularly thick subsequent platelet substrate and eventually a thick neointima.[42] Another study showed the contrary by comparing the same stent design with differing longitudinal flexibility in swine iliac arteries demonstrating less neointimal buildup in the flexible stent after 5 weeks.[43] In a recent study in swine carotid arteries, however, a stent with flexible extensions that accommodated the arterial wall at the transition zone showed coverage of the stent struts by an endothelium monolayer without upstream intimal thickening.[44] Hemodynamic disturbances due to compliance mismatch at the stent-vessel junction might invoke restenosis. The ability of an expanded stent to bend along with the vessel contour avoiding distortion at the stent-vessel junction is therefore to be preferred. Palmaz advocates the development of flexible endovascular devices to counteract the mechanical stress that causes intimal thickening and even fractures. He envisages stents with a surface promoting rapid stent endotheliasation to counter the biological effects of motion and microtrauma.[45]

The main purpose of this thesis is to evaluate the dynamic aspects of EVAR and CAS in a perspective aimed at the future. As forces and motions are inevitably responsible for long term performance, we focused on the dynamic properties of both treatments. Insights in stent and vessel wall behavior may aid in adjustment and modification of devices and techniques with, as ultimate goal, an improved long term outcome.

In the first part of this thesis clinical imaging studies of motion of aneurysm and stent-graft are described.
In **chapter 1**, Cine MRI is introduced as a standardized, less operator dependent, tool to quantify two-dimensional aneurysm pulsatile wall motion (2D-PWM). This MR technique provides 2-dimensional dynamic imaging of the aneurysm and its motions within the cardiac cycle. 2D-PWM was defined as the difference between the smallest (end-diastolic) and largest (peak-systolic) cross-sectional area of transverse sections of the aneurysm. As durability of EVAR is increasingly called into question, a means of predicting and identifying late endoleak is required. Increased aneurysm sac pressure is believed to be related with endoleak, aneurysm sac enlargement and might lead to eventual rupture. However direct pressure measurements are limited by their invasive nature. PWM has been proposed as an alternative.

In **chapter 2** we investigated aneurysm and stent-graft motions in transverse, sagittal and coronal planes with cine MRI. Translations in cranial-caudal, left-right and anteroposterior directions were measured by comparing the maximal displacement of the contours throughout the cardiac cycle. Angulations of the stent-grafts were measured in the sagittal and coronal planes in order to examine a possible relationship between the observed motions and the changing direction of the blood flow. 2D-PWM was calculated of the aneurysm before and after EVAR and of the stent-graft itself. Visualization of these motions can be of immense value to our understanding of the repetitive forces acting within the aorta and upon the stent-graft. Improved device design in terms of fixation and fabric strength is the key to successful long-term aneurysm repair.

In the second part of this thesis the influence of head movements with regard to CAS was studied.

In **chapter 3** we evaluated the morphology of the carotid artery after stent placement in five different head positions. The mobility of the carotid artery in CAS is a relatively unexplored subject despite the existence of long-term studies showing stent failure in other flexible arteries like the external iliac and popliteal arteries.[46-48] We performed 3D MR angiography, visualizing both carotid arteries in five different head positions (neutral, turned left and right and bent forward and backward). Maximum intensity projection reconstructions were obtained to measure angulation at the proximal and distal stent junction. Configuration changes of the stented section of the carotid artery and the unstented contralateral artery were judged. Secondly, transverse sections at the level of the carotid bifurcation and at the skull base were used to calculate torsion shear in the common and internal carotid arteries during turned left and right head position. Understanding these geometrical changes may lead to improved device design, which in turn can improve the long-term outcome of CAS.

Due to the results of this morphology study, in **chapter 4**, we expanded our MR study, using MR phase-contrast flow quantification to measure the Volumetric Flow Rate (VFR) in CAS and CEA. We investigated whether different head positions affect ICA geometry in patients following CAS and CEA. Subsequently we assessed correlation between its geometry and the VFR.

In **chapter 5** we performed an experimental in vitro study using commonly deployed carotid artery stents in the expanded bare state and after insertion in a porcine common carotid artery. We hypothesized that a stent design with high flexibility

and low torsion potential, implying that limited force is needed to rotate the stent along its axis, might be favorable to avoid stress passed on to the stented and remaining unstented segments of the CCA and the ICA. We evaluated flexibility and torsion of the stent designs within the range of motion of common head movements.

In the third part of this thesis in vitro as well as in vivo animal experiments are described of a stent-graft system with side branches for treatment of complex aneurysms. In infrarenal aneurysm repair the competition with the results of an OPEN repair is a challenge for EVAR. In contrast, aneurysms that involve segments of the aorta that contain essential branch arteries, such as suprarenal, thoraco-abdominal and aortic arch aneurysms, morbidity and mortality with OPEN is considerable and poses a formidable challenge to both surgeon and patient. Complications are related to the invasive nature of the procedure, often requiring thoracotomy, laparotomy and phrenicotomy, and to temporary or permanent organ ischemia due to aortic cross-clamping. Thus, with these extended aneurysms in particular a tremendous potential for improvement arises if repair could be accomplished via a minimally invasive, endoluminal method.
In **chapter 6** the results of our study in an animal experimental model are described in which complex aneurysms are treated with a side branched stent-graft. In this chapter the dynamic viewpoint expressed in this thesis can be interpreted as an effort to expand the current boundaries of endovascular intervention. In a porcine model supra- and juxtarenal aortic aneurysms were created by suturing a saccular dacron patch into an anterior aortotomy. Accordingly, a main graft with separate side branch grafts was subsequently placed in the renal arteries and the complex aneurysm was excluded from the circulation. Outcome was evaluated by postoperative angiography and autopsy results and by measuring operating time, blood loss and use of contrast agent.
In **chapter 7** we assessed the problem of proximal stent-graft migration. Fixation of stent-grafts at the level of or even above the renal arteries might improve fixation. We performed a traction study using an in vitro bench pull model comparing proximal fixation of stent-grafts with three different fixation configurations; an uncovered suprarenal part; a covered suprarenal part with renal artery orifice fenestrations; and a covered suprarenal part with renal artery side branches.

REFERENCES

1. Dubost C, Allary M, Oeconomos N. Resection of an aneurysm of the abdominal aorta: reestablishment of the continuity by a preserved human arterial graft with result after five months. *Ama Arch Surg*. 1952;64:405-408.

2. Greenhalgh RM, Brown LC, Kwong GPS, Powell JT, et al. Comparison of endovascular aneurysm repair with open repair in patients with abdominal aortic aneurysm (EVAR trial 1), 30-day operative mortality results: randomised controlled trial. *Lancet.* 2004;364:843-848.

3. Prinssen M, Verhoeven ELG, Buth J, Cuypers PWM, et al. A randomized trial comparing conventional and endovascular repair of abdominal aortic aneurysms. *N Eng J Med.* 2004;351:1607-1618.

4. Rutherford RB, Krupski WC. Current status of open versus endovascular stent-graft repair of abdominal aortic aneurysm. *J Vasc Surg*. 2004;39:1129-1139.

5. Hertzer NR, Mascha EJ, Karafa MT, O'Hara PJ, et al. Open infrarenal abdominal aortic aneurysm repair: The Cleveland Clinic experience from 1989 to 1998. *J Vasc Surg.* 2002;35:1145-1154.

6. Parodi JC, Palmaz JC, Barone HD. Transfemoral intraluminal graft implantation for abdominal aortic aneurysms. *Ann Vasc Surg.* 1991;5:491-499.

7. Criado FJ, Fairman RM, Becker GJ. Talent LPS AAA stent graft: Results of a pivotal clinical trial. *J Vasc Surg.* 2003;37:709-715.

8. Greenberg RK, Chuter TAM, Sternbergh WC, Fearnot NE. Zenith AAA endovascular graft: Intermediate-term results of the US multicenter trial. *J Vasc Surg.* 2004;39:1209-1218.

9. Matsumura JS, Brewster DC, Makaroun MS, Naftel DC. A multicenter controlled clinical trial of open versus endovascular treatment of abdominal aortic aneurysm. *J Vasc Surg.* 2003;37:262-271.

10. Moore WS, Matsumura JS, Makaroun MS, Katzen BT, et al. Five-year interim comparison of the Guidant bifurcated endograft with open repair of abdominal aortic aneurysm. *J Vasc Surg.* 2003;38:46-55.

11. Schmittling ZC, McLafferty RB, Danetz JS, Ramsey DE, et al. The AneuRx modular endograft device for the treatment of abdominal aortic aneurysms. Overview of 7 years of clinical use. *J Cardiovasc Surg*. 2004;45:301-306.

12. Zarins CK, Bloch DA, Crabtree T, Matsumoto AH, et al. Aneurysm enlargement following endovascular aneurysm repair: AneuRx clinical trial. *J Vasc Surg*. 2004; 39:109-117.

13. Buth J, Laheij RJ. Early complications and endoleaks after endovascular abdominal aortic aneurysm repair: report of a multicenter study. *J Vasc Surg*. 2000;31:134-146.

14. Fairman RM, Velazquez OC, Carpenter JP, Woo E, et al. Midterm pivotal trial results of the Talent Low Profile System for repair of abdominal aortic aneurysm: Analysis of complicated versus uncomplicated aortic necks. *J Vasc Surg*. 2004;40:1074-1082.

15. Brewster DC, Cronenwett JL, Hallett JW, Johnston KW, et al. Guidelines for the treatment of abdominal aortic aneurysms. Report of a subcommittee of the Joint Council of the American Association for Vascular Surgery and Society for Vascular Surgery. *J Vasc Surg*. 2003;37:1106-1117.

16. European Carotid Surgery Trialists'Collaborative Group. Randomised trial of endarterectomy for recently symptomatic carotid stenosis: final results of the MRC European Carotid Surgery Trial (ECST). *Lancet*.1998;351:1379-1387.

17. North American Symptomatic Carotid Endarterectomy Trial Collaborators. Beneficial effect of carotid endarterectomy in symptomatic patients with high-grade carotid stenosis. *N Engl J Med*. 1991;325:445-453.

18. Rothwell PM, Eliasziw M, Gutnikov SA, Fox AJ, et al. Analysis of pooled data from the randomised controlled trials of endarterectomy for symptomatic carotid stenosis. *Lancet.* 2003;361:107-116.

19. Frericks H, Kievit J, van Baalen JM, van Bockel JH. Carotid recurrent stenosis and risk of ipsilateral stroke. A systematic review of the literature. *Stroke*. 1998;29:244-250.

20. Moore WS, Kempczinski RF, Nelson JJ, Toole JF. Recurrent carotid stenosis: Results of the ACAS trial. *Stroke.* 1998;29:2018-25.

21. Diethrich EB. Carotid angioplasty and stenting. Will they match the gold standard? *Tex Heart Inst J*. 1998;25:1-9.

22. Roubin GS, New G, Iyer SS, Vitek JJ, et al. Immediate and late clinical outcomes of carotid artery stenting in patients with symptomatic and asymptomatic carotid artery stenosis. A 5-year prospective analysis. *Circulation.* 2001;103:532-537.

23. Brown MM, Rogers J, Bland JM, CAVATAS investigators. Endovascular versus surgical treatment in patients with carotid stenosis in the Carotid and Vertebral Artery Transluminal Angioplasty study (CAVATAS): a randomised trial. *Lancet.* 2001;357:1729-1737.

24. Groschel K, Riecker A, Schulz JB, Ernemann U, et al. Systematic review of early recurrent stenosis after carotid angioplasty and stenting. *Stroke*. 2005;36:367-373.

25. Criado FJ, Lingelbach JM, Ledesma DF, Lucas PR. Carotid artery stenting in a vascular surgery practice. *J Vasc Surg*. 2002;35:430-434.

26. Malina M, Lanne T, Ivancev K, Lindblad B, et al. Reduced pulsatile wall motion of abdominal aortic aneurysms after endovascular repair. *J Vasc Surg.* 1998;27:624-631.

27. Schurink GW, Aarts NJ, Malina M, van Bockel JH. Pulsatile wall motion and blood pressure in aneurysms with open and thrombosed endoleaks-comparison of a wall track system and M-mode ultrasound scanning: An in vitro and animal study. *J Vasc Surg*. 2000;32:795-803.

28. Lindblad B, Dias N, Malina M, Ivancev K, et al. Pulsatile wall motion (PWM) measurements after endovascular abdominal aortic aneurysm exclusion are not useful in the classification of endoleak. *Eur J Vasc Endovasc Surg*. 2004;28:623-628.

29. Faries PL, Agarwal G, Lookstein R, Bernheim JW, et al. Use of cine magnetic resonance angiography in quantifying aneurysm pulsatility associated with endoleak. *J Vasc Surg* 2003;38:652-656.

30. Liffman K, Lawrence-Brown MM, Semmens JB, Bui A, et al. Analytical modeling and numerical simulation of forces in an endoluminal graft. *J Endovasc Ther.* 2001;8:358-371.

31. Li Z, Kleinstreuer C. Blood flow and structure interactions in a stented abdominal aortic aneurysm model. *Med Eng Phys.* 2005;27:369-382.

32. Flora HS, Woodhouse N, Robson S, Adiseshiah M. Micromovements at the aortic aneurysm neck measured during open surgery with close-range photogrammetry: implications for aortic endografts. *J Endovasc Ther.* 2001;8:511-520.

33. Beebe HG, Cronenwett JL, Katzen BT, Brewster DC, et al. Results of an aortic endograft trial: impact of device failure beyond 12 months. *J Vasc Surg.* 2001; 33:S55-63.

34. Matsumura JS, Ryu RK, Ouriel K. Identification and implications of transgraft microleaks after endovascular repair of aortic aneurysms. *J Vasc Surg*. 2001;34:190-197.

35. Roberts B, Hardesty WH, Holling HE, Reivich M., et al. Studies on extracranial cerebral blood flow. *Surgery*. 1964;56:826-833.

36. Eikelboom BC, Lawson JA, Moll FL, Taks AC, et al. The hemodynamic significance of carotid coiling. *J Cardiovasc Surg (Torino*). 1988;29:437-440.

37. Kroger K, Santosa F, Goyen M. Biomechanical incompatibility of popliteal stent placement. *J Endovasc Ther*. 2004;11:686-694.

38. Greil O, Pflugbeil G, Weigand K, Weiss W, et al. Changes in carotid artery flow velocities after stent implantation: A fluid dynamics study with laser Doppler anemometry. *J Endovasc Ther*. 2003;10:275-284.

39. Duda SH, Wiskirchen J, Tepe G, Bitzer M, et al. Physical properties of endovascular stents: an experimental comparison. *J Vasc Interv Radiol*. 2000;11:645-654.

40. Dyet JF, Watts WG, Ettles DF, Nicholson AA. Mechanical properties of metallic stents: how do these properties influence the choice of stent for specific lesions? *Cardiovasc Intervent Radiol.* 2000;23:47-54.

41. Ormiston JA, Dixon SR, Webster MW, Ruygrok PN, et al. Stent longitudinal flexibility: a comparison of 13 stent designs before and after balloon expansion. *Catheter Cardiovasc Interv.* 2000;50:120-124.

42. Palmaz JC. Intravascular Stents - Tissue-Stent Interactions and Design Considerations. *Am J Roentgen*. 1993;160:613-618.

43. Fontaine AB, Spigos DG, Eaton G, Dospassos S, et al. Stent-induced intimal hyperplasia: are there fundamental differences between flexible and rigid stent designs. *JVIR*. 1994;5:739-744.

44. Rolland PH, Mekkaoui C, Vidal V, Berry JL, et al. Compliance matching stent placement in the carotid artery of the swine promotes optimal blood flow and attenuates restenosis. *Eur J Vasc Endovasc Surg*. 2004;28:431-438.

45. Palmaz JC. Intravascular stents in the last and the next 10 years. *J Endovasc Ther*. 2004;11:200-206.

46. Powell RJ, Fillinger M, Bettmann M, Jeffery R, et al. The durability of endovascular treatment of multisegment iliac occlusive disease. *J Vasc Surg.* 2000;31:1178-1184.

47. Ramaswami G, Marin ML. Stent grafts in occlusive arterial disease. *Surg Clin North Am.* 1999;79:597-609.

48. Babalik E, Gulbaran M, Gurmen T, Ozturk S. Fracture of popliteal artery stents. *Circ J.* 2003;67:643-645.

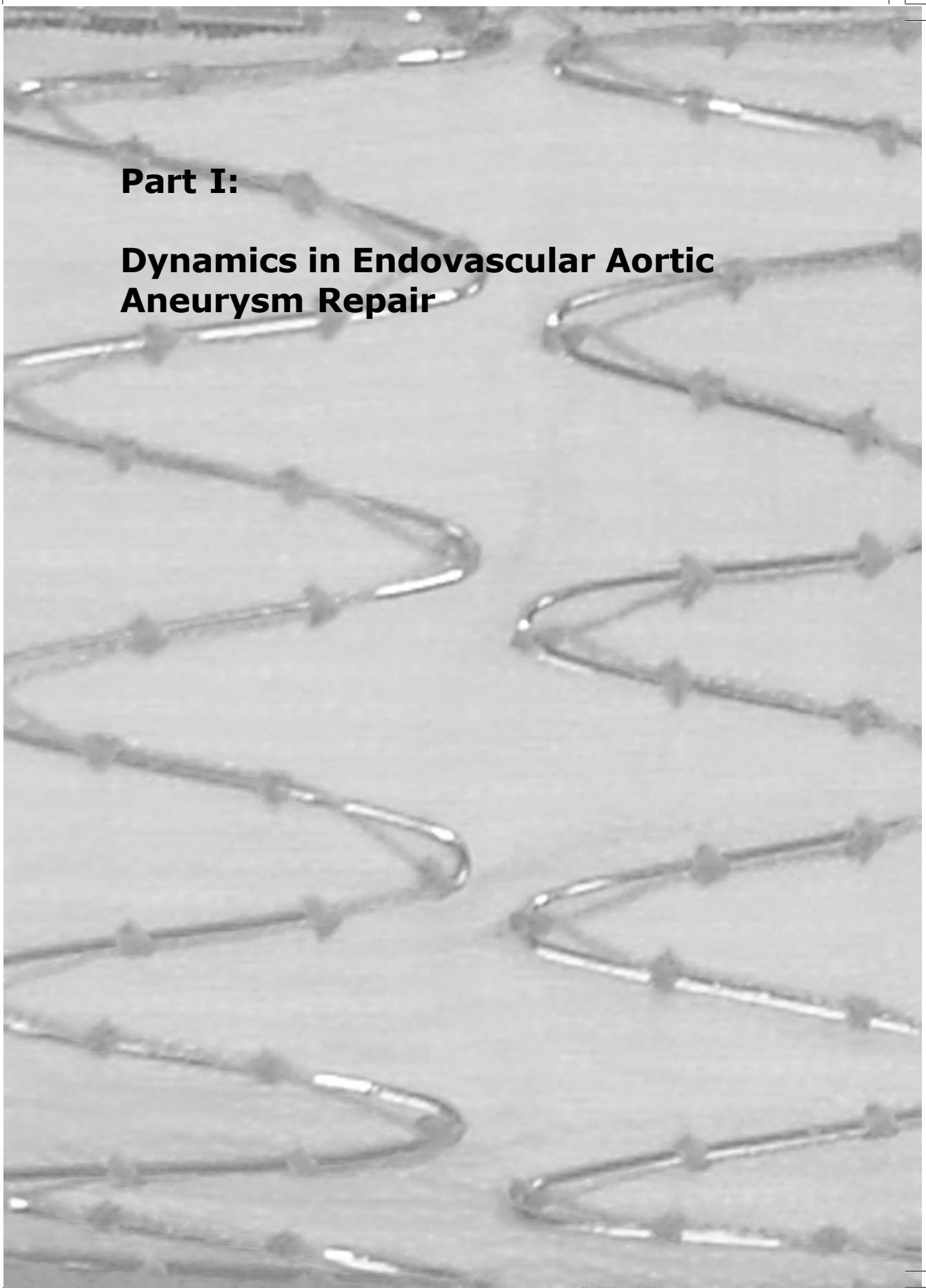

Part I:

Dynamics in Endovascular Aortic Aneurysm Repair

1

A.W. Floris Vos
Willem Wisselink
J. Tim Marcus
Radu A. Manoliu
Jan A. Rauwerda

Aortic Aneurysm Pulsatile Wall Motion Imaged by Cine MRI: A Tool to Evaluate Efficacy of Endovascular Aneurysm Repair?

European Journal of Vascular and Endovascular Surgery 2002;23:158-161

INTRODUCTION

The durability of endovascular aneurysm repair (EVAR) is increasingly being called into question. A means of predicting and identifying late endoleak is urgently required.[1-10] Direct pressure measurements are limited by their invasive nature.[11-14] Uni-dimensional pulsatile wall motion (PWM) has been proposed as an alternative.[15] In this institution, cine MRI has been shown to be an excellent tool to measure PWM of the heart and great vessels in two dimensions.[16,17] To date, no cine MRI acquisition studies have been published monitoring wall motion of aortic aneurysms. The aim of this study was to evaluate cine MRI as a standardized, less operator dependent tool to measure 2D-PWM in abdominal aortic aneurysms (AAAs).

METHODS

Twenty-one patients (17 men) of median age (range) 74 (57-87) years with AAA of median (range) diameter 62 (42-80) mm underwent cine MRI. At the point of greatest cross-sectional area cine images were obtained at a range of 12 per heartbeat. See the appendix for more technical details.

The images were processed on a Sun Sparcstation (Sun Microsystems, Mountain View, CA, USA) using the MASS software package (Dept. of Radiology, Leiden University Medical Center, Leiden, The Netherlands).

In patients where the AAA could not be delineated from the vertebral column a different slice 10 mm above or below was selected. The AAA contour was traced twice by two independent blinded observers. 2D-PWM was defined as the difference between the smallest (end-diastolic, ED) and largest (peak-systolic, PS) cross-sectional area. Left brachial pressure was measured using sphygmomanometry.

Statistical analyses were performed with SPSS software. A value of $p<0.05$ was considered statistically significant. The reliability coefficient of the 2D-PWM measurements was calculated for the means of the two observers.[18]

RESULTS

The median (IQR) 2D-PWM was 0.25 (0.1-0.4) cm^2 and the median (IQR) ED area was 28 (22-31) cm^2. The reliability coefficient for the two observers was 0.81. There was no significant difference between the 2D-PWM measured using the standard and high resolution techniques. The 2D-PWM represents only a 1% increase in cross-sectional area and, assuming the transverse section is circular, only a 0.3 mm increase in median diameter. However, localized wall displacements (up to 2mm) in various directions were observed (Fig. 1). The median MAP was 107 mmHg in the standard resolution and 100 mmHg in the high resolution group (p=0.12). Median pulse pressures were 60 vs 68 mmHg, respectively (p=0.47).

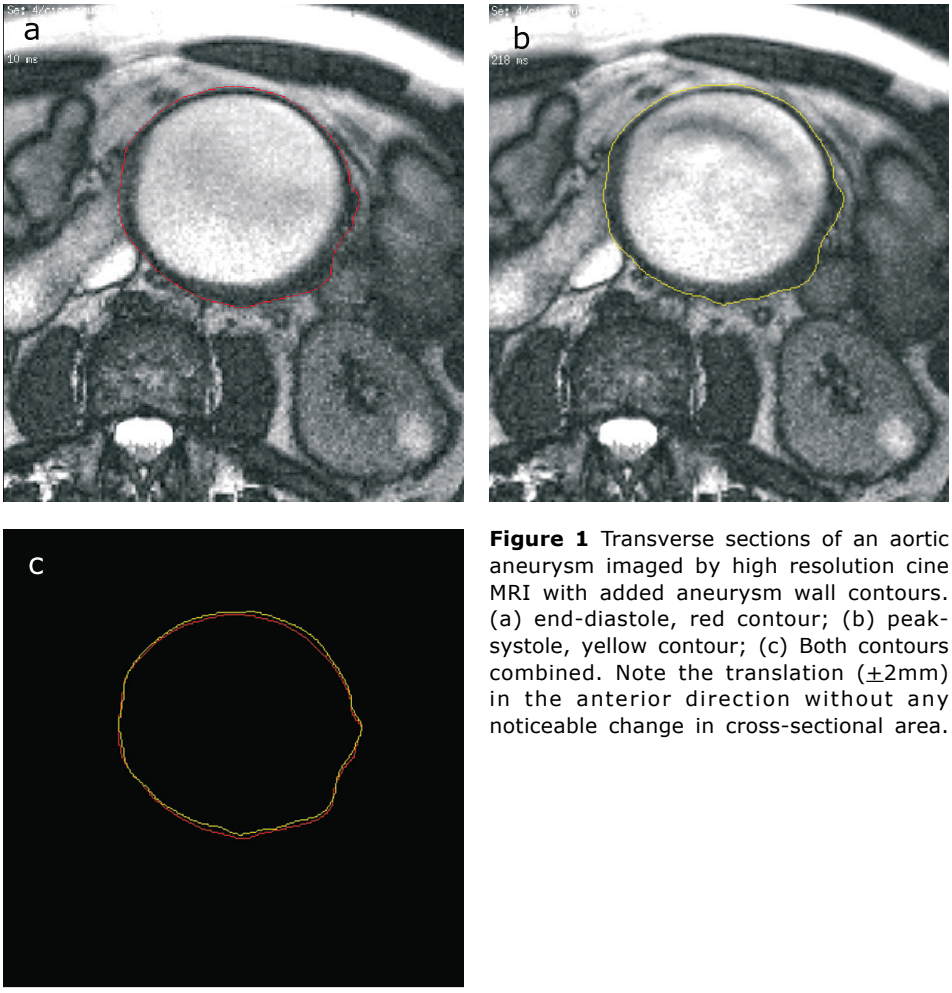

Figure 1 Transverse sections of an aortic aneurysm imaged by high resolution cine MRI with added aneurysm wall contours. (a) end-diastole, red contour; (b) peak-systole, yellow contour; (c) Both contours combined. Note the translation (±2mm) in the anterior direction without any noticeable change in cross-sectional area.

DISCUSSION

Ultrasound and MRI allow indirect intra-vascular pressure measurement to be made on the basis of diameter, cross-sectional area and volume changes.[19-24] Several groups have previously studied AAA.[25-27] One application of this technology may be the detection of endoleak following EVAR.[28] In the present study the PWM as determined by cine MRI (about 1%) is less than that found in ultrasound-based studies (about 4%).[15,26] There may be several reasons for this. Ultrasound-based techniques are uni-dimensional and assume equal wall movements in all directions.[15,23] Furthermore, they cannot distinguish this PWM from the movement of the whole AAA. And lastly, pressure from the transducer may affect distensibility. This study was initiated to determine if aneurysm wall motion can be accurately monitored by cine MRI to possibly determine efficacy of EVAR.[29-31] However, the true 2D-PWM is so small that it falls within the variation of measurements.
In conclusion, using high resolution, 2D cine MRI, we have demonstrated that true pressure related pulsatile wall motion is negligible and therefore not useful as a potential tool to assess efficacy of endovascular aneurysm exclusion.

Appendix

Technical specifications:

Cine MRI	Standard resolution (n=11)	High resolution (n=10)
Scanner	1.5T Siemens 'Vision'	1.5T Siemens 'Sonata'
Pulse sequence	gradient echo	steady state free precession
Excitation angle	25 deg	60 deg
# Phase-encoding lines/heartbeat	9	15
Acquisition time window	100 ms	72 ms
Temporal resolution	50 ms (echo-sharing)	72 ms (no echo-sharing)
# Acquisitions	6	6
Slice thickness	6 mm	5 mm
Echo time	4.8 ms	2.48 ms
Receiver bandwidth	195 Hz/pixel	574 Hz/pixel
Field of view	240 x 320 mm	227 x 280 mm
Acquisition matrix	162 x 256 pixels	416 x 512 pixels
Pixel size	1.48 x 1.25 mm	0.55 x 0.55 mm

REFERENCES

1. Parodi JC, Palmaz JC, Barone HD. Transfemoral intraluminal graft implantation for abdominal aortic aneurysms. *Ann Vasc Surg.* 1991;5:491-499.

2. Wisselink W, Hollier LH. Principles in the technique of endovascular grafting. In: Yao JST and Pearce WH. *Aneurysms: New Findings and Treatments.* Appleton & Lange, 1994: 317-324.

3. Marin ML, Veith FJ, Cynamon J, Sanchez LA, et al. Initial experience with transluminally placed endovascular grafts for the treatment of complex vascular lesions. *Ann Surg.* 1995;222:449-465.

4. May J, White GH, Yu W, Waugh RC, et al. Early experience with the Sydney and EVT prostheses for endoluminal treatment of abdominal aortic aneurysms. *J Endovasc Surg.* 1995;2:240-247.

5. Balm R, Eikelboom BC, May J, Bell PR, et al. Early experience with transfemoral endovascular aneurysm management (TEAM) in the treatment of aortic aneurysms. *Eur J Vasc Endovasc Surg.* 1996;11:214-220.

6. Moore WS, Rutherford RB. Transfemoral endovascular repair of abdominal aortic aneurysm: results of the North American EVT phase 1 trial. EVT Investigators. *J Vasc Surg.* 1996;23:543-553.

7. Gilling-Smith GL, Martin J, Sudhindran S, Gould DA, et al. Freedom from endoleak after endovascular aneurysm repair does not equal treatment success. *Eur J Vasc Endovasc Surg.* 2000;19:421-425.

8. Wolf YG, Hill BB, Rubin GD, Fogarty TJ, et al. Rate of change in abdominal aortic aneurysm diameter after endovascular repair. *J Vasc Surg.* 2000;32:108-115.

9. Harris PL, Vallabhaneni SR, Desgranges P, Becquemin JP, et al. Incidence and risk factors of late rupture, conversion, and death after endovascular repair of infrarenal aortic aneurysms: the EUROSTAR experience. *J Vasc Surg.* 2000;32:739-749.

10. White GH, May J, Petrasek P, Waugh R, et al. Endotension: an explanation for continued AAA growth after successful endoluminal repair. *J Endovasc Surg.* 1999;6:308-315.

11. Chuter TA, Ivancev K, Malina M, Resch T, et al. Aneurysm pressure following endovascular exclusion. *Eur J Vasc Endovasc Surg.* 1997;13:85-87.

12. Stelter W, Umscheid T, Ziegler P. Three-year experience with modular stent-graft devices for endovascular AAA treatment. *J Endovasc Surg.* 1997;4:362-369.

13. Treharne GD, Loftus IM, Thompson MM, Lennard N, et al. Quality control during endovascular aneurysm repair: monitoring aneurysmal sac pressure and superficial femoral artery flow velocity. *J Endovasc Surg.* 1999;6:239-245.

14. Baum RA, Carpenter JP, Cope C, Golden MA, et al. Aneurysm sac pressure measurements after endovascular repair of abdominal aortic aneurysms. *J Vasc Surg.* 2001;33:32-41.

15. Malina M, Lanne T, Ivancev K, Lindblad B, et al. Reduced pulsatile wall motion of abdominal aortic aneurysms after endovascular repair. *J Vasc Surg.* 1998;27:624-631.

16. Marcus JT, Vonk Noordegraaf A, De Vries PMJM, van Rossum AC, et al. MRI evaluation of right ventricular pressure overload in chronic obstructive pulmonary disease. *J Magn Res Im.* 1998;8:999-1005.

17. Marcus JT, Goette MJW, DeWaal LK, Stam MR, et al. The influence of through-plane motion on left ventricular volumes measured by Magnetic Resonance Imaging: Implications for Image acquisition and analysis. *J Cardiov Magn Res.* 1999;1:1-6.

18. Fleiss JL. The Design and Analysis of Clinical Experiments. In: *Anonymous*. John Wiley & Sons, 1986;1-31.

19. Boese JM, Bock M, Schoenberg SO, Schad LR. Estimation of aortic compliance using magnetic resonance pulse wave velocity measurement. *Phys Med Biol.* 2000;45:1703-1713.

20. Hansen F, Bergqvist D, Mangell P, Ryden A, et al. Non-invasive measurement of pulsatile vessel diameter change and elastic properties in human arteries: a methodological study. *Clin Physiol.* 1993;13:631-643.

21. Higgins CB, Sakuma H. Heart disease: functional evaluation with MR imaging. *Radiology.* 1996;199:307-315.

22. Mogelvang J, Stokholm KH, Saunamaki K, Reimer A, et al. Assessment of left ventricular volumes by magnetic resonance in comparison with radionuclide angiography, contrast angiography and echocardiography. *Eur Heart J.* 1992;13:1677-1683.

23. Kool MJ, van Merode T, Reneman RS, Hoeks AP, et al. Evaluation of reproducibility of a vessel wall movement detector system for assessment of large artery properties. *Cardiovasc Res.* 1994;28:610-614.

24. Semelka RC, Tomei E, Wagner S, Mayo J, et al. Normal left ventricular dimensions and function: interstudy reproducibility of measurements with cine MR imaging. *Radiology.* 1990;174:763-768.

25. Macsweeney ST, Young G, Greenhalgh RM, Powell JT. Mechanical properties of the aneurysmal aorta. *Br J Surg.* 1992;79:1281-1284.

26. Lanne T, Sonesson B, Bergquist D, Bengtsson H, et al. Diameter and compliance in the male human abdominal aorta: Influence of age and aortic aneurysm. *Eur J Vasc Surg*. 1992;6:178-184.

27. Wilson KA, Lindholt JS, Hoskins PR, Heickendorff L, et al. The relationship between abdominal aortic aneurysm distensibility and serum markers of elastin and collagen metabolism. *Eur J Vasc Endovasc Surg*. 2001;21:175-178.

28. Schurink GW, Aarts NJ, Malina M, van Bockel JH. Pulsatile wall motion and blood pressure in aneurysms with open and thrombosed endoleaks-comparison of a wall track system and M-mode ultrasound scanning: An in vitro and animal study. *J Vasc Surg.* 2000;32:795-803.

29. Wills A, Thompson MM, Crowther M, Sayers RD, et al. Pathogenesis of abdominal aortic aneurysms-cellular and biochemical mechanisms. *Eur J Vasc Endovasc Surg.* 1996;12:391-400.

30. Forbat SM, Mohiaddin RH, Yang GZ, Firmin DN, et al. Measurement of regional aortic compliance by MR imaging: a study of reproducibility. *J Magn Reson Imaging.* 1995;5:635-639.

31. Hilfiker PR, Quick HH, Pfammatter, Schmidt M, et al. Three-dimensional MR angiography of a nitinol-based abdominal aortic stent graft: assessment of heating and imaging characteristics. *Eur Radiol*. 1999;9:1775-1780.

2

A.W. Floris Vos
Willem Wisselink
J. Tim Marcus
Anco C. Vahl
Radu A. Manoliu
Jan A. Rauwerda

Cine MRI Assessment of Aortic Aneurysm Dynamics Before and After Endovascular Repair

Journal of Endovascular Therapy 2003;10:433-439

INTRODUCTION

Whether endovascular aneurysm repair (EVAR) will be the treatment of choice for the majority of patients with abdominal aortic aneurysms (AAA) is still undetermined. The excellent technical and short-term clinical success rates are in contrast with the 3% per year risk of late failure (aneurysm rupture or conversion).[1] The main risk factors are proximal endoleak, material disintegration, and stent-graft migration.[1] All are inevitably related to repetitive forces acting within the pressurized aorta and upon the stent-graft. Adequate visualisation of aneurysm and stent-graft motions might aid in our understanding of the complex patterns of those forces.
The established noninvasive methods to measure aneurysm and stent-graft dynamics consist of either 1-dimensional imaging techniques or mathematical simulation models.[2-4] In both, a number of assumptions are made to obtain the desired data. Cine magnetic resonance imaging (MRI) in transversal, sagittal, and coronal planes provides 2-dimensional dynamic imaging of the complex configurations of the aneurysm and its motions within the cardiac cycle without any assumption.[5] In this study, we have attempted to measure pulsatile motions of the aneurysm and stent-graft. A thorough understanding of these motions might lead to improved device design, fixation, and durability, as those are the key features to successful long-term stent-graft repair.

METHODS

Seven consecutive patients (5 men, median age 71 years, range 58-87) with AAAs suitable for EVAR underwent a cine MRI scan prior to and after the operation. The median maximum diameter of the aneurysms was 61 mm (range 46-75), with a median proximal neck length of 20 mm (range 18-27). In all patients, the iliac arteries were not severely calcified or tortuous, and in 5 aneurysms, the aortic bifurcation was involved. In all subjects, conventional AneuRx (Medtronic Sunnyvale, CA) or Talent (Medtronic World Medical, Sunrise, FL) stent-grafts containing low-artifact nitinol metallic components were used. Informed consent was obtained from all subjects in accordance with the requirements of the institutional ethics committee.

Cine MRI

Cine MRI was performed prior to EVAR and again postoperatively, after a median of 34 days (range 14-660). A 1.5-T Sonata MRI whole body system (Siemens AG, Munich, Germany) was used. The aneurysm was localized by 2D true-FISP (Free Induction with Steady State Precession). Sections of the aneurysm and stent-graft were selected in transverse, sagittal and coronal planes, and 12 cine loops per heartbeat were obtained. Examples of these cine loops (movies A-D) are included in the cd version of this article. The cine image acquisition was prospectively triggered by the R-wave of the electrocardiogram. The cardiac gated acquisition window was 72 ms. The highest in-plane spatial resolution was 0.55x0.55 mm, obtained with a matrix size of 416x512 pixels and a 227 x 280 mm field of view (see the Appendix for more technical details).

Data Collection

The images were processed on a Sun Sparcstation (Sun Microsystems, Mountain View, CA, USA) using the MASS software package (Dept. of Radiology, Leiden University Medical Center, Leiden, The Netherlands). Two independent observers blinded to the aim of the study manually traced aneurysm and stent-graft contours (Fig. 1) on the images obtained during peak-systole and end-diastole to evaluate configuration changes. Tracings were performed at the outside of the aneurysm and stent-graft to avoid confounding effects of through-plane flow on the observed endocontour. With regard to the stent-graft, locations were chosen distant from the proximal and distal ends to avoid measurement faults by flow related artefacts. Furthermore, tracings were solely performed at locations of the aneurysm wall and stent-graft when a clear delineation with the surrounding tissue was present. Translations in cranial-caudal (CC), left-right (LR) and anteroposterior (AP) directions were defined as maximal displacement of the contours. Angulation of the stent-graft was measured in the sagittal and coronal planes in order to examine a possible relationship between the observed motions and the changing direction of the blood flow. The surface area changes in the transverse sections throughout the cardiac cycle were calculated for the aneurysm at the level of the maximal diameter and of the stent-graft itself, as described in a previous study, and expressed as the 2-dimensional pulsatile wall motion (2D-PWM).[5] In all patients, sufficient data was obtained to perform the calculations.

Statistical Analysis

Maximal translations of each patient were calculated as the mean of the measurement results of the 2 observers. For the entire group of patients, maximal translations were

expressed as the median (range). Absent translation implied a motion within the limits of the pixel size (0.5 x 0.5 mm); therefore, wherever applicable, absent translation was expressed as <0.5mm. When performing calculations, all values of <0.5mm were replaced by 0 mm. Correlations between CC translation change after EVAR and stent-graft angulation were calculated using the Spearman test for comparison of continuous variables. Nonparametric Wilcoxon rank sum paired tests were used to evaluate statistical significance. Statistical analyses were performed with SPSS software, (version 9.0; SPSS, Chicago, IL, USA). P<0.05 was considered significant.

Click on the picture to see movie A-D

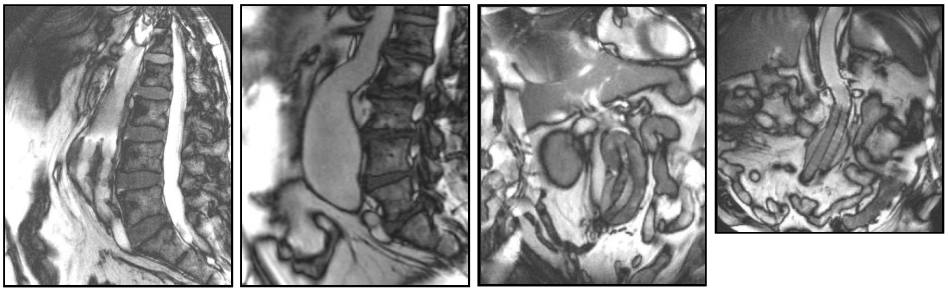

A **B** **C** **D**

RESULTS

All maximal translations are summarized in Fig. 2. The median AP translation of the aneurysm (Table) decreased from a baseline 1.05 mm (range<0.5 - 1.29) to within pixel size (<0.5 mm) after EVAR (p=0.04, Fig. 1A)[Movie A is a sagittal cine MRI of an aortic aneurysm after EVAR demonstrating increased CC translation and absent AP translation. Movie B is a sagittal cine MRI of an aortic aneurysm with AP translation before EVAR.] The median preprocedural CC translation (Fig. 1B) of 1.01 mm (range <0.5–1.51) increased after EVAR with 67% to 1.69 mm (range 1.1–1.99; p=0.02). In 2 patients, a LR translation (1.35 and 1.83 mm, respectively) after EVAR was observed at the level of 45° and 35° stent-graft angulation, respectively (Fig. 1C). In 4 patients, configuration changes were observed at the site of maximal angulation of the stent-graft (Fig. 3) [Movies C en D are coronal cine MRIs of stent-grafts bending at the site of maximal anguation.]. No significant change between 2D-PWM before (0.25, range 0.07–0.29) and after EVAR (0.18, range 0.08–0.42) was observed (p=0.79). The stent-graft showed no 2D-PWM. The correlation coefficient between angulation and CC translation change after EVAR was 0.67 (p>0.05).

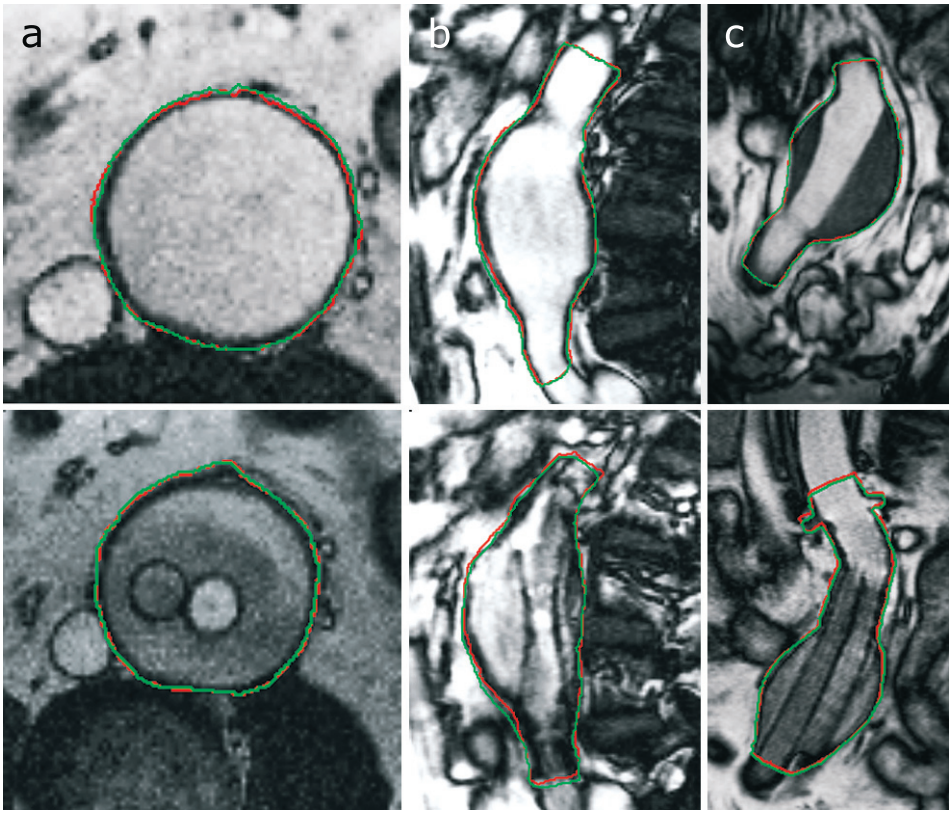

Figure 1 (A) Transverse, (B) sagittal, and (C) coronal sections from a cine MRI study of an aortic aneurysm at peak-systole before (above) and after (below) EVAR. The superimposed contours at peak systole (green) and end-diastole (red) show patterns of translation.

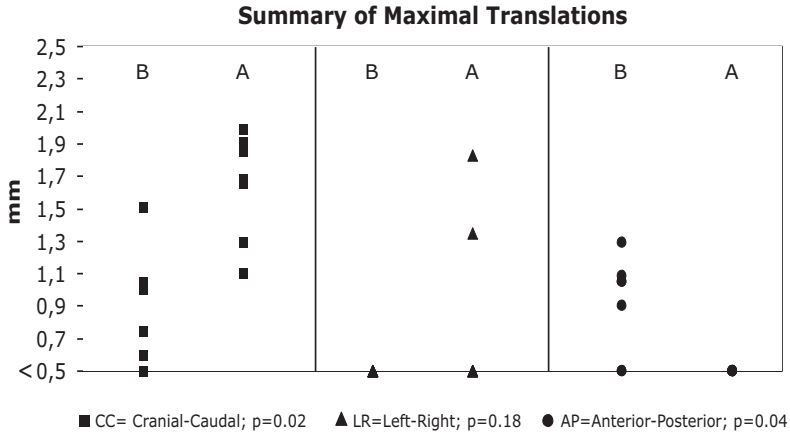

Figure 2 Maximal aneurysm wall translation in 3-Dimensions before (B) and after (A) EVAR.

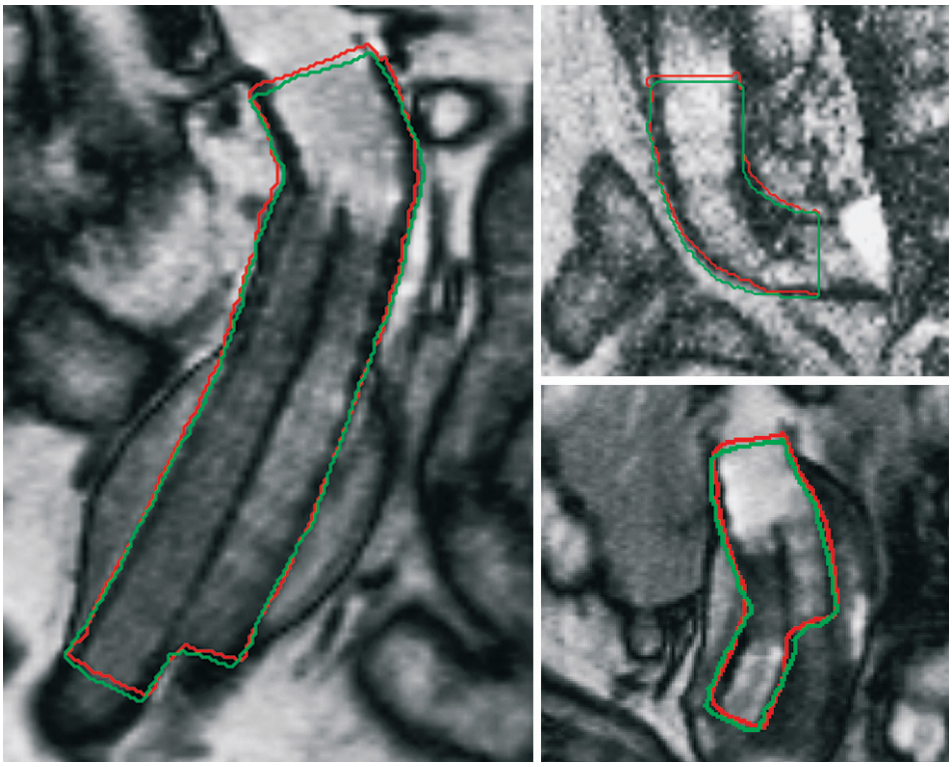

Figure 3 Cine MRI of stent-graft at peak-systole (green contour) and added red contour (end-diastole). Note the subtle bending of the stent-grafts at sites of maximal angulation.

	Before EVAR	After EVAR	
CC Translation	1.01 mm(<0.5 – 1.51)	1.69 mm(1.1 – 1.99)	p=0.02
AP Translation	1.05 mm(<0.5 – 1.29)	<0.5 mm	p=0.04
LR Translation	<0.5 mm	0.5 mm(<0.5 – 1.83)	p=0.18
2D-PWM Aneurysm	0.25 cm^2(0.07 – 0.29) 1%	0.18 cm^2(0.08 – 0.42) <1%	p=0.79
2D-PWM Stent-graft	X	0.05 (0 – 0.06)cm^2 <1%	
Stent-graft Angulation	X	30°(20 – 80)†	

Table Dynamic measurements taken from cine MR images of the aneurysm and stent-graft. Continuous variables are given as median (range). Surface increase in the systolic contour versus the diastolic contour is given as a percentage. EVAR: endovascular aneurysm repair, 2D-PWM: 2-dimensional pulsatile wall motion. †Correlation coeficient = 0.67 (angulation versus cc translation change).

DISCUSSION

Cine MRI, may be a useful non-invasive 2-dimensional tool to measure the complex patterns of force influencing aortic aneurysm motion before and after endovascular repair. Previous reports investigating the forces acting within the pressurized aorta and upon the stentgraft were either invasive or based on mathematical analyses and computational fluid dynamics studies.[2,6]

With regard to our evaluation procedures, we wish to stress that results from manual tracings of the vessel wall should be carefully assessed because the method is observer dependent. However, we had 2 independent blinded observers trace the aneurysm and stent-graft only when the vessel wall was clearly visible, so we believe that the main motions of the aneurysm and stent-graft have been accurately measured. More sophisticated methods with automatic contour detection or subtraction images have been tried, but they proved insufficient because of the highly irregular diseased vessel wall.

In the debate over suitability of short- or no- neck aneurysms for endograft repair, our findings of increased cranial-caudal translation provide useful insights. The pulsatile pressure variations caused by blood flowing through a noncompliant, tapering graft apparently result in an increased pulling force that may eventually induce a proximal displacement of the graft.[7] In aneurysms with short proximal necks, transrenal graft fixation with uncovered stents or even branched stent-grafts are indicated to avoid migration in the long term.[8-11]

Besides migration, there is an almost universal awareness that the long term durability of stent-grafts must be carefully assessed because fabric erosion (type III endoleak) and wire fracture are increasingly common at longer follow-up.[12-14]

In 4 patients, we observed the stent-graft bend with each systole at sites of angulation (Fig. 3), which supports the notion that metal fatigue and fabric damage are most likely to occur at these locations. Therefore, especially angulated stent-grafts should be closely monitored by means of plain abdominal radiography in addition to computed tomography. We did note in one patient an absence of motion in the aneurysm and stent-graft despite a significant angulation of the graft, but we surmise that lack of aneurysm wall compliance due to calcifications and surrounding tissues (retroperitoneal fibrosis) might have been responsible for this observation.

In an ultrasound study, Malina et al. recorded decreased pulsatility of the aortic aneurysm after EVAR by measuring aneurysm wall motions in one dimension.[3] In our study, we observed only minimal pulsatility of either the aneurysm or stent-graft before and after aneurysm exclusion. Perhaps the authors interpreted the

true disappearance of AP translation after EVAR, as observed in our MRI study, as a loss of pulsatility on the ultrasound study.

Possible limitations of this study are the artifacts of endovascular implants in the magnetic field. Previously published studies showed that the image quality around and within the stents is very much dependent on the magnetic properties of the stent material and the imaging sequence.[15-17] Generally, 3 types of artifacts may arise while imaging a region containing a stent: susceptibility artefacts, which arise from local field inhomogenities induced by metal, radio frequency artifacts caused by the induction of eddy currents in the implant, and flow artefacts. Because we avoided the proximal and distal ends and inner lumen of the stent-graft and based our comparison at the same location in end-diastole and peak-systole, these artefacts did not interfere with our measurements.

In conclusion, cine MRI is a useful tool to obtain dynamic information on the various repetitive translations and shape changes to which an aneurysm and stent-graft are subjected. Increased translation caused by a pulling longitudinal force at the aortic neck was observed, which might be due to the absence of radial compliance and a tapering angulated graft. The mechanism causing stent frame fractures, broken sutures, and fabric material disintegration, especially at sites of angulation, are inevitably related to the vector forces causing translation and bending. With regard to future stent-graft design, this relatively small study supports the use of strong proximal fixation, suprarenal if necessary, and a flexible, compliant mid zone without metallic components.

Appendix

Technical Specifications of Cine MRI Studies:

Excitation angle:	60°
Phase-encoding lines/heartbeat:	15
Acquisition time window:	72 ms
Temporal resolution:	72 ms (no echo-sharing)
# Acquisitions:	6
Slice thickness:	5 mm
Echo time:	2.48 ms
Receiver bandwidth:	574 Hx/pixel
Field of view:	227x280 mm to 340x340 mm
Acquisition matrix	416x512 pixels to 208x256 pixels
Pixel size:	0.55 x 0.55 mm-1.63x1.33 mm

REFERENCES

1. Harris PL, Vallabhaneni SR, Desgranges P, Becquemin JP, et al. Incidence and risk factors of late rupture, conversion, and death after endovascular repair of infrarenal aortic aneurysms: the EUROSTAR experience. *J Vasc Surg.* 2000;32:739-749.

2. Liffman K, Lawrence-Brown MM, Semmens JB, Bui A, et al. Analytical modeling and numerical simulation of forces in an endoluminal graft. *J Endovasc Ther*. 2001;8:358-371.

3. Malina M, Lanne T, Ivancev K, Lindblad B, et al. Reduced pulsatile wall motion of abdominal aortic aneurysms after endovascular repair. *J Vasc Surg*. 1998;27:624-631.

4. Sonesson B, Sandgren T, Lanne T. Abdominal aortic aneurysm wall mechanics and their relation to risk of rupture. *Eur J Vasc Endovasc Surg.* 1999;18:487-493.

5. Vos AW, Wisselink W, Marcus JT, Manoliu RA, et al. Aortic Aneurysm Pulsatile Wall Motion Imaged by Cine MRI: a Tool to Evaluate Efficacy of Endovascular Aneurysm Repair? *Eur J Vasc Endovasc Surg.* 2001; 23:158-161.

6. Flora HS, Woodhouse N, Robson S, Adiseshiah M. Micromovements at the aortic aneurysm neck measured during open surgery with close-range photogrammetry: implications for aortic endografts. *J Endovasc Ther*. 2001;8:511-520.

7. Resch T, Ivancev K, Brunkwall J, Nyman U, et al.Distal migration of stent-grafts after endovascular repair of abdominal aortic aneurysms. *J Vasc Interv Radiol*. 1999;10:257-264.

8. Marin ML, Parsons RE, Hollier LH, Mitty HA,et al. Impact of transrenal aortic endograft placement on endovascular graft repair of abdominal aortic aneurysms. *J Vasc Surg*. 1998;28:638-646.

9. Chuter TA, Gordon RL, Reilly LM, Goodman JD, et al. An endovascular system for thoracoabdominal aortic aneurysm repair. *J Endovasc Ther*. 2001;8:25-33.

10. Wisselink W, Abruzzo FM, Shin CK, Ramirez JR, et al. Endoluminal repair of aneurysms containing ostia of essential branch arteries: an experimental model. *J Endovasc Surg.* 1999;6:171-179.

11. Anderson JL, Berce M, Hartley DE. Endoluminal aortic grafting with renal and superior mesenteric artery incorporation by graft fenestration. *J Endovasc Ther*. 2001;8:3-15.

12. Beebe HG, Cronenwett JL, Katzen BT, Brewster DC, et al. Results of an aortic endograft trial: impact of device failure beyond 12 months. *J Vasc Surg.* 2001;33:S55-S63.

13. Matsumura JS, Ryu RK, Ouriel K. Identification and implications of transgraft microleaks after endovascular repair of aortic aneurysms. *J Vasc Surg.* 2001;34:190-197.

14. Collin J, Murie JA. Endovascular treatment of abdominal aortic aneurysm: a failed experiment. *Br J Surg.* 2001;88:1281-1282.

15. Bartels LW, Smits HF, Bakker CJ, Viergever MA. MR imaging of vascular stents: effects of susceptibility, flow, and radiofrequency eddy currents. *J Vasc Interv Radiol*. 2001;12:365-371.

16. Klemm T, Duda S, Machann J, Seekamp-Rahn K, et al. MR imaging in the presence of vascular stents: A systematic assessment of artifacts for various stent orientations, sequence types, and field strengths. *J Magn Reson Imaging*. 2000;12:606-615.

17. Merkle EM, Klein S, Wisianowsky C, Boll DT, et al. Magnetic resonance imaging versus multislice computed tomography of thoracic aortic endografts. *J Endovasc Ther*. 2002;9:II-2-13.

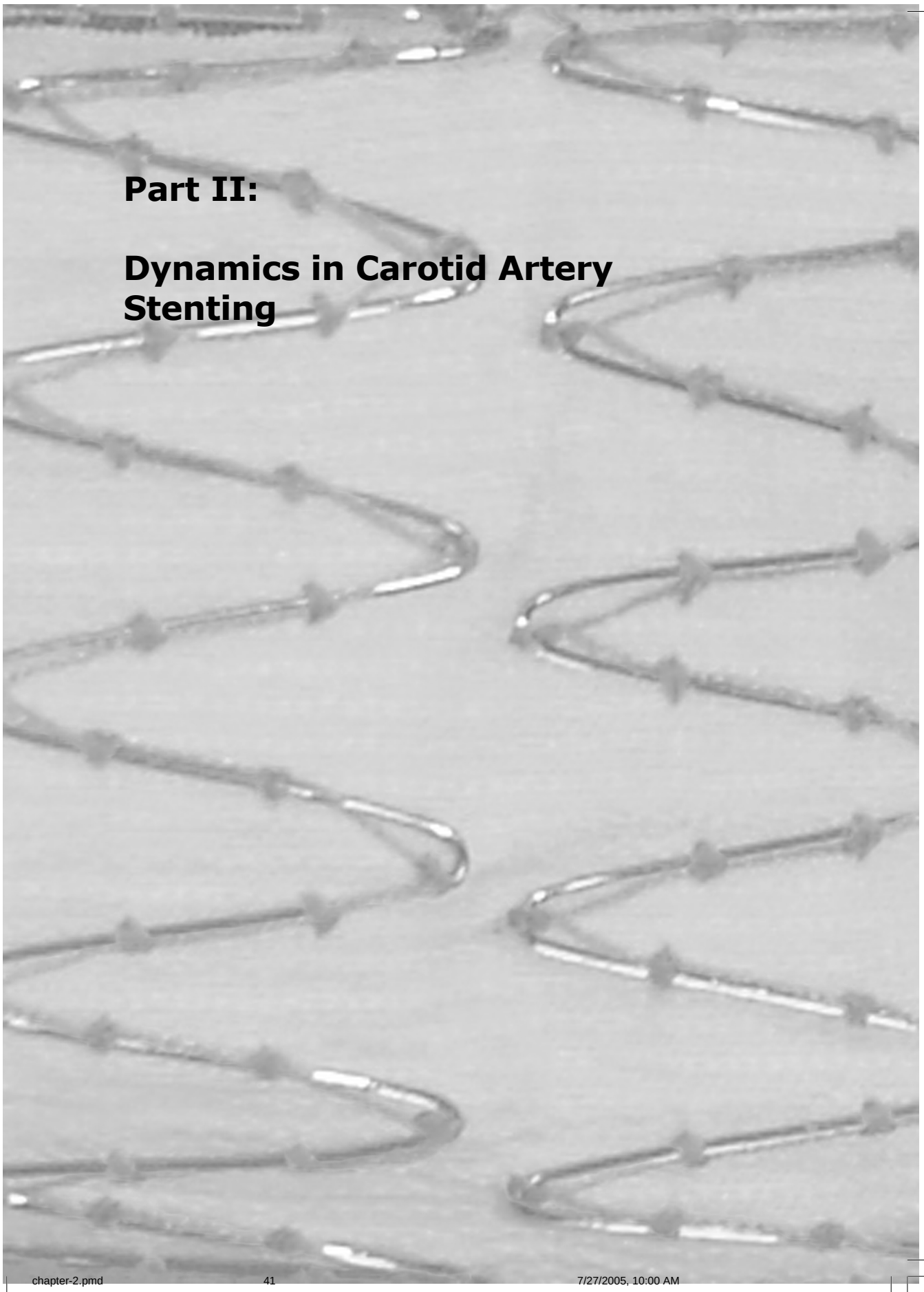

Part II:

Dynamics in Carotid Artery Stenting

3

A.W. Floris Vos
Matteus A.M. Linsen
J. Tim Marcus
Jos C. van den Berg
Jan Albert Vos
Jan A. Rauwerda
Willem Wisselink

Carotid Artery Dynamics During Head Movements: A Reason for Concern with Regard to Carotid Stenting?

Journal of Endovascular Therapy 2003;10:862-869

INTRODUCTION

Carotid angioplasty/stenting (CAS) is currently being widely embraced due to the perceived advantages of a less invasive treatment for carotid artery occlusive disease. Several studies suggest that early complication rates may be comparable to those of carotid endarterectomy.[1,2] However, long-term durability of CAS in preventing stroke and maintaining patency are being questioned for various reasons.[3] Interestingly, to date, very little attention has been directed towards the mobile features of the carotid artery, whereas repetitive motions of lower extremity vessels such as the external iliac and popliteal arteries, have been widely implicated in long-term stent failure.[4-6] The purpose of this study was to describe the geometric changes of the carotid artery during head movements in patients following CAS. A thorough understanding of these geometrical changes might lead to improved device design, which may in turn improve the long-term outcome of CAS.

METHODS

Patient Sample

Between November 2001 and September 2002, 7 patients (all men; mean age 69 years, range 65-76) were treated with CAS for high grade stenosis of the left carotid artery (Table 1). All patients had a high-resolution magnetic resonance (MR) scan at a mean 154 days postoperatively (range 50-229). In all subjects, stents were specifically designed for the carotid artery and contained low-artifact nitinol metallic components: Carotid SE (Medtronic, Minneapolis, MN, USA), Acculink (Guidant, Indianapolis, IN, USA) or Precise (Cordis, Miami, FL, USA). Patients who had a Carotid Wallstent (Boston scientific, Natick, MA, USA) were excluded because of the well-known MR artifacts caused by this stainless-steel device. Informed

Age, y	Stenosis	Stented Location	Stent Model	Size, mm
65	80-90%	Left bifurcation	Carotid SE,	20 x 6
70	90-99%	Left ICA	Carotid SE,	20 x 6
69	80-90%	Left ICA	Carotid SE,	30 x 8
67	90-99%	Left bifurcation	Precise,	30 x 9
66	90-99%	Left ICA	Acculink,	30 x 9
76	90%	Left bifurcation	Acculink,	30 x 7
73	80-90%	Left CCA	Precise,	40 x 9

Table 1 Patient characteristics and stent data for 7 men with carotid stents. ICA: internal carotid artery, CCA: common carotid artery.

consent was obtained from all subjects in accordance with the requirements of institutional ethics committee.

Imaging

A 1.5 T MR whole body system (Siemens Sonata, Erlangen, Germany) was used. First, the carotid artery was localized first using 2-dimensional (2D) true-FISP (Fast Imaging with Steady State Precession with balancing gradients in all spatial orientations) in transversal, sagittal and coronal planes. Then, a 3-dimensional (3D) "time of flight" (TOF) angiograpic acquisition was performed in transverse slabs covering the full range of both carotid arteries from the aortic arch to the skull base. This 3D-TOF sequence was a Fast Low Angle Shot (FLASH) gradient echo sequence. The acquisition was obtained with the head in 5 positions: neutral, turned left, turned right, bent forward, and bent backward. The in-plane spatial resolution was 1.0x0.8 mm, obtained with a matrix size of 168x256 pixels and a field of view of 175x200 mm. Slice thickness was 1.4 mm (for more technical details see the Appendix). Transverse and sagittal planes are defined as fixed planes related to the position of the MR field uninfluenced by the position of the head. Additional sagittal localizing images were acquired in the bent forward and bent backward positions to measure the exact bending angle in each patient. Finally, from the 3D acquisition, a maximum intensity projection (MIP) was reconstructed of the full range of the carotid arteries in all head positions. This MIP was constructed in such a way that the observer's viewpoint rotated from the left, via anterior, to the right in 6° increments.

Data Collection

Patients were asked to place their head in all positions to the maximal possible. Head positions were defined by measuring the angle between bony structures of the head and the thorax. The neutral position was considered to be 0° in both transverse and sagittal planes. The median angle of the head positions was 54.1° (40.0°-74.8°) in turned left, 51.5° (32.1°-67.4°) in turned right, 22.2° (18.3°-25.6°) in bent forward, and 26.4° (21.4°-36.0°) in bent backward positions. Maximal angulations at the proximal and distal carotid stent junction in neutral head position were selected by measuring all angulations in every viewpoint of the 3D MIP reconstructions. These maximal angulations were compared with angulations at the same viewpoint in the other head positions (Fig. 1). Shape changes of the stented section of the carotid artery were evaluated.

For torsion shear measurements of both carotid arteries, transverse sections at

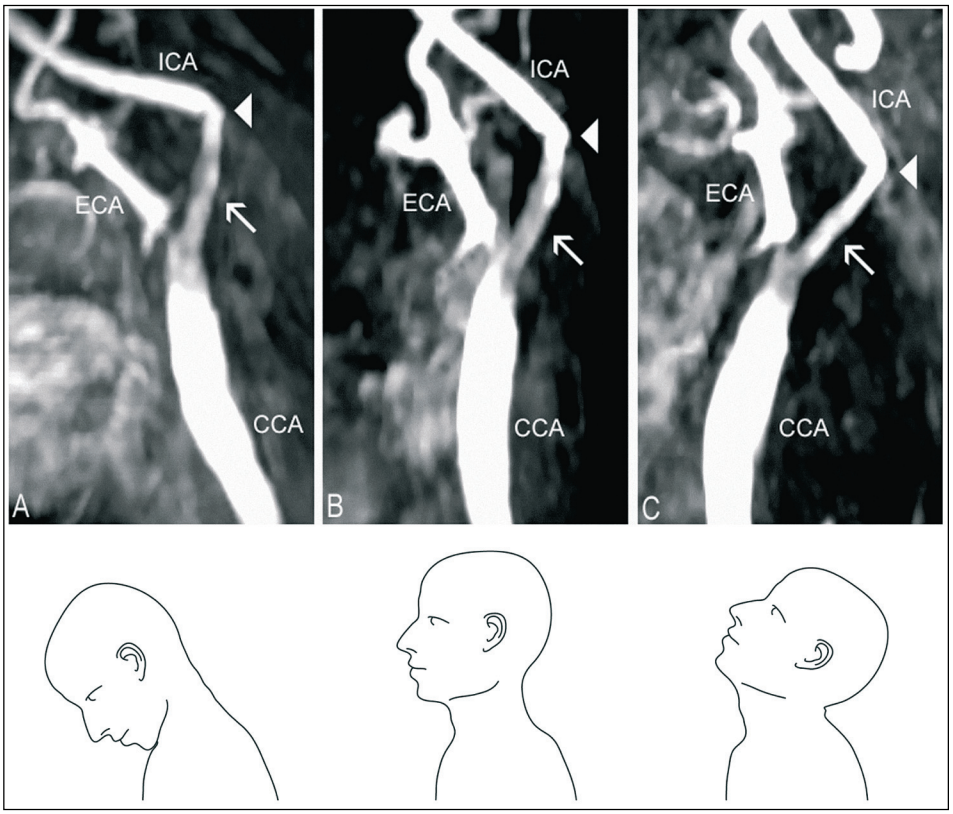

Figure 1 MR images of a 66-year-old man following stent placement (arrows in A, B, C) taken from the same viewpoint during the 3 illustrated head positions. In the neutral head position (B), there is 56° angulation of the distal stent junction (arrowheads in all images). Note the increase in this angulation up to 85° when the head is bent forward (A). In the bent backward position (C), the angulation is decreased to 49°. ICA: internal carotid artery, CCA: common carotid artery, ECA: external carotid artery.

the level of the carotid bifurcation and the carotid artery at the skull base were used to calculate torsion shear in the common (CCA) and internal carotid artery (ICA) during turned left and turned right head positions. The assumption was made that at the level of the skull base there is no rotation of the ICA relative to the bone (i.e., the ICA is "fixed" in the carotid foramen). By measuring both rotation of the skull, as well as rotation of the carotid bifurcation, we were able to differentiate degrees of torsion shear of the CCA and ICA, respectively (Fig. 2). Measurements of the stented and the contralateral side were compared, where possible. Two independent observers blinded to the aim of the study made all measurements. The images were processed on a RadWorks 5.1 diagnostic radiology workstation (IBM Corp, White Plains, NY, USA).

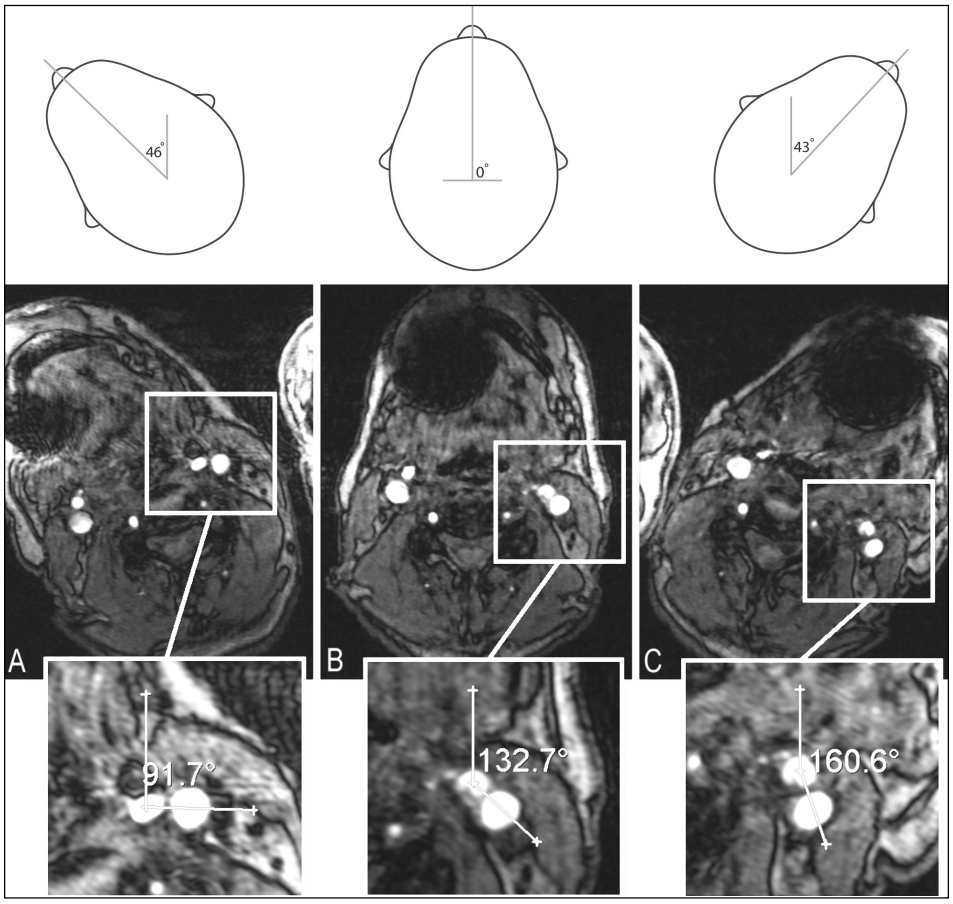

Figure 2 MR images of a 69-year-old man following stent placement in the left ICA. Transverse sections at the level of the bifurcation in different head positions, turned right (A), neutral (B), and turned Left (C), were used to measure torsion shear of the carotid artery. Common carotid artery torsion shear equals the rotation of the bifurcation; ICA torsion shear equals the head rotation minus rotation of the bifurcation.

Statistical Analysis

Maximal angulations and torsion shear of each patient were calculated as the mean of the measurement results of the 2 observers. For the entire group of patients, measurements were expressed as the median (range). Maximal angulations in neutral head position were compared with angulations at the same viewpoint in the other head positions using the Wilcoxon rank sum paired nonparametric test to evaluate statistical significance. The same test was used to compare torsion shear of the carotid artery at the stented and contralateral side. $P<0.05$ was considered statistically significant. Statistical analyses were performed with SPSS software (version 9; SPSS, Chicago, IL, USA).

RESULTS

In neutral head position, maximal angulation at the proximal stent junction was 24.1° (15.9°-32.3°) and 34.3° (32.3°-55.6°) at the distal junction. From the same viewpoint, angulation at the distal stent junction changed significantly up to 47.6° (42.6°-85.2°, p=0.028) in bent forward and 26.5° (25.0°-48.7°, p=0.027) in bent backward head positions. In turned left head position, angulation at the proximal stent junction showed a significant change of 27.5° (16.9°-38.2°, p=0.028). All other compared angulations showed no significant change (Table 2). In all patients, configuration changes of the stented section of the carotid artery were absent. No differences were seen between the respective stent models used. In one patient, the contralateral unstented side was occluded and could not be visualized; the remaining 6 patients showed diffuse configuration changes in the carotid artery during head movements without specific angulation at one location. Of all angulation data, the mean difference between both observers was 0.16°$\pm$3.49°.

At the stented side in turned left and turned right head positions, the CCA was subjected to 28.6° (13.6°-53.7°) and 24.9° (2.0°-50.6°) of torsion shear, respectively. Torsion shear of the ICA at the stented side was subsequently 18.1° (12.7°-40.5°) and 15.2° (2.9°-69.4°). At the contralateral side, the values were not significantly different compared to the stented side: CCA: 34.3° (20.4°-82.5°, p=0.46) and 26.9° (14.3°-38.1°,p=0.60) and ICA: 15.4° (13.6°-53.7°,p=0.35) and 28.6° (5.2°-65.4°,p=0.46) (Table 3). Of all torsion shear data, the mean difference between both observers was 0.82°$\pm$5.25°.

Angulation	**Head position**				
Stent junction	Neutral	Bent Forward	Bent Backward	Turned Left	Turned Right
Distal	34.3° (32.3-55.6)	47.6° * (42.6-85.2)	26.5° * (25.0-48.7)	34.8° (30.7-59.5)	34.7° (32.6-55.4)
Proximal	24.1° (15.9-32.3)	23.5° (16.4-40.2)	24.8° (16.1-30.9)	27.5° * (16.9-38.2)	21.5° (13.0-32.9)

Table 2 Results of angulation at the proximal and distal stent junctions.
Values are expressed as median (range). * P < 0.05 versus neutral head position.

Torsion shear		Head position	
		Turned Left	Turned Right
Stented side	ICA	18.1° (12.7-40.5)	15.2° (2.9-69.4)
	CCA	28.6° (13.6-53.7)	24.9° (2.0-50.6)
Contralateral side	ICA	15.4° (13.6-53.7)	28.6° (5.2-65.4)
	CCA	34.3° (20.4-82.5)	26.9° (14.3-38.1)

Table 3 Torsion shear results. Values are expressed as median (range). ICA: internal carotid artery, CCA: common carotid artery.

DISCUSSION

Percutaneous carotid balloon angioplasty with stent placement has been branded as potentially safer, less traumatic, and more cost-effective than carotid endarterectomy. It is applicable in high-risk patients and is not limited to the cervical carotid artery.[7-9] However, broad variations in success and complication rates have been reported.[1,10-13] Despite promising early results, long-term performances may theoretically be hampered by the mobile features of the carotid artery. Stent failure in arteries that are subject to repetitive motion has been broadly described. van Lankeren et al. observed stent remodelling leading to early onset neointimal hyperplasia and continued plaque and thrombus formation in mobile arteries of the knee region.[14] Edelman and Rogers postulated that dynamic arteries oppose the strain caused by the stent struts through increased collagen deposition, marked destruction of elastin, and persistent inflammation.[15] Moreover, stent implantation has been shown to cause changes in 3D vessel geometry in such a way that regions with decreased and increased shear stress may occur close to the stent edges.[16] Alterations in shear stress, in turn, have been commonly implicated in recurrent plaque and thrombus formation.[17,18] Even the occurrence of stent fracture has been described in an otherwise flexible artery as the superficial femoral artery.[19]
Our results show major changes in 3D carotid artery geometry, especially at the distal junction site in bent forward and bent backward head positions. In this study, the flexible properties of the stents were demonstrated to be absent following deployment in the carotid artery. Despite the manufactures' claims that nitinol stents are more flexible and conformable than the commonly used Wallstent, the stented segment of the artery appears as a stiff, inflexible unit in all head positions. This leaves the unstented segments to accommodate head movements by increased flexion and torsion, inevitably leading to friction at both ends of the stent. For example, the sharply angled carotid artery shown in Figure 1 represents the fairly

common position of a patient asleep in a chair with the head bent forward. In comparison, the carotid artery of the opposite side showed a diffuse shape change throughout the complete artery, causing a far more subtle change in 3D geometry. Furthermore, our results showed the carotid artery to be subject to considerable torsion shear with turning of the head. Most currently used carotid stents have negligible ability to accommodate torsion shear, so the unstented parts of the artery must respond to all torsion shear movements, which is likely to cause friction at the stent limits. For example, by turning the head 46.9° to the left, we measured 18.1° of torsion shear in the ICA, normally executed by the entire length of the ICA.

MR imaging is noninvasive and provides high-resolution images of the carotid artery without use of ionizing radiation or nephrotoxic contrast media. In our institution, extensive experience has been obtained with various MR techniques, which have proven to be excellent tools to measure motion of the heart and great vessels.[20-23] MR imaging can provide morphologic information about caliber and course of the arteries, as well as functional information about velocity and flow.[24-26] Possible limitations of MR techniques are the artifacts produced by the endovascular implants in the magnetic field. Previously published studies showed that the image quality around and within the stents is very much dependent on the magnetic properties of the stent material and the imaging sequence used.[27-29] In this study, the 3D MIP in combination with the high-resolution transverse plane images showed sufficient data to objectify major angulation changes and torsion shear of the carotid artery, including the stented segment and its junction sites (Fig. 1).

Based on these findings, CAS might be reserved for selected series of patients who have a limited life expectancy or are poor candidates for carotid endarterectomy because of previous neck surgery or radiation therapy. Our results might strengthen the theoretical rationale for drug-eluting stents in future practice to overcome the hyperplastic reaction to the frictional forces described.[30] With regard to follow-up examinations, attention should be given to the distal ICA at the level of the distal stent junction, as this location might be prone to restenosis after CAS.

In conclusion, the carotid artery is a highly mobile artery; by stenting a major part of the vessel, its flexibility and rotational capacities are lost, leading to sharp angles at the end of the stent that are aggravated by head movement as well as rotational friction. Based on this study and the similarity to observations following stent placement in the mobile arteries of the lower extremity, we speculate that the highly mobile features of the carotid artery may well hamper long-term results of CAS. Effort should be put into development of carotid stents with in vivo flexibility and torsion capacities.

Appendix

Technical Specifications of MRI Studies:

Coils:	circularly polarized (CP) neck array, CP head array, CP spine array.
Pulse sequence:	3D time of flight angiography (3D-TOF) Fast Low Angle Shot (FLASH) acquisition.
Specifications:	
3D slabs:	3 slabs in a transverse plane; a tracking saturation band (gap 10 mm, thickness 40 mm) was applied at the cranial side, in order to suppress venous blood.
Tilted Optimized Nonsaturating Excitation (TONE) pulse:	In 3D-TOF angiography, a TONE radiofrequency (RF) pulse was applied using a ramped RF pulse. A 1-3 ramped RF pulse was selected, which was empirically determined in volunteers to be the optimal pulse in our conditions.
Distance factor:	-36.54%, the 3 slabs are partially overlapping.
Gap:	-26.6 mm.
Phase encoding direction:	R>>L.
Slice oversampling:	8%.
Slice thickness:	1.4 mm.
Number of slices per slab:	52.
Pixel size:	field of view in read direction: 200 mm. in phase encoding direction: 175 mm.
Matrix:	168x256 pixels.
Voxel:	1 x 0.8 x 1.4 mm.
Slice resolution:	64%.
Phase partial Fourier:	6/8.
Slice partial Fourier:	6/8.
Repetition time:	25 ms.
Echo time:	6.90 ms.
Bandwidth:	81 Hz/pixel.
Flip angle:	25°.

REFERENCES

1. Brown MM, Rogers J, Bland JM, CAVATAS investigators. Endovascular versus surgical treatment in patients with carotid stenosis in the Carotid and Vertebral Artery Transluminal Angioplasty study (CAVATAS): a randomised trial. *Lancet.* 2001;357:1729-1737.

2. Criado FJ, Lingelbach JM, Ledesma DF, Lucas PR. Carotid artery stenting in a vascular surgery practice. *J Vasc Surg.* 2002;35:430-434.

3. Leger AR, Neale M, Harris JP. Poor durability of carotid angioplasty and stenting for treatment of recurrent artery stenosis after carotid endarterectomy: an institutional experience. *J Vasc Surg.* 2001;33:1008-1014.

4. Cikrit DF, Dalsing MC. Lower-extremity arterial endovascular stenting. *Surg Clin North Am.* 1998;78:617-629.

5. Powell RJ, Fillinger M, Bettmann M, Jeffery R, et al. The durability of endovascular treatment of multisegment iliac occlusive disease. *J Vasc Surg.* 2000;31:1178-1184.

6. Ramaswami G, Marin ML. Stent grafts in occlusive arterial disease. *Surg Clin North Am.* 1999;79:597-609.

7. Diethrich EB, Gordon MH, Lopez-Galarza LA, Rodriguez-Lopez JA, et al. Intraluminal Palmaz stent implantation for treatment of recurrent carotid artery occlusive disease: a plan for the future. *J Interv Cardiol.* 1995;8:213-218.

8. Phatouros CC, Higashida RT, Malek AM, Meyers PM, et al. Carotid artery stent placement for atherosclerotic disease: rationale, technique, and current status. *Radiology.* 2000;217:26-41.

9. Veith FJ, Amor M, Ohki T, Beebe HG, et al. Current status of carotid bifurcation angioplasty and stenting based on a consensus of opinion leaders. *J Vasc Surg.* 2001 ;33:S111-S116.

10. Biasi GM, Ferrari SA, Nicolaides AN, Mingazzini PM, et al. The ICAROS registry of carotid artery stenting. Imaging in Carotid Angioplasties and Risk of Stroke. *J Endovasc Ther.* 2001;8:46-52.

11. Diethrich EB, Ndiaye M, Reid DB. Stenting in the carotid artery: initial experience in 110 patients. *J Endovasc Surg.* 1996;3:42-62.

12. Mathur A, Roubin GS, Gomez CR, Iyer SS, et al. Elective carotid artery stenting in the presence of contralateral occlusion. *Am J Cardiol.* 1998;81:1315-1317.

13. Theron JG, Payelle GG, Coskun O, Huet HF, et al. Carotid artery stenosis: treatment with protected balloon angioplasty and stent placement. *Radiology.* 1996;201:627-636.

14. van Lankeren W, Gussenhoven EJ, van Kints MJ, van der Lugt A, et al. Stent remodeling contributes to femoropopliteal artery restenosis: an intravascular ultrasound study. *J Vasc Surg.* 1997;25:753-756.

15. Edelman ER, Rogers C. Pathobiologic responses to stenting. *Am J Cardiol.* 1998;81:4E-6E.

16. Wentzel JJ, Whelan DM, van der Giessen WJ, van Beusekom HM, et al. Coronary stent implantation changes 3-D vessel geometry and 3-D shear stress distribution. *J Biomech.* 2000;33:1287-1295.

17. Ku DN, Giddens DP, Zarins CK, Glagov S. Pulsatile flow and atherosclerosis in the human carotid bifurcation. Positive correlation between plaque location and low oscillating shear stress. *Arteriosclerosis.* 1985;5:293-302.

18. Samijo SK, Willigers JM, Barkhuysen R, Kitslaar PJ, et al. Wall shear stress in the human common carotid artery as function of age and gender. *Cardiovasc Res.* 1998;39:515-522.

19. Duda SH, Pusich B, Richter G, Landwehr P, et al. Sirolimus-eluting stents for the treatment of obstructive superficial femoral artery disease: six-month results. *Circulation.* 2002;106:1505-1509.

20. Marcus JT, Vonk Noordegraaf A, De Vries PMJM, Van Rossum AC, et al. MRI evaluation of right ventricular pressure overload in chronic obstructive pulmonary disease. *J Magn Res Im.* 1998;8:999-1005.

21. Marcus JT, Goette MJW, DeWaal LK, Stam MR, et al. The influence of through-plane motion on left ventricular volumes measured by Magnetic Resonance Imaging: Implications for Image acquisition and analysis. *J Cardiov Magn Res.* 1999;1:1-6.

22. Mattle HP, Kent KC, Edelman RR, Atkinson DJ, et al. Evaluation of the extracranial carotid arteries: correlation of magnetic resonance angiography, duplex ultrasonography, and conventional angiography. *J Vasc Surg.* 1991;13:838-844.

23. Vos AW, Wisselink W, Marcus JT, Manoliu RA, et al. Aortic Aneurysm Pulsatile Wall Motion Imaged by Cine MRI: a Tool to Evaluate Efficacy of Endovascular Aneurysm Repair? *Eur J Vasc Endovasc Surg.* 2001;23:158-161.

24. Botnar R, Rappitsch G, Scheidegger MB, Liepsch D, et al. Hemodynamics in the carotid artery bifurcation: a comparison between numerical simulations and in vitro MRI measurements. *J Biomech.* 2000;33:137-144.

25. Milner JS, Moore JA, Rutt BK, Steinman DA. Hemodynamics of human carotid artery bifurcations: computational studies with models reconstructed from magnetic resonance imaging of normal subjects. *J Vasc Surg.* 1998;28:143-156.

26. Stokholm R, Oyre S, Ringgaard S, Flaagoy H, et al. Determination of wall shear rate in the human carotid artery by magnetic resonance techniques. *Eur J Vasc Endovasc Surg.* 2000;20:427-433.

27. Bartels LW, Smits HF, Bakker CJ, Viergever MA. MR imaging of vascular stents: effects of susceptibility, flow, and radiofrequency eddy currents. *J Vasc Interv Radiol.* 2001;12:365-371.

28. Juergens KU, Tombach B, Reimer P, Vestring T, et al. Three-dimensional contrast-enhanced MR angiography of endovascular covered stents in patients with peripheral arterial occlusive disease. *AJR Am J Roentgenol.* 2001;176:1299-1303.

29. Merkle EM, Klein S, Wisianowsky C, Boll DT, et al. Magnetic resonance imaging versus multislice computed tomography of thoracic aortic endografts. *J Endovasc Ther.* 2002;9 Suppl 2:II2-13.

30. Fattori R, Piva T. Drug-eluting stents in vascular intervention. *Lancet.* 2003;361:247-249.

4

Jan Albert Vos
A.W. Floris Vos
Matteus A. M. Linsen
J. Tim Marcus
Timotheus Th. C. Overtoom
Jos C. van den Berg
Willem Wisselink

Impact of Head Movements on Morphology and Flow in the Internal Carotid Artery after Carotid Angioplasty and Stenting vs Endarterectomy

Journal of Endovascular Therapy 2003;10:862-869

INTRODUCTION

Several large controlled trials have proven carotid endarterectomy (CEA) to be superior to medical treatment alone for symptomatic stenoses of the carotid bifurcation.[1-3] More recently, an alternative treatment has emerged that has obviated the need for instrumentation of the neck, namely, carotid angioplasty and stenting (CAS).[4-7] This treatment was initially used mainly in patients with an increased surgical risk. Initial results appeared promising, and the popularity of CAS has increased substantially over the last few years; currently, CAS is more often being advocated as an alternative to CEA. Several controlled trials comparing CAS with CEA are currently being conducted.[8-10] However, long-term results of CAS are still sparse, and several issues regarding the inherent differences between treatment modalities have not been elucidated. One of these is the increased stiffness of the internal carotid artery (ICA) resulting from the introduction of a stent as compared with the situation after CEA.[11-13] The carotid bifurcation is located in a highly mobile part of the human anatomy, and after the introduction of a stent, it is only partially able to accommodate the changes in geometry that result from physiologic movements of the head, which may lead to kinking at the distal end of the stent.[14] Although the clinical importance of carotid artery kinking remains controversial, significant flow changes during head movements have been found to be associated with ICA kinking.[15] Magnetic resonance (MR) phase-contrast flow quantification is a non-invasive technique that can measure the blood flow in separate arteries.[16,17] It can be used to evaluate the volumetric flow rate (VFR) in the ICA distal to the stented or surgically treated segment. Furthermore, in the same session, MR angiography (MRA) can depict the anatomy of the ICA in the same head position, thus allowing assessment of the correlation between its geometry and the VFR. The aim of this study was to use MRA and MR flow quantification to assess whether different head positions affect ICA geometry and flow in patients after CAS and CEA.

METHODS

Study design and study population

Six patients treated with CEA and six treated with CAS between January 2002 and September 2003 were asked to participate in this study. Only CAS patients treated

with nonferromagnetic self-expandable stents were eligible. Patients treated with stainless-steel stents were excluded because the inherent properties of these stents may produce artifacts on MR imaging and MR flow measurements. Patients with significant preprocedural carotid elongation were also excluded in both groups, because this might influence the results of this study. All patients had been treated for symptomatic stenoses at the carotid bifurcation of more than 70% according to the North American Symptomatic Carotid End-arterectomy Trial criteria. There were four men and two women in the CAS group; three were treated on the left and three on the right carotid bifurcation. The median age of this group was 70 years (interquartile range [IQR], 67-71 years). Four patients were treated with a Precise stent (Cordis J&J, Minneapolis, Minn; 7x20 mm, n=2; 8x20 mm, n=1; 8x30 mm, n=1), one with a 7x30-mm Carotid SE stent (Medtronic, Minneapolis, Minn), and one with a 6 to 8x40-mm Acculink stent (Guidant, Indianapolis, Ind). This last stent was placed across the carotid bifurcation; all others were placed in the ICA only. The CEA group consisted of five men and one woman (median age, 67 years; IQR, 63-72 years). Four patients were treated on the right and two on the left side. In all cases, a patch was used: two with autologous venous material and four with Dacron grafts (DuPont, Wilmington, Del). After a median interval of 7 months (IQR, 5-8 months) in CAS patients and 8 months (IQR, 7-8 months) in CEA patients, MR imaging and MR flow measurements were performed. The study was approved by the institutional human research committees, and prior written informed consent was obtained from all subjects.

Imaging

All MR investigations were performed with a 1.5-T MR whole-body system (Sonata; Siemens Medical Solutions, Erlangen, Germany). A circularly polarized head array coil, a circularly polarized neck array coil, and a spine coil were simultaneously used. First, a three-dimensional time-of-flight (3D-TOF) MRA was performed. Sagittal and coronal maximum-intensity projections were then calculated. By using both of these maximum-intensity projections, the image plane for flow quantification was adjusted orthogonally to the treated ICA 1 cm downstream from the distal stent edge in CAS patients. In CEA patients, the plane was positioned 4 cm downstream from the carotid bifurcation. Subsequently, an MR flow measurement was performed. The specifications of the MRA and MR flow quantification sequence used are summarized in Appendices I and II, respectively. Both sequences were performed in five different head positions: neutral, bent forward, bent backward, turned toward

the treated side (ipsilateral), and turned away from the treated side (contralateral). Neutral was always used as the starting position, but the subsequent order of positions was randomized. Patients were asked to place their heads in the forward, backward, ipsilateral, and contralateral positions in the maximum possible way. Head positions were defined by measuring the angle between bony structures of the head and the thorax for the forward and backward positions. For measurement of the ipsilateral and contralateral positions, the angle between the midsagittal plane of the head was compared with the anteroposterior axis. The neutral position was considered to be 0° in both the transverse and the sagittal plane. All angulation measurements were performed on a RadWorks 5.1 diagnostic radiology workstation (IBM Corp, White Plains, NY). Flow measurements were performed on a Sun Sparcstation (Sun Micosystems, Mountain View, Calif) by using the software package FLOW (Medis, Leiden, The Netherlands). The cross section of the ICA was delineated by drawing contours on the magnitude images through the cardiac cycle (Fig. 1). Then, from the velocity and the cross-sectional area, the volumetric flow (milliliters per second) was derived. Subsequently, integrating flow over the cardiac cycle yielded the stroke volume in milliliters per heart beat, which was equal to the area under curve (Fig. 2). Finally, multiplying the volumetric flow per heart beat with the heart rate yielded the VFR in milliliters per minute.

Statistical analysis

In each individual, neutral was considered to be the standard for both ICA angulation and BFV. In all head positions other than neutral, the angulation and BFV were compared with neutral, and the difference was recorded. This then excluded baseline data and allowed comparison between groups of the effect of the head movements. Data that were not normally distributed are presented with median and IQR. For this type of data, differences between groups were tested by using the Mann-Whitney *U* test. $P<.05$ was regarded as statistically significant. Statistical analyses were performed with SPSS 11.5/2002 (SPSS Inc, Chicago, Ill).

RESULTS

The median degree of forward angulation of the head was 15.8° in CAS patients and 18.9° in CEA patients. The median backward angulations were 19.1° and 20.0°, respectively. The median ipsilateral rotation of the head was 46.9° in CAS patients

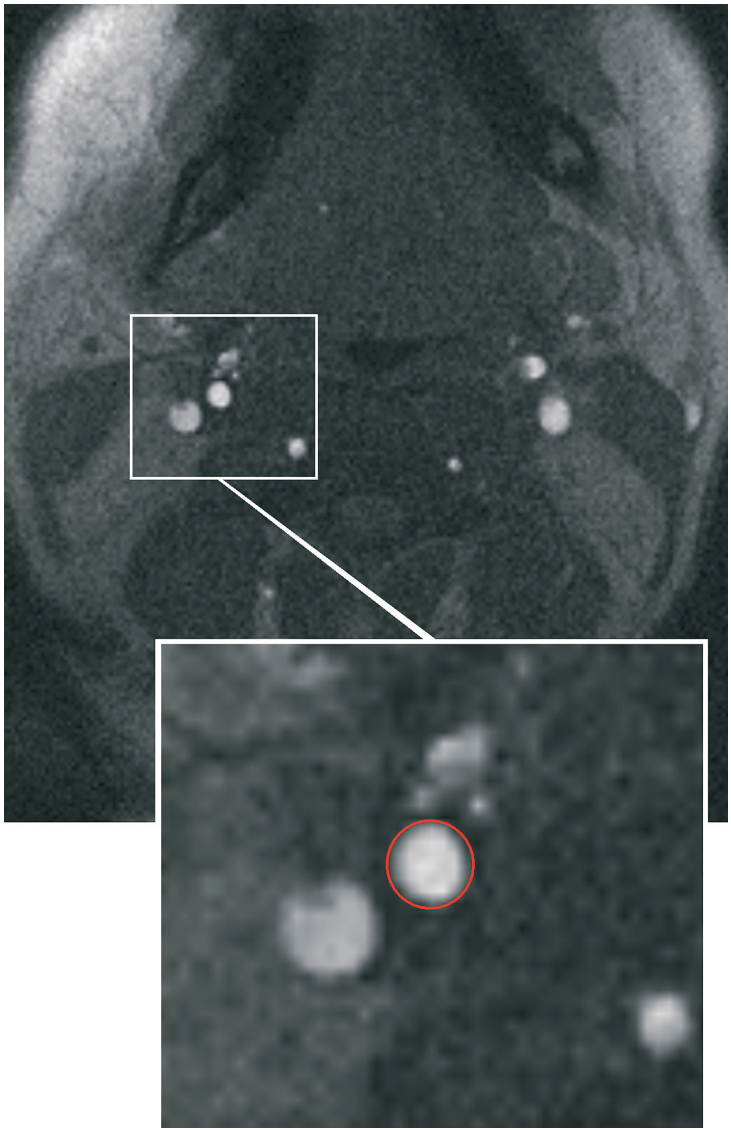

Figure 1 A magnitude image of the MR flow measurement in a patient after stent placement in the right internal carotid artery. The cross section of the internal carotid artery was delineated by drawing contours on the magnitude images through the cardiac cycle.

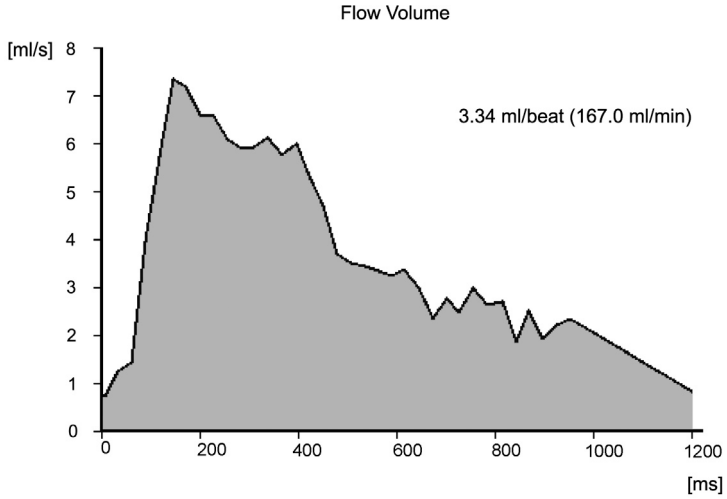

Figure 2 Example of flow curve across the cardiac cycle. The area under the curve (Gray) represents the total cerebropetal volumetric flow through this internal carotid artery during one cardiac cycle.

CAS	N		F		B		I		C	
	Head (°)	ICA (°)	Head (°)	ICA Δ to N (°)	Head (°)	ICA Δ to N (°)	Head (°)	ICA Δ to N (°)	Head (°)	ICA Δ to N (°)
1	0	12	16.5	20.1	-20.6	-2.8	35.7	-1.7	51.4	3.0
2	0	63.9	10.6	11.2	-14.2	-1.4	46.3	-1.4	39	6.0
3	0	77.9	27.1	6.7	-17.7	-9.3	54	-3.7	59.2	-1.7
4	0	3.9	14	9.1	-18.4	-3.7	42.1	-0.5	38.9	13.4
5	0	24.6	15	2.1	-23	-3.9	47.4	4.2	45.5	0.9
6	0	37.4	18.7	47.3	-21.8	-11.9	56.3	11.9	47.8	-11.6
Median (IQR)				10.2 (7.3 to 17.9)		-3.7 (-3.9 to -2.8)		-1.4 (-1.7 to-0.5)		3.0 (0.9 to 6.0)

Table I Head position and corresponding change in angulation of the internal carotid artery (ICA) in five different head positions (CAS patients). *CAS,* Carotid angioplasty and stenting; *N,* neutral; *F,* forward; *B,* backward; *I,* ipsilateral; *C,* contralateral; *Δ to N,* difference in ICA angulation compared with neutral; *IQR,* interquartile range.

CEA	N		F		B		I		C	
	Head (°)	ICA (°)	Head (°)	ICA Δ to N (°)	Head (°)	ICA Δ to N (°)	Head (°)	ICA Δ to N (°)	Head (°)	ICA Δ to N (°)
1	0	36.3	15.2	0	-12.7	-16.3	42.8	12.5	55.7	0
2	0	5.5	24.4	0.4	-12.5	-0.8	44.6	1.6	54.0	-0.5
3	0	50.3	13.5	-2.0	-20	-7.3	51.9	-1	61.6	-1.5
4	0	15.9	34.4	7.8	-33.7	1.3	52	3.5	46.3	1.1
5	0	52.2	14	-1.3	-22.7	-11.6	59.8	-9.6	55.1	-3.6
6	0	12	15.1	3.1	-17.7	1.9	38.7	3.4	33.8	-0.3
Median (IQR)				0.2 (-1.0 to 2.4)		-4.1 (-10.5 to 0.8)		2.5 (-0.4 to 3.5)		-0.4 (-1.3 to -0.1)
P value compared with CAS				.016*		.7		.7		.4

Table II Head position and corresponding change in angulation of the internal carotid artery (ICA) in five different head positions (CEA patients). *CEA,* Carotid endarterectomy; *N,* neutral; *F,* forward; *B,* backward; *I,* ipsilateral; *C,* contralateral; *Δ to N,* difference in ICA angulation compared with neutral;*IQR,* interquartile range; CAS, carotid angioplasty and stenting.* Statistically significant.

and 48.3° in CEA patients. The median contralateral rotations were 46.7° and 54.6°, respectively. The degree of head movement and the concomitant angulation change of the ICA, as observed on the MRA images in individual subjects, are shown in Table I for CAS patients and in Table II for CEA patients. In CAS patients, the median increase of angulation at the distal stent end during forward motion of the head was 10.2° (IQR, 7.3°- 17.9°). In CEA patients, it was 0.2° (-1.0° to 2.4°), a difference that was statistically significant (P=.016; Fig. 3). In all other head positions, there was no statistically significant difference between groups in angulation change. The corresponding VFR data are presented in Tables III and IV for CAS and CEA patients, respectively. There was no statistically significant difference between groups in VFR change in any of the head positions tested. The case with the most profound kinking of the ICA (forward position in CAS case 6), in which the angulation of the ICA increased from 37.4° to 84.7°, showed an increase rather than a decrease of VFR in the ipsilateral ICA.

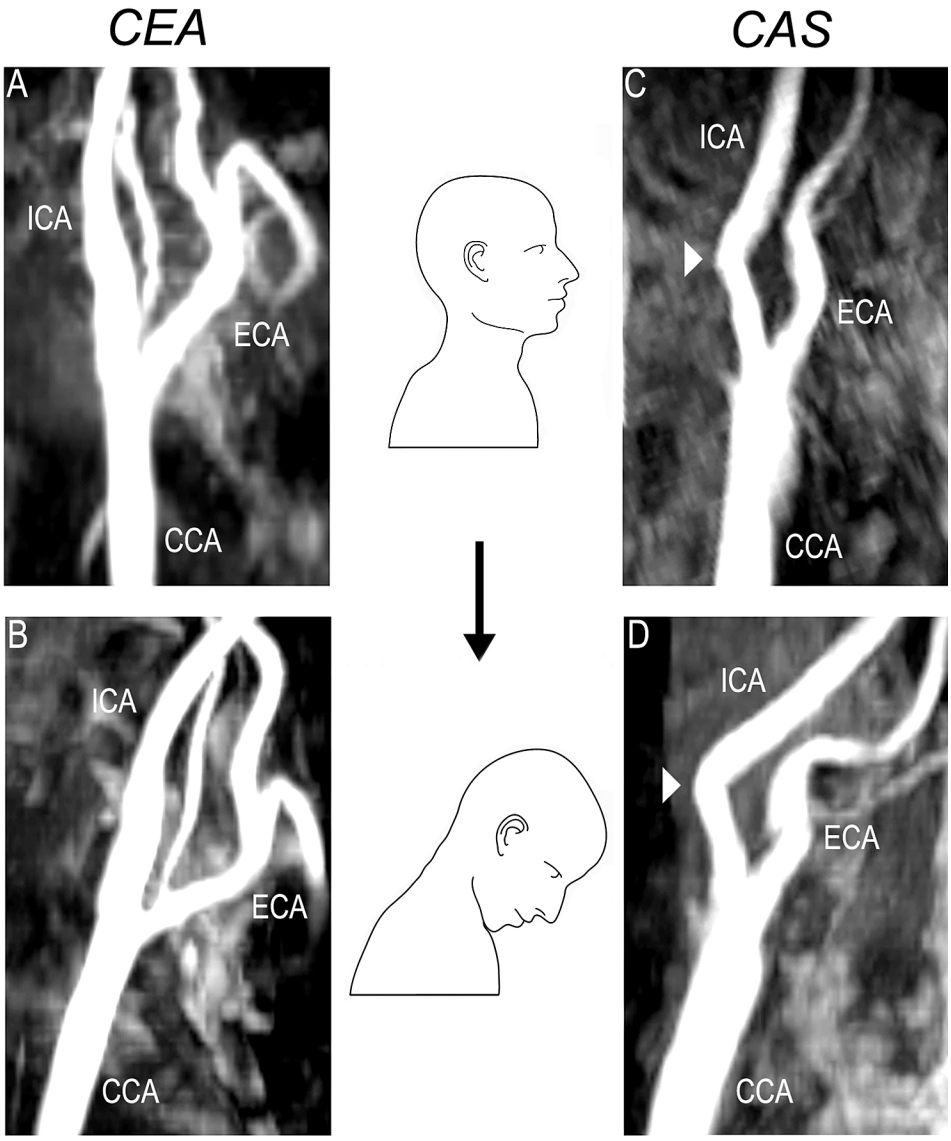

Figure 3 Maximum-intensity projection images of a patient after CEA with a dilatation patch *(left)* and a patient after CAS *(right)* in the neutral and forward head positions. Images show the carotid artery from the same viewpoint. In the CAS patient, the stent is situated in the ICA, and the distal stent junction is marked *(arrowhead)*. Note the increase in angulation at the distal stent junction when the head is bent forward. The ICA shows a much more global curvature in the CEA patient. In both patients, there was a mild increase rather than a decrease of volumetric flow rate in the ipsilateral ICA in the forward position. *CEA,* Carotid endarterectomy; *CAS,* carotid angioplasty and stenting; *ICA,*internal carotid artery, *CCA,* common carotid artery; *ECA,* external carotid artery.

Patient	N VFR (mL/min)	F		B
		VFR (mL/min)	Δ to N (mL/min)	VFR (mL/min)
1	279	292	13	267
2	260	237	-23	241
3	216	193	-23	219
4	196	236	40	229
5	286	285	-1	265
6	396	509	113	425
Median (IQR)	270 (245 to 284)	261 (236 to 290)	6 (-18 to 33)	253 (232 to 267)

Table III Volumetric flow rate (VFR) in the internal carotid artery distal to the treated segment (CAS patients) *CAS,* Carotid angioplasty and stenting; *N,* neutral; *F,* forward;

Patient	N VFR (mL/min)	F		B
		VFR (mL/min)	Δ to N (mL/min)	VFR (mL/min)
1	167	167	0	156
2	380	321	-59	331
3	178	197	19	185
4	181	171	-10	166
5	234	266	34	254
6	202	272	70	224
Median (IQR)	192 (177 to 226)	232 (178 to 271)	10 (-8 to 30)	205 (171 to 247)
P value compared with CAS			1	

Table IV Volumetric flow rate (VFR) in the internal carotid artery distal to the treated segment (CEA patients) *CEA,* Carotid endarterectomy; *N,* neutral; *F,* forward; *B,*

DISCUSSION

The fact that head movements can cause changes in carotid blood flow in healthy subjects is well known and was described as early as 1964.[18] These changes may be aggravated by the increased kinking of the ICA that is observed in some patients after CAS and might be the cause of cerebral hypoperfusion in these head positions. In this study, the increased stiffness of the ICA after CAS was confirmed as a potential cause of increased angulation at the distal stent end during forward bending

	I		C	
Δ to N (mL/min)	VFR (mL/min)	Δ to N (mL/min)	VFR (mL/min)	Δ to N (mL/min)
-12	287	8	325	46
-19	171	-89	208	-52
3	166	-50	303	87
33	238	42	247	51
-21	271	-15	268	-18
29	406	10	489	93
-5 (-17 to 23)	255 (188 to 283)	-4 (-41 to 10)	286 (252 to 320)	49 (-2 to 78)

B, backward; *I,* ipsilateral; *C,* contralateral; *Δ to N,* difference in VFR compared with neutral; *IQR,* interquartile range.

	I		C	
Δ to N (mL/min)	VFR (mL/min)	Δ to N (mL/min)	VFR (mL/min)	Δ to N (mL/min)
-9	161	-6	155	-12
-49	367	-13	340	-40
7	147	-31	139	-39
-15	204	23	184	3
20	230	-4	216	-18
22	197	-5	221	19
-1 (-14 to 17)	201 (170 to 224)	-6 (-11 to -4)	200 (162 to 220)	-15 (-34 to -1)
.9		.9		.2

backward; *I,* ipsilateral; *C,* contralateral; *Δ to N,* difference in VFR compared with neutral; *IQR,* interquartile range; *CAS,* carotid angioplasty and stenting.

of the head. This phenomenon was not observed in CEA patients, in whom there was a much more global curvature of the entire ICA as a result of changes in head position. Conceptually, this increased angulation in CAS patients might lead to a decrease in volumetric flow through the ICA during flexion of the neck, a head position that may very well occur physiologically in daily life, for instance, when a patient falls asleep while sitting in a chair. There was, however, no statistically significant decrease in VFR associated with increased angulation in our series. The wide range of normal cerebropetal BFV is reflected in the results, which show a

substantial variation between head positions and between subjects. As mentioned previously, the subject with the most profound increase in angulation at the distal stent edge showed an increase rather than a decrease of BFV in this head position. A significant reduction of BFV, which we had hypothesized might occur, was not found in any of our subjects. In a controlled study by Malek et al, patients with known internal carotid elongation were examined with transcranial Doppler imaging.[19] In the eight head positions tested in their series, no reduction of middle cerebral artery flow was found. Apparently, the ICA is able to conform to geometric changes in physiologic situations even in the presence of significant tortuosity. Berkefeld et al proposed a method of measuring the common carotid artery–ICA angle and the ICA offset before and after carotid stenting.[13] They found a significant reduction in both common carotid artery–ICA angulation and ICA offset after CAS, compared with baseline, in their patients. The measurements in their series were all performed in the neutral head position with the patient supine on the angiography table. Kinking at the distal stent end was observed in several cases, even in this neutral position, but not structurally evaluated.

Although no acute reduction in cerebropetal blood flow was found to be associated with the increased angulation of the ICA caused by neck flexion in our series, the repetitive changes in morphology may very well be associated with more chronic detrimental effects. The increased stiffness caused by the introduction of stents has previously been implicated as the cause of recurrent stenosis in arteries subject to physiological flexion.[20,21] The mechanism of this re-stenosis formation has been hypothesized to entail primarily the deposition of collagen as a reaction of the vessel to oppose the strain caused by the stent struts.[22] This same mechanism may very well lead to similar effects in the stented carotid artery. Angles at stent edges are instrumental in the velocity of overgrowth of endothelial cells to cover the stent struts.[23] Delayed overgrowth is associated with an increased risk of neointimal hyperplasia and re-stenosis.[24] Even fracturing of stents placed in highly mobile parts of the human anatomy has been reported.[25,26] So far, these reports have been confined to arteries of the extremities. No reports on fractured carotid stents have been published, but this may change, and the clinical consequences of this eventuality remain to be awaited. Our study was limited to patients treated with segmented nitinol stents. The most frequently used carotid stent to date, both in our series and worldwide, is the Wallstent (Boston Scientific, Natick, Mass), which is a stainless-steel stent with continuous filaments. This type of stent was not included in our current study on account of the artifacts it might induce on MR imaging. The geometry changes of this type of stent could conceivably be quite different from

our current findings. In an in vitro study by Tanaka et al, the conformity of five different types of self-expandable carotid stents was tested.[27] They found better wall apposition and less straitening and kinking of their carotid bifurcation model when segmented nitinol stents were used as compared with stents with continuous filaments. Even these segmented nitinol stents, however, showed considerable angulation in our in vivo study when the position of the head changed.

We used MR imaging and MR phase-contrast flow quantification to examine patients in our study. With these techniques, no ionizing radiation is used. Increasing evidence suggests that gadolinium-enhanced MRA may be superior to 3D-TOF MRA for the grading of carotid bifurcation stenoses. We nevertheless decided to use 3D-TOF because it was the morphology of the ICA that we were trying to depict, rather than a possible stenosis, and this method does not require the administration of intravenous contrast agents. For the flow quantification sequence, we used prospective cardiac triggering. This implies that flow was measured from the electrocardiogram R wave to late diastole. The end-diastolic phase coincides with the refractory period of the sequence when a new R wave of the electrocardiogram is awaited. This does not seem to influence the results of our study, because the same sequence was used in all head positions and in all patients, as suggested by Ho et al.[28] Furthermore, this part of the cardiac cycle plays only a minor role in the total cerebropetal blood flow. The choice of the location of the plane for BFV measurement may seem rather arbitrary. Four centimeters distal to the bifurcation and 1 cm distal to the stent both equate to roughly the same segment of the vessel. This segment did not contain significant tortuosity in any of the subjects tested, which allowed accurate measurement. Because volumetric flow was measured rather than velocity and because there are no side branches in this segment, a variation in location along this segment will not lead to a difference in flow.

In conclusion, this study confirmed significant increases in ICA angulation in patients treated with CAS if the head was bent forward; this was not observed in patients treated with CEA. Although this increased angulation did not lead to acute changes in cerebropetal bloodflow, it is possible that such angulation might result in chronic changes, such as re-stenosis. This, however, remains to be tested in future studies.

Appendix I

Parameters of three-dimensional time-of- flight magnetic resonance angiography

Variable	Setting
Distance factor:	-36.54% (3 partially overlapping slabs).
Gap:	-26.6 mm.
Phase-encoding direction:	Right to left.
Slice oversampling:	8%.
Slice thickness:	1.4 mm.
Number of slices per slab:	52.
Field of view in read:	200 mm.
Field of view in phase:	175 mm.
Matrix:	168x256 pixels.
Voxel:	1x0.8x1.4 mm.
Slice resolution:	64%.
Phase partial Fourier:	6/8.
Slice partial Fourier:	6/8.
Repetition time:	25 ms.
Echo time:	6.90 ms.
Receiver bandwidth:	81 Hz/pixel.
Flip angle:	25°.

For three-dimensional slabs, there were three slabs in a transverse plane; a tracking saturation band (gap, 10 mm; thickness, 40 mm) was applied cranially for venous signal suppression. For tilted optimized nonsaturating excitation (TONE) pulse, in three-dimensional time-of-flight, a TONE radiofrequency (RF) pulse was applied by using a ramped RF pulse. A 1-3 ramped RF pulse was selected, which was empirically determined in volunteers to be the optimal pulse in our setting.

Appendix II

Parameters of magnetic resonance flow quantification

Variable	Setting
Phase-encoding direction:	Anterior to posterior.
Field of view in read:	200 mm.
Field of view in phase:	81.3%.
Slice thickness:	6 mm.
Temporal resolution:	35 ms (echo-shared).
Echo time:	4.8 ms.
Flip angle:	25°.
In-plane resolution:	208x256 pixels, or 0.8x0.8 mm.
Triggering:	Prospectively triggered by the ECG R wave.
Velocity sensitivity:	120 cm/s in the through-plane direction.
Receiver bandwidth:	331 Hz/pixel.
Phase-encoding lines per beat:	3.

ECG, Electrocardiogram.

REFERENCES

1. Barnett HJ, Taylor DW, Eliasziw M, Fox AJ, et al. Benefit of carotid endarterectomy in patients with symptomatic moderate or severe stenosis. North American Symptomatic Carotid Endarterectomy Trial Collaborators. *N Engl J Med.* 1998;339:1415-25.

2. European Carotid Surgery Trialists' Collaborative Group. Randomised trial of endarterectomy for recently symptomatic carotid stenosis: final results of the MRC European Carotid Surgery Trial (ECST). *Lancet*. 1998;351:1379-87.

3. Executive Committee for the Asymptomatic Carotid Atherosclerosis Study. Endarterectomy for asymptomatic carotid artery stenosis. *JAMA*. 1995;273:1421-8.

4. Yadav JS, Roubin GS, Iyer S, Vitek J, et al. Elective stenting of the extracranial carotid arteries. *Circulation*. 1997;95:376-81.

5. Wholey MH, Wholey M, Bergeron P, Diethrich EB, et al. Current global status of carotid artery stent placement. *Cathet Cardiovasc Diagn*. 1998;44:1-6.

6. Henry M, Amor M, Masson I, Henry I, et al. Angioplasty and stenting of the extracranial carotid arteries. *J Endovasc Surg* 1998;5:293-304.

7. Diethrich EB, Ndiaye M, Reid DB. Stenting in the carotid artery: initial experience in 110 patients. *J Endovasc Surg.* 1996;28:397-403.

8. Hobson RW II. CREST (Carotid Revascularization Endarterectomy versus Stent Trial): background, design, and current status. *Semin Vasc Surg.* 2000;13:139-43.

9. Featherstone RL, Brown MM, Coward LJ. International carotid stenting study: protocol for a randomised clinical trial comparing carotid stenting with endarterectomy in symptomatic carotid artery stenosis. *Cerebrovasc Dis.* 2004;18:69-74.

10. Ringleb PA, Kunze A, Allenberg JR, Hennerici MG, et al. The Stent-Supported Percutaneous Angioplasty of the Carotid Artery vs. Endarterectomy Trial. *Cerebrovasc Dis*. 2004;18:66-8.

11. Lal BK, Hobson RW II, Goldstein J, Chakhtoura EY, et al. Carotid artery stenting: is there a need to revise ultrasound velocity criteria? *J Vasc Surg*. 2004;39:58-66.

12. Vernhet H, Jean B, Lust S, Laroche JP, et al. Wall mechanics of the stented extracranial carotid artery. *Stroke*. 2003;34: e222-4.

13. Berkefeld J, Martin JB, Theron JG, Zanella FE, et al. Stent impact on the geometry of the carotid bifurcation and the course of the internal carotid artery. *Neuroradiology*. 2002;44:67-76.

14. Vos AW, Linsen MA, Marcus JT, van den Berg JC, et al. Carotid artery dynamics during head movements: a reason for concern with regard to carotid stenting? *J Endovasc Ther*. 2003;10:862-9.

15. Stanton PE Jr, McClusky DA Jr, Lamis PA. Hemodynamic assessment and surgical correction of kinking of the internal carotid artery. *Surgery*. 1978;84:793-802.

16. Van Goethem JW, van den Hauwe L, Ozsarlak O, Parizel PM. Phasecontrast magnetic resonance angiography. *JBR-BTR*. 2003;86:340-4.

17. Langerak SE, Kunz P, Vliegen HW, Jukema JW, et al. MR flow mapping in coronary artery bypass grafts: a validation study with Doppler flow measurements. *Radiology.* 2002;222:127-35.

18. Roberts B, Hardesty WH, Holling HE, Reivich M, et al. Studies on extracranial blood flow. *Surgery*. 1964;56:826-33.

19. Malek AK, Hilgertner L, Szostek M. The effect of internal carotid artery elongation on intracranial blood flow. *Eur J Vasc Surg*. 1994;8:677-81.

20. van Lankeren W, Gussenhoven EJ, van Kints MJ, van der Lugt A, et al. Stent remodeling contributes to femoropopliteal artery restenosis: an intravascular ultrasound study. *J Vasc Surg*. 1997;25:753-6.

21. Andrews RT, Venbrux AC, Magee CA, Bova DA. Placement of a flexible endovascular stent across the femoral joint: an in vivo study in the swine model. *J Vasc Interv Radiol*. 1999;10:1219-28.

22. Edelman ER, Rogers C. Pathobiologic responses to stenting. *Am J Cardiol. 1998;81:4E-6E.*

23. Hamuro M, Palmaz JC, Sprague EA, Fuss C, et al. Influence of stent edge angle on endothelialization in an in vitro model. *J Vasc Interv Radiol*. 2001;12:607-11.

24. Doornekamp FN, Borst C, Post MJ. Endothelial cell recoverage and intimal hyperplasia after endothelium removal with or without smooth muscle cell necrosis in the rabbit carotid artery. *J Vasc Res*. 1996;33:146-55.

25. Duda SH, Pusich B, Richter G, Landwehr P, et al. Sirolimus-eluting stents for the treatment of obstructive superficial femoral artery disease: six-month results. *Circulation*. 2002;106:1505-9.

26. Babalik E, Gulbaran M, Gurmen T, Ozturk S. Fracture of popliteal artery stents. *Circ J*. 2003;67:643-5.

27. Tanaka N, Martin JB, Tokunaga K, Abe T, et al. Conformity of carotid stents with vascular anatomy: evaluation in carotid models. *AJNR Am J Neuroradiol*. 2004;25:604-7.

28. Ho SS, Chan YL, Yeung DK, Metreweli C. Blood flow volume quantification of cerebral ischemia: comparison of three noninvasive imaging techniques of carotid and vertebral arteries. *AJR Am J Roentgenol*. 2002;178:551-6.

5

A.W. Floris Vos
Matteus A.M. Linsen
Jeroen Diks
Jan A. Rauwerda
Willem Wisselink

Carotid Stent Mobility with Regard to Head Movements: In Vitro Analysis

Vascular 2004;12:369-373

INTRODUCTION

Carotid angioplasty stenting (CAS) is currently being widely embraced owing to the perceived advantages of a less invasive treatment for carotid artery occlusive disease. Several studies suggest that early complication rates are comparable to those of carotid endarterectomy.[1,2] However, 1-year restenosis rates up to 22%, although often asymptomatic, are reported.[1,3] The results of CAS in de novo lesions are encouraging because CAS for recurrent carotid artery occlusive disease after carotid endarterectomy seems partially responsible for the high incidence of restenosis.[4,5] Nevertheless, with long-term results becoming available, restenosis, even for CAS, in de novo lesions is increasing.[6] This ongoing process of restenosis might be inflicted by stent friction during motions of the carotid artery similar to widely implicated long-term stent failure of mobile lower extremity vessels such as the external iliac and popliteal arteries.[7–9] In a recently published study, we found average angulation changes of 21° after CAS during head movements, leading to sharp angulations up to 85° at stent-artery junctions, whereby the stented segment of the artery behaved as a stiff unit.[10] This leaves the unstented segments to accommodate head movements by increased flexion, inevitably leading to friction. The same study reported a considerable amount of torsion of common and internal carotid arteries (CCA, ICA) of 28.6° and 18.1°, respectively, while turning the head. We hypothesized that a stent design with high flexibility and low torsion, implying a low force to rotate the stent along its axis, might be favourable to avoid stress imparted to the stented and remaining unstented segments of the CCA and the ICA. The aims of this study were to compare the flexibility (or, conversely, stiffness) of commonly used carotid stents in the expanded bare state and after deployment in a porcine common carotid artery, as well as compare torsion of the stent designs within the range of motion of common head movements.

METHODS

Five stents commonly used for treating carotid artery stenosis were included in this study: Wallstent (Boston Scientific Corp., Natick, MA), Precise (Cordis Corp., Johnson & Johnson Company, Warren, NJ), Acculink (Guidant Corp., Indianapolis, IN), Carotid SE (Medtronic AVE, Santa Rosa, CA), and Protégé (EV3, Plymouth, MN). All stents are self-expandable nitinol stents, with the exception of the Wallstent, which is

made of elgiloy (an alloy of cobalt and chromium) and tantalum. All stents were 8 mm in unconstrained diameter and 40 mm in length. Each stent was deployed according to the manufacturer's directions. All stents were assessed for flexibility and torsion. For each stent type, two identical stents were tested, and measurements were made in triplicate. All measurements were carried out at a temperature of 37°C to ensure that the nitinol stents were within their optimal operating conditions.

Flexibility

Stents were bent up to an angulation of 25°, representing the average angulation change in the carotid artery during head movements using the three-point bend test method previously described by Ormiston and colleagues.[10,11] In our study, we adjusted the setup by applying a more diffuse physiologic traction using an element with a convex surface instead of the ''hook'' representing the third point in the Ormiston and colleagues model (Fig. 1). The bending load (BL) in grams required to flex each stent to 25° was determined. Increased BL implies decreased flexibility. Healthy CCAs were harvested from 10 pigs that were used for another study (median weight 90 kg, range 88–95 kg; median age 6 months); the tests were performed within 2 hours after obtaining the arteries. The artery itself was cut into a standardized length of 100 mm and was placed into the testing device. The internal diameters of the arteries were 7 mm (range 6–7.5 mm). A 0.9% saline drip with a pressure-bag was used to simulate an in vivo blood pressure of 80 mm Hg. First, flexibility of the carotid artery itself was evaluated to avoid variances between the carotid arteries, interfering with our results. Subsequently, in each

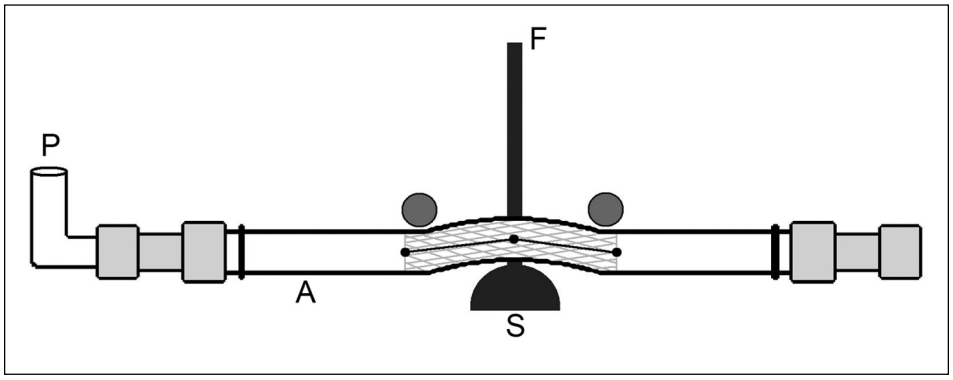

Figure 1 The modified three-point bend test for measuring stent flexibility. Force (F) is applied to an element with a convex surface (S), resulting in a 25° angulation of the stent. The artery (A) was placed into the testing device, and a 0.9% saline drip with a pressure-bag (P) was used to simulate an in vivo blood pressure of 80 mm Hg.

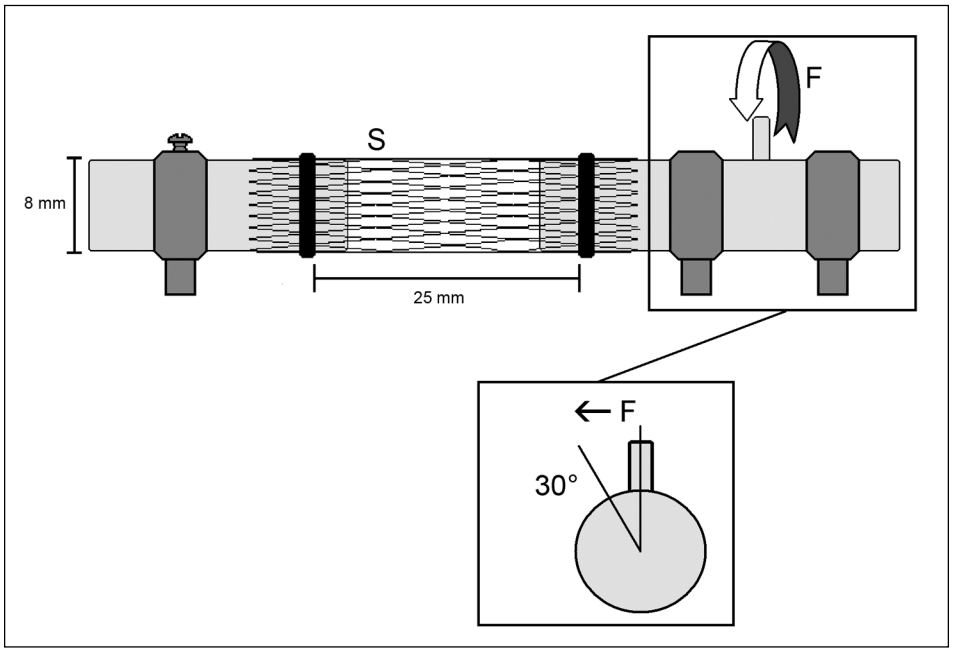

Figure 2 The testing device for measuring torsion. Force (F) is applied to rotate the stent (S) 30° along its axis.

carotid artery, one stent was deployed by the same investigator. Flexibility measurements were performed at the center of the stent. Thereafter, the artery was sacrificed; the expanded stent was placed in the testing device, and flexibility measurements of the bare stents were done.

Torsion

Bare expanded stents were placed into a testing device constructed for torsion measurements (Fig. 2). The stent was fixated at two points, 25 mm apart. The rotation load (RL) in grams required to rotate the stent 30° was measured. Increased RL implies increased torsion.

In both tests, an unster was used with an accuracy of $\pm$ 2 g of the absolute value and a range of 0 to 100 g. Calibration was performed using standard weights (2, 10, 20, 50, 75, and 100 g; Netherlands Calibration Organization /International Standards Organization certified).

Statistical Analysis

The results were expressed as the median (range) of the triplicate measurements of the two identical stents. To analyze differences in the flexibility of the carotid arteries, we compared the repetitive measurements of the carotid arteries by means of analysis of variance (ANOVA), with the individual carotid arteries as the between factor and the repetitions as the within factor. The differences between the several types of bare stents and the stents after deployment in carotid arteries were evaluated using one-way ANOVA with the factor; type of stent with post hoc Bonferroni tests. Statistical analyses were performed with SPSS, version 11.0 (SPSS, Chicago, IL). A p value < .05 was considered significant.

RESULTS

In the bare expanded state, the median BL was 6 g, with a wide spread varying from 4 g (range 1–5 g, Wallstent) to 20 g (range 18–22 g, Acculink), depending on the stent design. The BLs for the Acculink and Protégé stents were significantly higher (20 g and 14 g, respectively) in the bare state compared with the other stents ($p<.0001$). After deployment in the carotid artery, the overall BL increased to 38 g (range 20–41 g). The BL for the Carotid SE and Wallstent stents was significantly lower, 21 g (range 20–22 g; $p<.0001$) and 36 g (range 34–37 g; $p=.0016$)

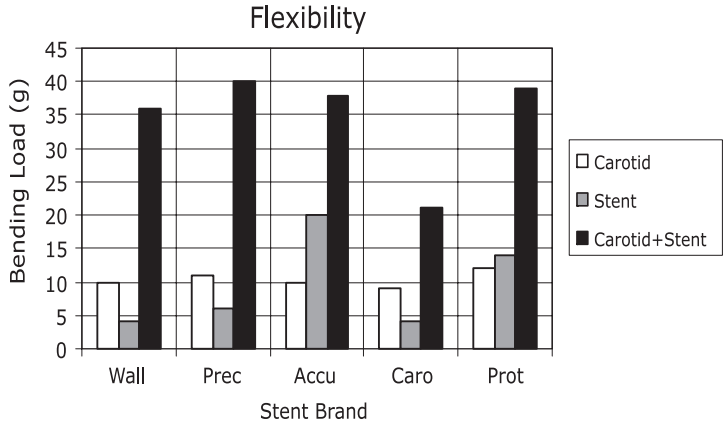

Figure 3 Comparison of flexibility of the carotid artery, the five bare expanded stent designs and subsequently flexibility of the stents while deployed in the carotid artery. Flexibility is expressed as bending load in grams required to produce 25° of flexion. Values are expressed as the median. Accu = Acculink; Caro = Carotid SE; Prec = Precise; Prot = Protégé; Wall = Wallstent.

compared with the other stents. The BLs of bare carotid stents were not significantly related to the BLs after deployment in the carotid arteries (p=.089). No significant difference was found between the flexibility of the carotid arteries itself in all five groups (p = .14). A summary of all of the bending tests is shown in Fig. 3.
With regard to the torsion tests, all stents were capable of rotating along their axis, 11 g (range 1–76 g), although a significantly increased RL was applied on the Wallstent, 73 g (range 65–76 g), and the Precise, 20 g (range 19–22 g), to achieve a rotation of 30° (p<.0001) (Fig. 4). None of the stents showed signs of deforming or collapse during the flexibility or torsion test.

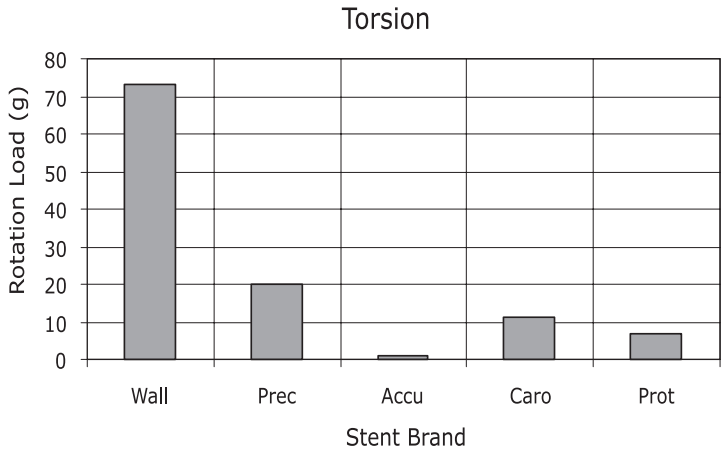

Figure 4 Comparison of torsion of the five stent designs. Torsion is expressed as rotation load in grams required to rotate the stent 30° along its axis. Values are expressed as the median. Accu = Acculink; Caro = Carotid SE; Prec = Precise; Prot = Protégé; Wall = Wallstent.

DISCUSSION

In a previous magnetic resonance angiography study describing the mobility patterns of the carotid artery after CAS during head movements, we demonstrated a complete lack of flexibility of the stented segment, although the carotid artery itself was highly flexible.[10] Angulations at stent junctions aggravated by bending the head and increased torsion in the unstented segment of the ICA were observed after rotation of the head.[10] Angulations and increased torsion might cause reduced patency because disturbed flow shear rates and a decreased rate of endothelialization by irregularities at the junction between the stent surface and the inner lumen of

the vessel wall result in increased intimal formation.[12,13] The extent of intimal hyperplasia has been shown to correlate with the degree of injury by penetration of the stent struts into the layers of the vessel wall.[14] Obviously, when the stented segment is incapable of torsion, the stent implanted in healthy landing zones of the CCA and ICA might cause deep injury to the arterial wall by torsional motions. Repetitive angulation changes and friction during head movements will inevitably result in repeated injury by this mechanism. With regard to torsion, we emphasize the unique rotational capacities of the carotid arteries. The CCA and ICA are subjected to considerable torsion shear (approximately 28° and 16°) by rotation of the head during average head movements.[10] To avoid such an injury, comparable flexibility and torsion of the stented and unstented segments of the carotid artery might be the ideal option. Caution in this matter is required because experimental results conflict. Studies by Palmaz and Barth and colleagues stated that the parameter of flexibility might hamper the development of a thin neointima.[15,16] The pulsatile nature of a flexible stent may induce platelet sloughing, embolization, and reaccumulation, thus leading to an irregularly thick subsequent platelet substrate and, eventually, a thick neointima. Another study showed the contrary by comparing the same stent design with differing longitudinal flexibility in swine iliac arteries showing less neointimal buildup in the flexible stent after 5 weeks.[17] In the case of a mobile artery such as the carotid, some flexibility is, in our opinion, preferable because sharp angulations with disturbance of the luminal geometry and repetitive trauma at stent edges are to be avoided. Several studies have assessed the mechanical properties of bare expanded stents.[11,18,19] In those, the flexibility and torsion of bare stents were objectified, and excellent results were obtained. However, in our study, increased stiffness was observed after stents were deployed in carotid artery specimens irrespective of their excellent flexible capacities in the bare state. The potential advantages especially provided by the flexible Wallstent, Precise, and Protégé stents decreased after the stents were inserted into a carotid artery. These variations are inevitably related to the gauge (thickness of wire), type of wire, and surface area of the stent. A similar finding of decreased compliance and progressive stiffness is observed after deployment in canine iliac arteries.[20] A limitation of this bench-test study is the lack of comparability between the porcine and the human carotid artery, whereby, in the latter, flexibility and torsion are likely to be decreased owing to the presence of atherosclerotic plaque. However, as stent placement extends into both the proximal and distal undiseased parts of

the carotid artery, which represent the areas of maximal shear stress in our study, our findings are likely to bear some resemblance to the human situation.

In conclusion, despite the highly flexible capacities of currently used stents ex vivo, decreased flexibility is present after deployment in the porcine carotid artery. Moreover, some of the currently used stents displayed increased torsion compared with the other stents. Restrictions in flexibility and torsion might inevitably lead to frictional forces and repetitive trauma, especially at the stent-vessel junctions, potentially causing intimal hyperplasia, stent migration, and stent breakdown. Although the restenosis rates for CAS in de novo lesions are encouraging, stent interaction with the mobile carotid artery can result in disappointing restenosis rates in the long term. For now, use of short stents limited to the diseased vessel wall might be preferable. Effort should be directed toward development of carotid stents with high flexibility and low torsion in vivo.

REFERENCES

1. Brown MM, Rogers J, Bland JM, CAVATAS Investigators. Endovascular versus surgical treatment in patients with carotid stenosis in the Carotid and Vertebral Artery Transluminal Angioplasty study (CAVATAS): a randomised trial. *Lancet*. 2001;357:1729–37.

2. Criado FJ, Lingelbach JM, Ledesma DF, Lucas PR. Carotid artery stenting in a vascular surgery practice. *J Vasc Surg*. 2002;35:430–4.

3. Christiaans MH, Ernst JMPG, Suttorp MJ, van den Berg JC, et al. Restenosis after carotid angioplasty and stenting: a follow-up study with duplex ultrasonography. *Eur J Vasc Endovasc Surg*. 2003;26:141–4.

4. Leger AR, Neale M, Harris JP. Poor durability of carotid angioplasty and stenting for treatment of recurrent artery stenosis after carotid endarterectomy: an institutional experience. *J Vasc Surg*. 2001;33:1008–14.

5. Setacci C, Pula G, Baldi I, de Donato G, et al. Determinants of in-stent restenosis after carotid angioplasty: a case control study. *J Endovasc Ther*. 2003;10:1031–8.

6. Lal BK, Hobson RW II, Goldstein J, Geohagan M, et al. In-stent recurrent stenosis after carotid artery stenting: life table analysis and clinical relevance. *J Vasc Surg*. 2003;38:1162–8.

7. Cikrit DF, Dalsing MC. Lower-extremity arterial endovascular stenting. *Surg Clin North Am*. 1998;78:617–29.

8. Powell RJ, Fillinger M, Bettmann M, Jeffery R, et al. The durability of endovascular treatment of multisegment iliac occlusive disease. *J Vasc Surg*. 2000;31:1178–84.

9. Ramaswami G, Marin ML. Stent grafts in occlusive arterial disease. *Surg Clin North Am.* 1999;79:597–609.

10. Vos AW, Linsen MA, Marcus JT, van den Berg JC, et al. Carotid artery dynamics during head movements: a reason for concern with regard to carotid stenting? *J Endovasc Ther*. 2003;10:862–9.

11. Ormiston JA, Dixon SR, Webster MW, Ruygrok P, et al. Stent longitudinal flexibility: a comparison of 13 stent designs before and after balloon expansion. *Catheter Cardiovasc Interv*. 2000;50:120–4.

12. Carlier SG, van Damme LC, Blommerde CP, Wentzel JJ, et al. Augmentation of wall shear stress inhibits neointimal hyperplasia after stent implantation: inhibition through reduction of inflammation? *Circulation*. 2003;107:2741–6.

13. Hamuro M, Palmaz JC, Sprague EA, Fuss C, et al. Influence of stent edge angle on endothelialization in an in vitro model. *J Vasc Interv Radiol*. 2001;12:607–11.

14. Schwartz RS, Huber KC, Murphy JG, Edwards WD, et al. Restenosis and the proportional neointimal response to coronary artery injury: results in a porcine model. *J Am Coll Cardiol.* 1992;19: 267–74.

15. Palmaz JC. Intravascular stents: tissue-stent interactions and design considerations. *AJR Am J Roentgenol*. 1993;160:613–8.

16. Barth KH, Virmani R, Froelich J, Takeda T, et al. Paired comparison of vascular wall reactions to Palmaz stents, Strecker tantalum stents, and Wallstents in canine iliac and femoral arteries. *Circulation*. 1996;93:2161–9.

17. Fontaine AB, Spigos DG, Eaton G, Dospassos S, et al. Stent-induced intimal hyperplasia: are there fundamental differences between flexible and rigid stent designs? *J Vasc Interv Radiol.* 1994;5:739–44.

18. Duda SH, Wiskirchen J, Tepe G, Bitzer M, et al. Physical properties of endovascular stents: an experimental comparison. *J Vasc Interv Radiol*. 2000;11:645–54.

19. Dyet JF, Watts WG, Ettles DF, Nicholson AA. Mechanical properties of metallic stents: how do these properties influence the choice of stent for specific lesions? *Cardiovasc Interv Radiol*. 2000;23:47–54.

20. Back M. Changes in arterial wall compliance after endovascular stenting. *J Vasc Surg.* 1994;19:905–11.

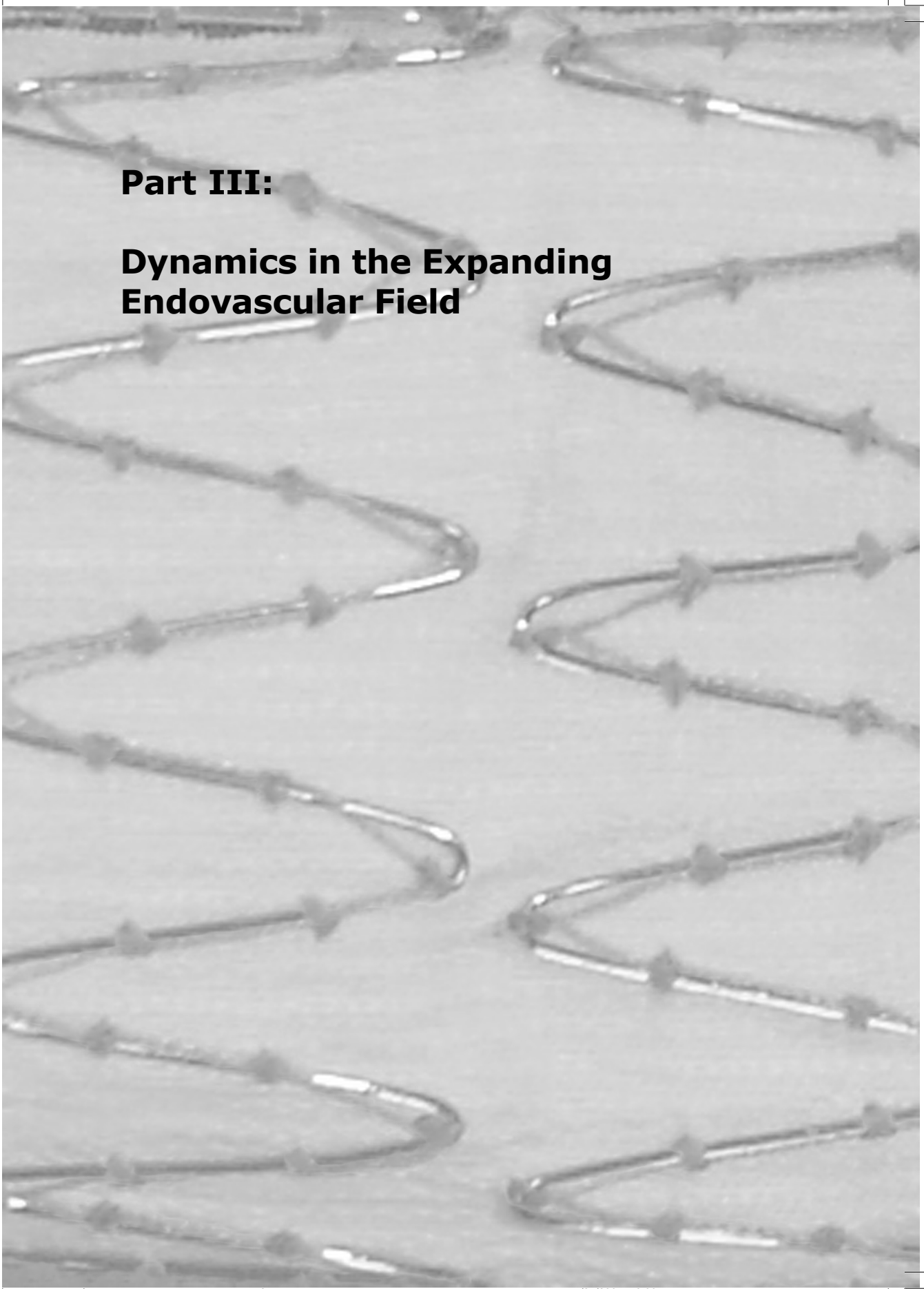

Part III:

Dynamics in the Expanding Endovascular Field

6

A.W. Floris Vos
Matteus A.M. Linsen
Willem Wisselink
Jan A. Rauwerda

Endovascular Grafting of Complex Aortic Aneurysms with a Modular Side Branch Stent-graft System in a Porcine Model

European Journal of Vascular and Endovascular Surgery 2004;27:492-497

INTRODUCTION

Aneurysms that involve segments of the aorta containing essential branch arteries, such as supra-renal, thoraco-abdominal and aortic-arch aneurysms, may pose difficult challenges to both surgeon and patient. Despite recent strides in surgical technique and perioperative care, morbidity and mortality for repair of these aneurysms is still considerable.[1–3] Thus, with these extended aneurysms in particular lies a potential for improvement if repair could be accomplished via minimally invasive, endoluminal methods. Reports of endovascular techniques of complex aneurysm repair containing essential branch arteries have been limited to animal studies and incidental case reports.[4–7] In the latter, technically demanding and time consuming procedures are being described that to date have not been reproduced by others. The complex devices were in most cases hand made and, therefore, unsuitable for use in a conventional endovascular unit.

The aim of this study was to develop and test, in cooperation with a major stent-graft manufacturer, a conventional, custom made branch graft system, that can be placed in a reliable, predictable and timely manner. If such a system would become commercially available, inclusion criteria for endovascular repair could potentially be extended to no-neck infrarenal aneurysms, aorto-iliac, as well as aortic arch and thoraco-abdominal aneurysms.

METHODS

Stent-graft system

The device is a modular system containing a main stent-graft and separate side branches. The main stent-graft is composed of a Talent^{TM} stent-graft (Medtronic AVE, Santa Rosa, CA, USA) customized with two fenestrations to match the renal artery origins (Fig. 1). Radiopaque markers are incorporated in the main graft to aid in accurate alignment with the arterial ostia. The delivery device is equipped with a partial deployment feature consisting of a bare top stent constrained by a spindle and sleeve (Fig. 2). Restraining sutures have been placed around the main graft to allow optimal maneuverability following initial deployment. The side branch grafts consist of a balloon expandable stent, mounted on a non-compliant balloon, and covered with an ePTFE tube that is overmolded with a silicone flange (Fig. 3). The ePTFE is held to the stent by an additional constraining suture that will brake when the branch graft is deployed. The silicone flanges are designed to easily slide

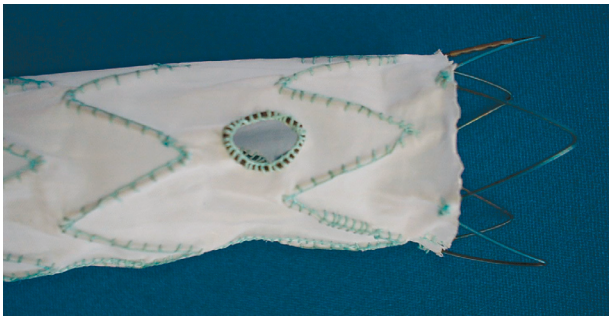

Figure 1 View of a fenestrated aortic stent-graft. Note the flexible radiopaque ring around the fenestration.

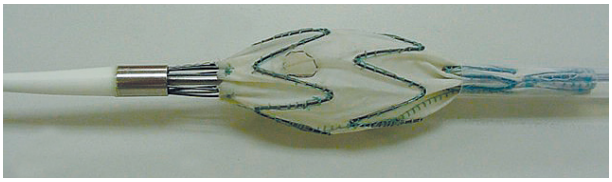

Figure 2 The aortic stent-graft partially deployed by constraining the bare stent with a spindle and sleeve just below the tip of the introducer device. When de device is unsheathed, the bare top stent remains securely constrained in the sleeve, allowing continued manipulation to align the fenestrations with the vessel ostia.

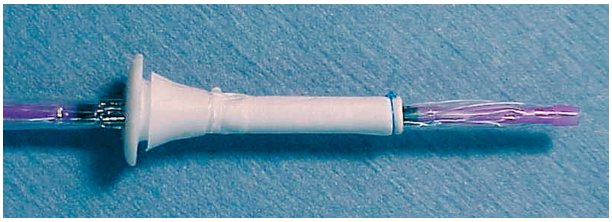

Figure 3 The side branch mounted on a catheter. The branch consists of a bare stent covered with an ePTFE tube overmolded with a silicone flange. The ePTFE is constrained by a suture and the flange specially designed to create a water tight seal between main body and branch graft.

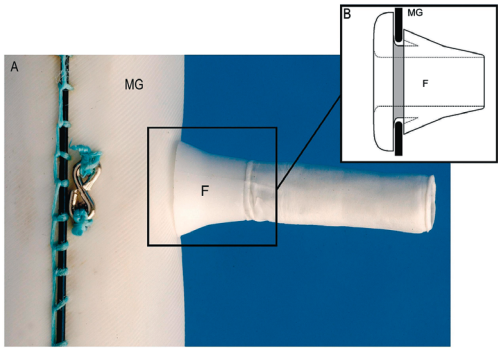

Figure 4 (A) The expanded side branch in position, sealed within the main graft (MG). (B) Schematic drawing of the flange (F) in detail.

into the fenestration, lock into place and create a seal between the main stent-graft and the side branch graft (Fig. 4).

Operative procedures

Once final adjustments to materials and techniques had been made, and successful grafting of a single branch artery was completed in a pig with an infra renal aneurysm, four fully conditioned Yorkshire pigs were obtained from a single vendor and underwent a 5 day pre-operative conditioning period. In four consecutive experiments, all animals underwent two operative procedures during the same anesthetic period: (1) creation of a complex aortic aneurysm (2) endovascular repair of the aneurysm. All experiments were conducted using the guidelines published in the Guide for the Care and Use of Laboratory Animals (NIH publication 85–23, revised 1985). The study protocol was approved by our institution's Animal Care and Use Committee.

Creation of the aneurysm

Pigs of 90 kg (70–100) were pre-anaesthetized with a mixture of intramuscular ketamine (800 mg), midazolam (35 mg) and atropine (1 mg). Endotracheal intubation was performed following a intravenous dose of fentanyl (150 mg) and ethomidate

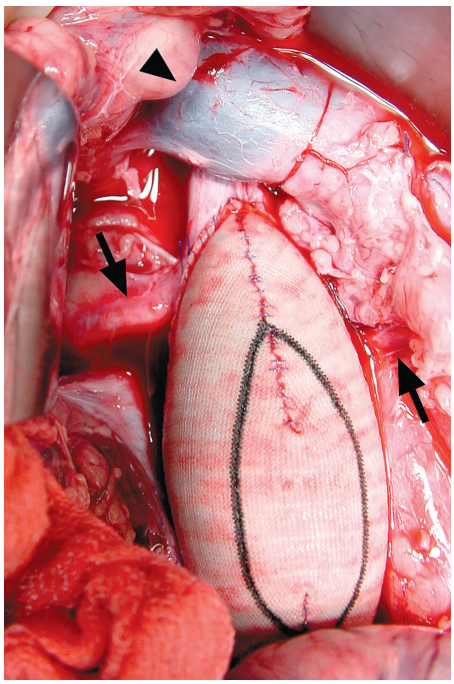

Figure 5 Supra renal aortic aneurysm created by suturing an artificial patch onto an anterior aortotomy. Note the renal arteries (arrows) and left renal vein (arrowhead).

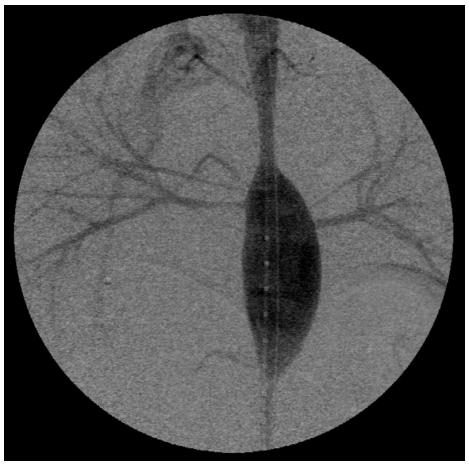

Figure 6 Angiogram of the created supra renal aortic aneurysm.

Figure 7 Completion angiogram. The renal arteries are patent and no contrast is visible in the aneurysm sac.

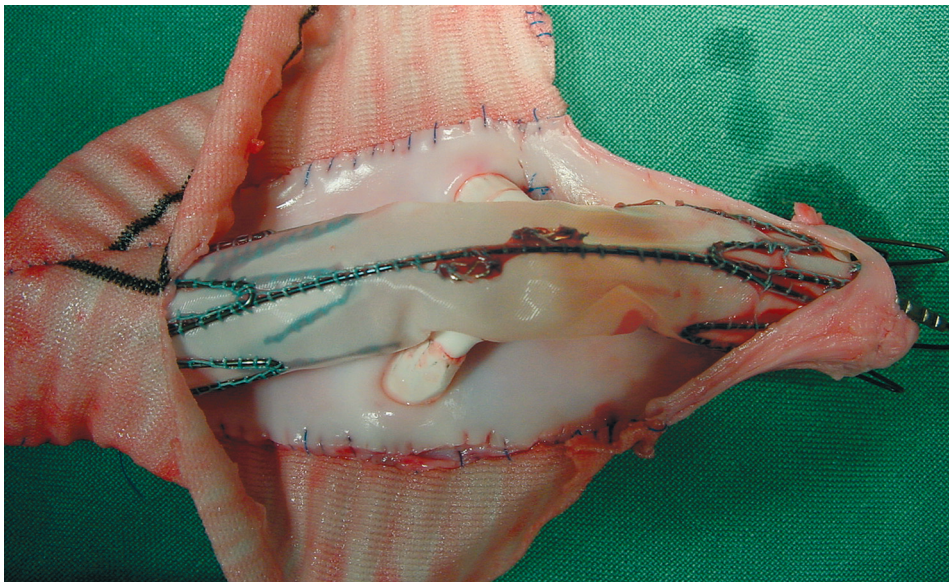

Figure 8 Post mortem specimen. The aorta has been opened longitudinally through the patch. Note the side branches connected to the main graft and located in the renal arteries.

(40 mg). General anaesthesia was continued with a mixture of intravenous fentanyl (500 mg/h), midazolam (20 mg/h) and pancuronium (20 mg/h) and inhaled isoflurane (2.4%). Tidal volume was initially set at 10 ml/kg, and respiratory rate at 13 per minute. These initial parameters were modified after serial blood gas

measurements to keep the pCO2 between 25 and 35, and the pH within normal limits. A jugular venous and carotid arterial access was obtained prior to the procedure. The electrocardiogram, carotid blood pressure, central venous pressure, blood gases, urine output, transcutaneous oxygen saturation and body temperature were monitored throughout the entire procedure. Glucose and Ringer's lactate solutions were administered for hydration. The surgical procedure of creating an aneurysm was previously described in a dog model.[4] In short, a longitudinal aortotomy was made and an elliptic artificial patch was sewn onto the aortotomy proximally starting above or at the level of the renal arteries (Fig. 5).

Endovascular aneurysm repair

During the endovascular procedure, blood loss, contrast use and operation time was monitored. Incisions were made in the left and right groin and common femoral arteries isolated. Following systemic heparinization (bolus of 5000 IU and 10,000 IU/h continuously), using the Seldinger technique, a .035" guide wire was entered into the right femoral artery and advanced into the supra renal aorta under fluoroscopic control (BV Pulsera, Philips Medical Systems, Andover, MA, USA). A sizing catheter was advanced over the guidewire and digital subtraction angiography was performed (Fig. 6). The diameter of the aorta, length of the aneurysm and location of the renal artery origins were measured (Table). Accordingly, 4 mm diameter fenestrations were created in an appropriately sized aortic stent-graft (diameter 14 mm, length 93 mm). The main stent-graft was placed in an introducer sheath (14F) and advanced over a .035" stiff guidewire (Back-up Meier, Boston Scientific, Natick MA, USA) into the aorta under fluoroscopic control. Subsequently, the sheath was retracted and the stent-graft partially deployed as described above. Partial deployment allows cannulation of the main graft from below without committing to definitive placement in the aorta. At this time, the device can still be rotated, or moved proximally or distally for proper alignment of the fenestrations with the vessel ostia. After retraction of the introducer sheath, a 16F sheath was introduced in the left femoral artery and a .035" guidewire and 5F directional catheter was used to gain access to the main graft. Using the same wire and catheter, the renal artery was cannulated through the fenestration in the main stent-graft. The side branch was placed into an introducer sheath via a loading cartridge that folds the flange, and reduces its profile. The side branch catheter was then tracked over a .035" guidewire, through the main stent-graft fenestration into the renal artery. By pushing the graft into the renal artery, the special flange design assures for a

Animal no.	Weight (kg)	Diameter (mm)		Aneurysm Length	Aneurysm Type	Side Branches	Distance	
		Aorta	Aneurysm				A	B
1.	100	12	30	75	Infra renal "no neck"	2	3	0
2.	70	10	35	80	Infra renal "no neck"	1	8	X
3.	95	10	30	80	Supra renal	2	15	10
4.	95	12	35	80	Supra renal	2	14	8

Table Summary of animal and stent-graft data. Distance A= axial distance between the beginning of the aneurysm and the most cranial artery, Distance B= axial distance between both renal arteries.

tight connection between main stent-graft and branch graft (Fig. 4). An integrated balloon was inflated to 3 atm. to deploy the stent to secure the landing site in the renal artery. The diameter of the side branch (5 mm) was oversized by 1 mm to achieve an effective sealing. Subsequently, the same procedure was performed for remaining branch arteries. Thereafter, the main stent-graft was fully deployed by unlocking the partial deployment mechanism and by inflating a noncompliant balloon (6 atm.) at the level of the landing sites and fenestrations. Extensions were placed distally in the main graft until distal fixation in the aorta was completed. As soon as the aneurysm was excluded from the circulation a completion angiography was performed (Fig. 7). Finally, the pigs were euthanised and at autopsy the aorta and aneurysm were carefully resected and the position of the device was photographed (Fig. 8).

RESULTS

The median endovascular procedure time was 126 min (90–160), with 575 ml (400–800) blood loss and 65 ml (50–80) contrast agent use. The median cannulation time for each side branch graft placement was 34 min (20–60). Angiographically, all aneurysms were excluded from aortic flow without signs of endoleak and all renal arteries were patent after the procedure (Fig. 7). At autopsy, the main stent-graft and all side branches were adequately placed with intact connections between main stent-graft and branches (Fig. 8).

DISCUSSION

To date, reports on the use of branched stent-graft systems for endovascular aneurysm exclusion have been limited to incidental small series and case reports from highly skilled pioneers. The devices described are mostly home made or put together with various components that have been initially designed for other purposes.[4–7] In these studies, considerable technical difficulties were encountered, procedure time, contrast use and morbidity were significant and moreover the techniques described have not been reproduced by others. In endovascular repair of complex aneurysms the optimal positioning of the main stent-graft is of prime importance. To avoid occlusion of essential branch arteries fenestrations should be positioned careful at artery origins. Chuter et al. cited concerns about this subject when a system with fenestrations is used. Nevertheless, its feasibility has been shown in earlier studies by Anderson and Stanley.[8,9] In our device, cannulation of the renal arteries is performed before the main graft was fully deployed thereby creating additional manoeuvrability and reversibility of the procedure. For example, in our first animal procedure the main stent-graft had been initially deployed erratically with the left renal fenestration directed to the right, prohibiting cannulation of the corresponding renal artery. When the error was noted, the partially deployed main stent-graft could be easily rotated 180° allowing successful cannulation of both renal arteries. Additionally, we were keen to develop a side branch with an 'aerodynamic' configuration in the predeployment state allowing smooth insertion of the graft into the branch artery, thus perhaps reducing long branch graft cannulations times reported by others.[5,7] The advantage of a modular system as described is mentioned earlier by Chuter et al.[5] A modular system can preserve branch artery perfusion during the entire procedure while the non-modular system described by Hosokawa causes considerable warm ischemia time when the main stent-graft is deployed and the side branches are not yet in place.[6] Obviously, success of the procedure as described depends on accurate pre-operative measurements of images in three dimensions, followed by custom made graft manufacturing to obtain correct alignment of side holes and branch artery orifices. In our study measurements were made during creation of the aneurysm and using angiography. In case of future use in humans we have to adjust the size of the side branches up to 6–8 mm diameter after deployment using an 18–20F introducer.
Various studies reported concerns about stent-graft migration in the long term.[10,11] Migration is associated with late aneurysm rupture, proximal endoleak, graft kinking

and graft limb thrombosis.[12,13] Poorly incorporated stent-grafts because of the defective healing process of the aortic wall in aneurysmal disease combined with chronic longitudinal 'pulling and pushing' mechanical forces at the proximal and distal fixation sites are of concern.[14,15] In case of so-called 'no-neck aneurysms', the side branch device might increase proximal stability by creating a sufficient landing zone in healthy visceral aorta. Likewise, in case of distal migration of previously placed infrarenal stent-grafts, an extension with side branches in the renal arteries may secure proximal fixation. Theoretically, branch graft placement as described in this study need not be limited to the renal arteries but, instead, can be implemented in aortic arch branches, visceral arteries, and internal iliacs, leading to a significant widening of the indication range for endovascular aneurysm repair. In conclusion, in this model, endovascular repair of complex aneurysms using a modular branch graft system has been shown to be feasible in a reliable, predictable and timely fashion.

Acknowledgements

This experimental research project has been supported by a grant from Medtronic AVE, Santa Rosa, CA, USA.

REFERENCES

1. Svensson LG, Crawford ES, Hess KR, Coselli JS, et al. Experience with 1509 patients undergoing thoracoabdominal aortic operations. *J Vasc Surg*. 1993;17:357–368.

2. Cambria RP, Clouse WD, Davison JK, Dunn PF, et al. Thoracoabdominal aneurysm repair: results with 337 operations performed over a 15-year interval. *Ann Surg*. 2002;236:471–479.

3. Rectenwald JE, Huber TS, Martin TD, Ozali CK, et al. Functional outcome after thoracoabdominal aortic aneurysm repair. *J Vasc Surg*. 2002;35:640–647.

4. Wisselink W, Abruzzo FM, Shin CK, Ramirez JR, et al. Endoluminal repair of aneurysms containing ostia of essential branch arteries: an experimental model. *J Endovasc Surg*. 1999;6:171–179.

5. Chuter TA, Gordon RL, Reilly LM, Goodman JD, et al. An endovascular system for thoracoabdominal aortic aneurysm repair. *J Endovasc Ther.* 2001;8:25–33.

6. Hosokawa H, Iwase T, Sato M, Yoshida Y, et al. Successful endovascular repair of juxtarenal and suprarenal aortic aneurysms with a branched stent-graft. *J Vasc Surg*. 2001;33:1087–1092.

7. Bleyn J, Schol F, Vanhandenhove I, Vercaeren P. Sidebranched modular endograft system for thoracoabdominal aortic aneurysm repair. *J Endovasc Ther*. 2002;9:838–841.

8. Anderson JL, Berce M, Hartley DE. Endoluminal aortic grafting with renal and superior mesenteric artery incorporation by graft fenestration. *J Endovasc Ther*. 2001;8:3–15.

9. Stanley BM, Semmens JB, Lawrence-Brown MM, Goodman MA, et al. Fenestration in endovascular grafts for aortic aneurysm repair: new horizons for preserving blood flow in branch vessels. *J Endovasc Ther*. 2001;8:16–24.

10. Kalliafas S, Albertini JN, Macierewicz J, Yusuf SW, et al. Stent-graft migration after endovascular repair of abdominal aortic aneurysm. *J Endovasc Ther*. 2002;9:743–747.

11. Mohan IV, Harris PL, van Marrewijk CJ, Laheij RJ, et al. Factors and forces influencing stent-graft migration after endovascular aortic aneurysm repair. *J Endovasc Ther*. 2002;9:748–755.

12. Harris PL, Vallabhaneni SR, Desgranges P, Bequemin JP, et al. Incidence and risk factors of late rupture, conversion, and death after endovascular repair of infrarenal aortic aneurysms: the EUROSTAR experience. *J Vasc Surg*. 2000;32:739–749.

13. Resch T, Ivancev K, Brunkwall J, Nyman U, et al. Distal migration of stent-grafts after endovascular repair of abdominal aortic aneurysms. *J Vasc Interv Radiol*. 1999;10:257–264.

14. Szilagyi DE. The problem of healing of endovascular stent-grafts in the repair of abdominal aortic aneurysms. *J Vasc Surg*. 2001;33:1283–1285.

15. Vos AW, Wisselink W, Marcus JT, Vahl AC, et al. Cine MRI assessment of aortic aneurysm dynamics before and after endovascular repair. *J Endovasc Ther*. 2003;10:433-439.

7

Matteus A.M. Linsen
A.W. Floris Vos
Jeroen Diks
Jan A. Rauwerda
Willem Wisselink

Fenestrated and Branched Endografts: Assessment of Proximal Aortic Neck Fixation

Accepted Journal of Endovascular Therapy

INTRODUCTION

Long-term performance of a vascular graft in open abdominal aortic aneurysm (AAA) repair depends on the durability of anastomosis and graft material. With the introduction of endovascular aneurysm repair (EVAR), both anastomosis and graft material changed, implying doubts with regard to its long-term performance. One of the worrisome complications in EVAR is proximal endograft migration. Migration of the device from its initial location can lead to late type I endoleak, aneurysm enlargement, and eventually rupture.[1,2]

Currently available endografts rely on columnar support, radial force, appendages like hooks and barbs, and suprarenal bare stent deployment for improved fixation. Mid-term results for these devices show migration rates varying from 0-13%.[3-6] However, the incidence of device migration seems to increases with length of follow-up, longer-term data is therefore important.[7,8]

Fenestrated and branched endografts might improve long-term fixation, with the advantage to deploy the endograft further into the non-aneurysmal section of the aorta. A larger surface contact between graft and aortic wall is created without impairing blood flow to the renal and visceral arteries. Such complex endografts are not yet available in regular practice. In future they might enlarge the pool of anatomically feasible aneurysms suitable for EVAR and also improve long-term success of EVAR in infrarenal aneurysms currently treated with standard endografts in terms of migration.

The purpose of this study is to investigate proximal fixation of a fenestrated endograft and a modular branch graft, in comparison with an infrarenal endograft with suprarenal bare stent fixation and a conventional hand-sewn anastomosis.

METHODS

Endografts

Three different endograft designs, based upon the Talent^{TM} (Medtronic AVE, Santa Rosa, CA, USA) were tested for proximal fixation capacities: an infrarenal endograft with suprarenal bare stent fixation; a fenestrated endograft with fenestrations aligning the renal artery orifices and a branched endograft (Fig. 1).

The branched endograft is modular system composed of a tubular main graft, customized with two fenestrations to match the renal artery origins. The branch

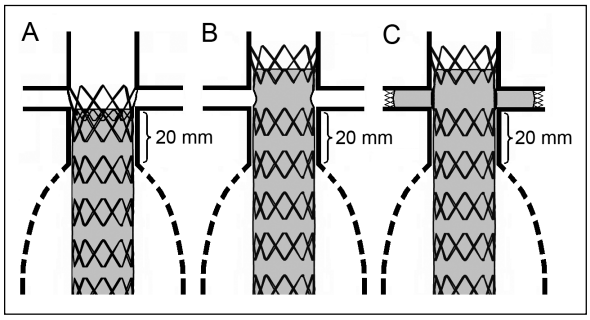

Figure 1 The three different endograft designs.
An infrarenal endograft, placed with the fabric below the lowest renal artery (A), a fenestrated endograft (B) and a branched endograft (C). Both B en C are placed with the fabric below the superior mesenteric artery. The infrarenal aneurysm neck of 20 mm was simulated.

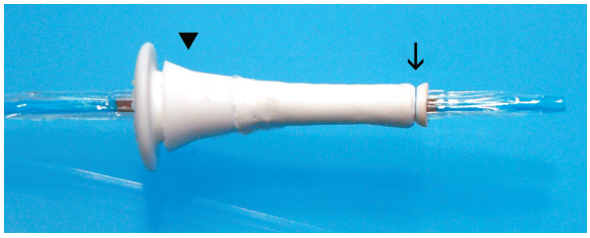

Figure 2 A side branch graft device. The ePTFE tube is over-molded with a silicone flange (arrowhead) and held to the stent-system with a constraining suture (arrow).

graft device is a Bridge Assurant^{TM} balloon expandable stent system, covered with an extended polytetrafluoroethylene (ePTFE) tube that is over-molded with a silicone flange (Fig. 2). The ePTFE is held to the stent-system by an additional constraining suture that will brake when the integrated stent is ballooned. The silicone flanges are designed to easily slide into the fenestration, lock into place and create a fluid tight seal between the main graft and the proximal end of the branch graft (Fig. 3).

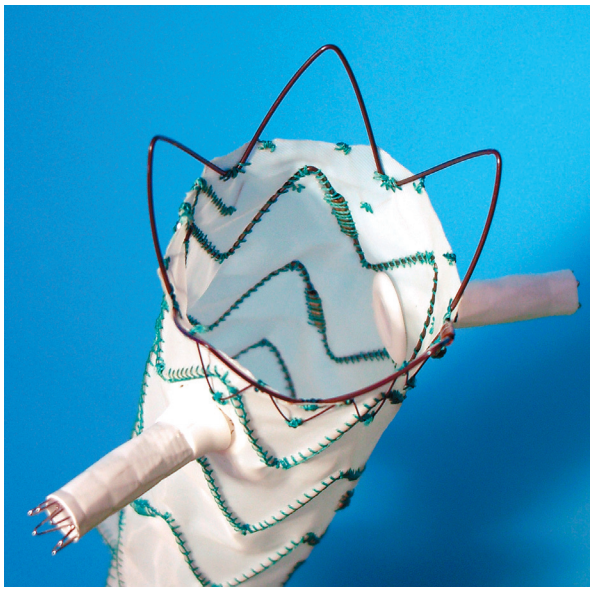

Figure 3 Both side branch grafts are locked into the fenestrations of the main graft, creating a fluid tight seal.

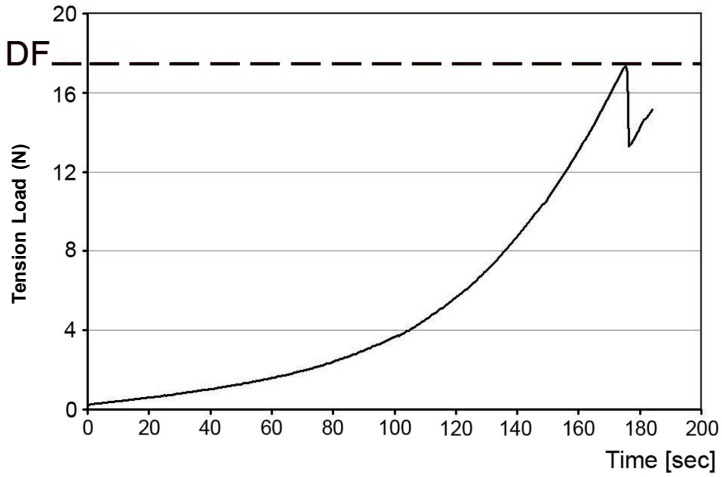

Figure 4 Longitudinal tension load curve of a branched endograft. Notice the increase in force (Newton) due to elastic elongation. At maximum tension load, static friction changed into dynamic friction, this point is defined as the Displacement Force (DF).

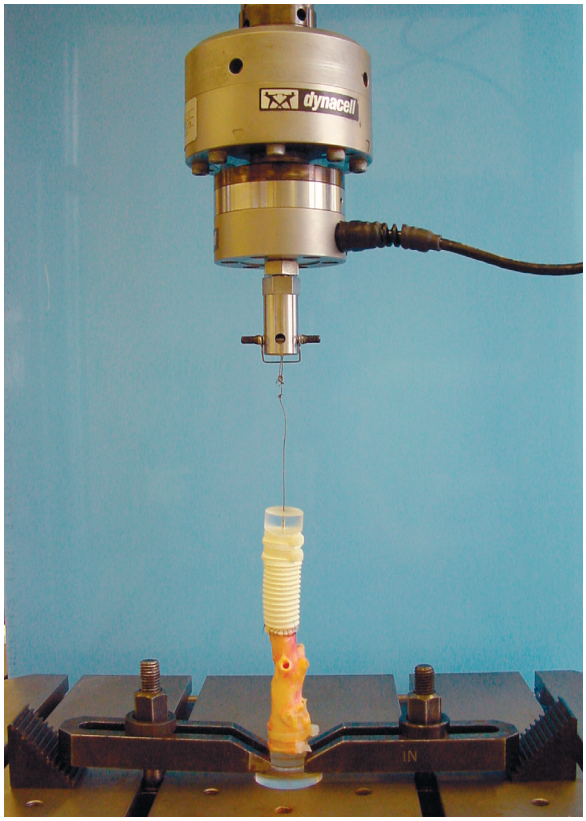

Figure 5 A conventional anastomosis is placed into the hydraulic material testing machine and longitudinal traction is applied.

Harvesting and preparation of the aortas

At autopsy human abdominal non-aneurysmal aortas (n=16) were obtained. After harvesting, the aortas were macroscopically classified following the scoring system proposed by Malina et al, (I) non-atherosclerotic, (II) soft intimal thickening, (III) calcified plaques engaging part of the aortic circumference, (IV) circumferentially located calcified plaques, (V) completely calcified, incompressible aorta.[9] Subsequently, the aortic diameter was measured. Ten aortas (n=10), group II and III classified, with diameters between 18 and 22 mm were considered suitable for proximal aortic neck fixation in EVAR and therefore used in the experimental set-up. The median age of the deceased (6 male, 4 female) was 69 years (range 60-75 years). To mimic an infrarenal aneurysm neck the aortas were transected 20 mm below the orifice of the lowest renal artery. Both renal arteries were preserved with a minimum length of 20 mm each. For conservation the aortas were placed in saline fluid and maintained below 4ºC until tests were performed (mean delay: 11.4 hours). All aortas were obtained in accordance with the requirements of the institutional ethical committee and the departments involved.

Experimental set-up

Endografts were deployed in the 20 mm aortic neck similar to clinical practice. Oversizing (10-20%) and post deployment dilatation was performed (6 atm.). The implanted grafts were flushed with saline solution at 37ºC to promote graft expansion. Using a hydraulic material testing machine (Model 8872, 250 N load cell, Instron Corporation, MA, USA) longitudinal traction (N) was applied to the distal end of each endograft. The aorta showed elastic elongation due to increasing tension load. At maximum tension load, static friction changed into dynamic friction. At this point endograft migration starts, this point was defined as the displacement force (DF) (Fig. 4). The three endografts were tested in a random order, once in each aorta. The aorta was examined for injury after each extraction and if necessary excluded from the test. Thereafter a 3-0 Prolene hand-sewn anastomosis was made using a Dacron graft and the force to dislodge the graft was measured (Fig. 5).

Statistical analysis

The results are presented as the median (range) of the 10 measurements. Multiple groups were compared using the Friedman test. The Wilcoxon signed ranks test was used for comparing two devices. A p value <0.05 was considered statistically significant. Statistical analyses were performed with *SPSS*, version 11.0 (SPSS, Chicago, IL).

RESULTS

The median DF ranged from 4.67 N (3.82 to 6.37) for the infrarenal endograft to 16.95 N (14.78 to 19.67) for the branched endograft (Fig. 6). DF for the fenestrated endograft was 9.17 N (8.03 to 10.81). Statistical analysis showed a significant increase in the DF between the infrarenal and the fenestrated endograft (p=0.005), as well as between the fenestrated and the branched endograft (p=0.005). The median force to dislodge the graft from the conventional anastomosis was 89.16 N (71.24 to 105.23), which is about five times higher than the branched endograft. During displacement of the endografts no macroscopic damage was made to the aortic segments. Displacement in case of the conventional anastomosis resulted in tearing of the aorta along the suture line.

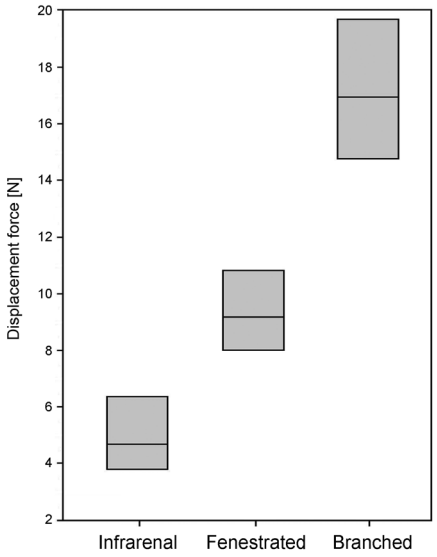

Figure 6 Displacement force (DF) in Newton of the three types of endografts.

DISCUSSION

Successful EVAR requires secure proximal endograft fixation. Failure in this fixation can lead to late type I endoleak, aneurysm enlargement, and rupture.[1,2] Factors influencing proximal endograft fixation are: aortic neck dilation, due to progressive aneurysm disease or stent oversizing; pulsatile blood flow causing longitudinal repetitive displacement forces; and in certain cases unfavorable neck morpho-

logy.[10-14] While biological incorporation into the aortic wall is generally inadequate, endograft manufacturers have sought to overcome this by introducing mechanical fixation techniques.[15] Besides columnar support and radial force, currently available endografts rely on appendages like hooks and barbs, and suprarenal bare stent deployment for increased surface contact.

Several experimental studies using human cadaveric aortas showed improved endograft fixation by addition of simple appendages like hooks and barbs.[9,16,17] These results are supported by low incidences of migration, in patients treated with infrarenal endografts with proximal barbs.[18,19] However, enthusiasm about hooks and barbs is somewhat tempered by reports of hook fractures due too material fatigue in patients after EVAR.[3,20] Long-term concerns may also rise with hooks and barbs penetrating the aortic wall and surrounding structures, although, to date such events have not been reported.

Another important development is suprarenal stent placement. By placing a proximal uncovered portion across the orifices of the renal arteries, a larger attachment area is created. According to large series from various centers short to medium-term results for suprarenal bare stent placement are satisfactory.[21-24] Due to these favorable results suprarenal bare stent placement is increasingly applied in EVAR. However, concerns remain as stent struts across the renal ostia, with or without foreign body induced neo intimal hyperplasia might alter renal blood flow and renal function.[19,25] Renal infarction and occasional renal artery occlusion have been reported in some patients.[26-28] More long-term information about these issues is essential to ensure the safety of suprarenal endograft implantation.[24,29] Both techniques combined, e.g. hooks or barbs and suprarenal fixation, has been described as the best possible fixation in ex vivo experiments, with a DF of approximately 25 N.[16] This is also confirmed by multicenter data reporting low incidence migration with suprarenal barbed endografts.[3,30]

To overcome stent struts covering renal artery orifices, some have propagated the use of fenestrated endografts.[31,32] By creating holes in the fabric of the graft, blood flow to renal, and if needed visceral arteries is preserved. The concept of graft fenestration has been developed into successful clinical application.[33,34] However, the risk of endoleaks remains present when these grafts are applied in treatment of aneurysms with very short or absent infrarenal necks. This concern has given rise to the development of branched endografts with fluid tight seals between the main and branch grafts. Reports have been mostly limited to animal studies and incidental case reports.[34-36] These procedures have been proven technically challenging and time consuming, and therefore are probably less suitable

for use in a conventional endovascular unit. The modular branched endograft system described in this study, has been specifically designed to overcome these problems. Although still in pre-clinical development, in an animal model, the branch system has proved it can be placed in a reliable, predictable and timely manner.[37]

The current study revealed improved proximal fixation by the fenestrated endograft (median DF 9.17N), caused by an increased attachment area (with approximately 35 mm length) at the proximal neck, compared to the 20 mm neck of the infrarenal graft. Increase in attachment area by the addition of two branch grafts in the renal arteries, resulted in an even better proximal fixation (median DF 16.95N). However, in this study the proximal fixation provided by the endografts was not nearly as good as that realized by the conventional hand-sewn anastomosis (median DF 89.16 N).

Although effort was put into reproducing the clinical situation, there are several limitations to this study design. Similar to other in vitro migration studies, we used a continuous longitudinal force instead of pulsatile blood flow with repetitive pulling and pushing forces.[9,16,17] Also, we focused on proximal neck fixation leaving columnar strength and distal fixation abandoned. Considering the aortic neck we believe, our selection of atherosclerotic post mortem aorta's at the level of the renal arteries with a short delay between harvest and test is the optimal condition possible mimicking situation in a living human being. Because of the absence of hooks and barbs in this study, no impairment of the aortic wall was discerned and therefore all endograft types were tested in a random order avoiding selection bias. Nevertheless caution is warranted while comparing our results with the other studies.[9,16,17] First, we positioned our devices in the exact location with regard to the renal arteries similar to the clinical situation as the other studies used varying aortic neck lengths (2-5cm) without taking the increased attachment area of the bare suprarenal part into account. Secondly, while even minimal displacement is essential in fenestrated and branched grafts, we selected the start of displacement as the important force factor, as other studies measured the force to completely dislodge the grafts from the aorta.

Although still technically challenging, fenestrated and branched endografts provide enhanced proximal fixation strength. As endograft migration and vulnerable renal perfusion are persisting concerns in EVAR, expansion of the endovascular field with the introduction of fenestrations and branch grafts in clinical practice seems worthwhile. Fenestrated endografts especially with the addition of branch grafts, combined with adjacent hooks or barbs might approach the gold standard, the hand-sewn anastomosis.

REFERENCES

1. Harris PL, Vallabhaneni SR, Desgranges P Becquemin JP, et al. Incidence and risk factors of late rupture, conversion, and death after endovascular repair of infrarenal aortic aneurysms: the EUROSTAR experience. European Collaborators on Stent/graft techniques for aortic aneurysm repair. *J Vasc Surg.* 2000;32:739-749.

2. Tonnessen BH, Sternbergh WC 3rd, Money SR. Late problems at the proximal aortic neck: migration and dilation. *Semin Vasc Surg.* 2004;17:288-293.

3. Greenberg RK, Chuter TA, Sternbergh WC 3rd, Fearnot NE. Zenith AAA endovascular graft: intermediate-term results of the US multicenter trial. *J Vasc Surg.* 2004;39:1209-1218.

4. Fairman RM, Velazquez OC, Carpenter JP, Woo E, et al. Midterm pivotal trial results of the Talent Low Profile System for repair of abdominal aortic aneurysm: analysis of complicated versus uncomplicated aortic necks. *J Vasc Surg.* 2004;40:1074-1082.

5. Kibbe MR, Matsumura JS. The Gore Excluder US multi-center trial: analysis of adverse events at 2 years. *Semin Vasc Surg.* 2003;16:144-150.

6. Schmittling ZC, McLafferty RB, Danetz JS, Ramsey DE, et al. The AneuRx modular endograft device for the treatment of abdominal aortic aneurysms. Overview of 7 years of clinical use. *J Cardiovasc Surg.(Torino).* 2004;45:301-306.

7. Cao P, Verzini F, Zannetti S, De Rango P, et al. Device migration after endoluminal abdominal aortic aneurysm repair: analysis of 113 cases with a minimum follow-up period of 2 years. *J Vasc Surg.* 2002;35:229-235.

8. Zarins CK, Bloch DA, Crabtree T, Matsumoto AH, et al. Stent graft migration after endovascular aneurysm repair: importance of proximal fixation. *J Vasc Surg.* 2003;38:1264-1272.

9. Malina M, Lindblad B, Ivancev K, Lindh M, et al. Endovascular AAA exclusion: will stents with hooks and barbs prevent stent-graft migration? *J Endovasc Surg.* 1998;5:310-317.

10. Resch T, Ivancev K, Brunkwall J, Nyman U, et al. Distal migration of stent-grafts after endovascular repair of abdominal aortic aneurysms. *J Vasc Interv Radiol.* 1999;10:257-264.

11. Mohan IV, Harris PL, Van Marrewijk CJ, Laheij RJ, et al. Factors and forces influencing stent-graft migration after endovascular aortic aneurysm repair. *J Endovasc Ther.* 2002;9:748-755.

12. Vos AW, Wisselink W, Marcus JT, Vahl AC, et al. Cine MRI assessment of aortic aneurysm dynamics before and after endovascular repair. *J Endovasc Ther.* 2003;10:433-439.

13. Liffman K, Lawrence-Brown MM, Semmens JB, Bui A, et al. Analytical modeling and numerical simulation of forces in an endoluminal graft. *J Endovasc Ther.* 2001;8:358-371.

14. Conners MS 3rd, Sternbergh WC 3rd, Carter G, Tonnessen BH, et al. Endograft migration one to four years after endovascular abdominal aortic aneurysm repair with the AneuRx device: a cautionary note. *J Vasc Surg.* 2002;36:476-484.

15. Malina M, Brunkwall J, Ivancev K, Jonsson J, et al. Endovascular healing is inadequate for fixation of Dacron stent-grafts in human aortoiliac vessels. *Eur J Vasc Endovasc Surg.* 2000;19:5-11.

16. Veerapen R, Dorandeu A, Serre I, Berthet JP, et al. Improvement in proximal aortic endograft fixation: an experimental study using different stent-grafts in human cadaveric aortas. *J Endovasc Ther.* 2003;10:1101-1109.

17. Resch T, Malina M, Lindblad B, Malina J, et al. The impact of stent design on proximal stent-graft fixation in the abdominal aorta: an experimental study. *Eur J Vasc Endovasc Surg.* 2000;20:190-195.

18. Matsumura JS, Brewster DC, Makaroun MS, Naftel DC. A multicenter controlled clinical trial of open versus endovascular treatment of abdominal aortic aneurysm. *J Vasc Surg.* 2003;37:262-271.

19. Sun Z, Zheng H. Effect of suprarenal stent struts on the renal artery with ostial calcification observed on CT virtual intravascular endoscopy. *Eur J Vasc Endovasc Surg.* 2004;28:534-542.

20. Guidoin R, Marois Y, Douville Y, King MW, et al. First-generation aortic endografts: analysis of explanted Stentor devices from the EUROSTAR Registry. *J Endovasc Ther.* 2000;7:105-122.

21. Alric P, Hinchliffe RJ, Picot MC, Braithwaite BD, et al. Long-term renal function following endovascular aneurysm repair with infrarenal and suprarenal aortic stent-grafts. *J Endovasc Ther.* 2003;10:397-405.

22. Izzedine H, Koskas F, Cluzel P, Mallet A, et al. Renal function after aortic stent-grafting including coverage of renal arterial ostia. *Am J Kidney Dis.* 2002;39:730-736.

23. Lobato AC, Quick RC, Vaughn PL, Rodrigues-Lopez J, et al. Transrenal fixation of aortic endografts: intermediate follow-up of a single-center experience. *J Endovasc Ther.* 2000;7:273-278.

24. Bove PG, Long GW, Shanley CJ, Brown OW, et al. Transrenal fixation of endovascular stent-grafts for infrarenal aortic aneurysm repair: mid-term results. *J Vasc Surg.* 2003;37:938-942.

25. Liffman K, Lawrence-Brown MM, Semmens JB, Sutalo ID, et al. Suprarenal fixation: effect on blood flow of an endoluminal stent wire across an arterial orifice. *J Endovasc Ther.* 2003;10:260-274.

26. Lau LL, Hakaim AG, Oldenburg WA, Neuhauser B, et al. Effect of suprarenal versus infrarenal aortic endograft fixation on renal function and renal artery patency: a comparative study with intermediate follow-up. *J Vasc Surg.* 2003;37:1162-1168.

27. Mehta M, Cayne N, Veith FJ, Darling AC, et al. Relationship of proximal fixation to renal dysfunction in patients undergoing endovascular aneurysm repair. *J Cardiovasc Surg.(Torino).* 2004;45:367-374.

28. Bockler D, Krauss M, Mannsmann U, Halawa M, et al. Incidence of renal infarctions after endovascular AAA repair: relationship to infrarenal versus suprarenal fixation. *J Endovasc Ther.* 2003;10:1054-1060.

29. Sun Z Transrenal fixation of aortic stent-grafts: current status and future directions. *J Endovasc Ther.* 2004;11:539-549.

30. Sternbergh WC 3rd, Money SR, Greenberg RK, Chuter TA. Influence of endograft oversizing on device migration, endoleak, aneurysm shrinkage, and aortic neck dilation: results from the Zenith Multicenter Trial. *J Vasc Surg.* 2004;39:20-26.

31. Stanley BM, Semmens JB, Lawrence-Brown MM, Goodman MA, et al. Fenestration in endovascular grafts for aortic aneurysm repair: new horizons for preserving blood flow in branch vessels. *J Endovasc Ther.* 2001;8:16-24.

32. Browne TF, Hartley D, Purchas S, Rosenberg M, et al. A fenestrated covered suprarenal aortic stent. *Eur J Vasc Endovasc Surg.* 1999;18:445-449.

33. Verhoeven EL, Prins TR, Tielliu IF, van den Dungen JJ, et al. Treatment of short-necked infrarenal aortic aneurysms with fenestrated stent-grafts: short-term results. *Eur J Vasc Endovasc Surg.* 2004;27:477-483.

34. Hosokawa H, Iwase T, Sato M, Yoshida Y, et al. Successful endovascular repair of juxtarenal and suprarenal aortic aneurysms with a branched stent graft. *J Vasc Surg.* 2001;33:1087-1092.

35. Wisselink W, Abruzzo FM, Shin CK, Ramirez JR, et al. Endoluminal repair of aneurysms containing ostia of essential branch arteries: an experimental model. *J Endovasc Surg.* 1999;6:171-179.

36. Tse LW, Steinmetz OK, Abraham CZ, Valenti DA, et al. Branched endovascular stent-graft for suprarenal aortic aneurysm: the future of aortic stent-grafting? *Can J Surg.* 2004;47:257-262.

37. Vos AW, Linsen MA, Wisselink W, Rauwerda JA. Endovascular grafting of complex aortic aneurysms with a modular side branch stent-graft system in a porcine model. *Eur J Vasc Endovasc Surg.* 2004;27:492-497.

SUMMARY AND CONCLUSIONS

This study focuses on several issues associated with endovascular abdominal aortic aneurysm repair (EVAR) and carotid angioplasty and stenting (CAS). In the first two parts the dynamic consequences of endovascular therapies are emphasized as we believe they are highly influential on long term outcome.

In **Chapter 1** two-dimensional pulsatile wall motion (2D-PWM) of abdominal aortic aneurysm (AAA) was determined by visualizing aneurysm wall motions with high resolution cine MRI.
We measured 2D-PWM by comparing the difference between the smallest (end-diastolic) and largest (peak-systolic) cross-sectional area of transverse sections of AAA in 21 patients.
The median diastolic area surface was 28 cm^2 (intraquartile range, IQR, 22-31) and the median (IQR) 2D-PWM was 0.25 cm^2 (0.10-0.40). Assuming that the AAA is circular in cross-section this represents a median (IQR) diameter increase of 0.3 mm (0.1-0.4). However, local wall displacements up to 2 mm were present in varying directions, without significant change in surface area.
In this study, 2D-PWM represents a 1% increase in cross sectional area as determined by cine MRI. This is less than that found in ultrasound studies (about 4%). This may be caused by several reasons. Ultrasound techniques, are uni-dimensional, which may lead to the assumption that equal wall movements take place in all directions. A uni-dimensional technique cannot distinguish between PWM and movement of the whole AAA.
In conclusion, using high resolution cine MRI, this study demonstrates that true pressure related pulsatile wall motion is negligible and therefore not useful as a potential tool to assess efficacy of endovascular aneurysm exclusion.

Chapter 2 outlines the effect of pulsatile blood flow on aneurysm and stent-graft. Prior to and after EVAR movements during the cardiac cycle were monitored using cine MRI in an effort to identify mechanisms leading to long-term failure of EVAR. Prior to and after EVAR in 7 patients with AAA, 12 MR images per cardiac cycle were acquired in transverse, sagittal, and coronal planes of the aneurysm. Two independent observers blinded to the aim of the study manually traced stent-graft and aneurysmal wall contours. Translation was defined as the maximal displacement of the contours in the peak-systolic image compared to the end-diastolic image. Aneurysmal wall motions before and after repair were compared. Stent-graft and aneurysmal configuration changes during the cardiac cycle were evaluated.

The anteroposterior translation of the aneurysm decreased from a median 1.05 mm (<0.5-1.29) before EVAR to within pixel size (<0.5 mm) after EVAR (p=0.04). The cranial-caudal translation of the aneurysm increased from a median 1.01 mm (<0.5-1.51) before to 1.69 mm (1.1-1.99) after EVAR (p=0.02). In 4 stent-grafts, bending during cardiac systole was observed at the site of maximal angulation of the device. After EVAR, increased longitudinal translation of both aneurysm and stent-graft was observed, indicating downward pulling forces at the proximal fixation site. Secondly, increased bending was seen at the site of maximal angulation, which implies a risk of metal fatigue and fabric damage.
These results show that cine MRI is a useful tool to obtain dynamic information on the various repetitive translations and shape changes to which an aneurysm and stent-graft are subjected. With regard to future stent-graft design, this relatively small study supports the use of strong proximal fixation, suprarenal if necessary, and a flexible, compliant mid zone without metallic components.

Chapter 3 deals with carotid artery mobility patterns during head movements following CAS. CAS has been advocated as potentially safer, less traumatic, and more cost-effective than carotid endarterectomy (CEA). Despite promising initial results, long-term performance theoretically may be hampered by the mobile features of the carotid artery. Stent failure caused by neointimal hyperplasia and stent fractures in arteries that are subject to repetitive motion has been broadly described. In this present study, 7 patients after unilateral CAS, were examined, using 3D time-of-flight MR angiography, visualizing both carotid arteries in 5 different head positions (neutral, turned left and right and bent forward and backward). Maximum intensity projection reconstructions were obtained to measure angulation at the proximal and distal stent junction. Configuration changes of the stented section of the carotid artery and the unstented contralateral artery were judged. Secondly, transverse sections at the level of the carotid bifurcation and at the skull base were used to calculate torsion shear in the common and internal carotid arteries (CCA, ICA) during turned left and right head position.
In neutral head position, maximal angulation at the distal stent junction was 34.3º (32.3-55.6). With the head bent forward, this angulation changed to 47.6º (42.6-85.2, p=0.028) and when bent backward to 26.5º (25.0-48.7, p=0.027). In all patients, configuration changes of the stented sections were absent. The contralateral unstented side showed diffuse configuration changes without specific angulation at one location. With the head turned left and right, the CCA on the stented side was

subjected to 28.6º (13.6-53.7) and 24.9º (2.0-50.6) of torsion shear, respectively. Torsion of the ICA was subsequently 18.1º (12.7-40.5) and 15.2º (2.9-69.4).
Concluding, following carotid stenting, sharp ICA angulations that are aggravated by forward bending of the head occur at the distal stent junction. In all patients the stented section of the carotid artery shows complete lack of flexibility despite highly flexible features of the stents ex vivo. Both the CCA and ICA are subjected to considerable torsion shear with the head turned to the left and to the right. This shear is not accommodated by the current stent designs. Based on this study and the similarity to observations following stent placement in mobile arteries of the lower extremity, we speculate that the highly mobile features of the carotid artery may well hamper long-term results in CAS. Effort should be put into development of carotid stents with in vivo flexibility and torsion capacities.

Due to the results of the morphology study described in the previous chapter we questioned whether the vessel angulations caused by stents influence cerebropetal bloodflow. In **Chapter 4**, the use of MR phase-contrast flow quantification is described to measure the Volumetric Flow Rate (VFR) in the ICA after CAS and CEA in various head positions. Furthermore, in the same session, the anatomy of the ICA in the same head position was depicted, thus allowing assessment of the correlation between its geometry and the VFR. Results were compared between patients treated with CAS versus CEA.
In CAS patients, there was a median change in ICA angulation of 10.2° (IQR, 7.3-17.9) in the forward position, compared with 0.2°(IQR, -1.0 to 2.4) in CEA patients (p=0.016). In all other head positions, there was no statistically significant difference in angulation change. Neither was a statistically significant difference in VFR change present between groups in any of the head positions tested.
Therefore, this study confirmed significant increases in ICA angulation in patients treated with CAS if the head was bent forward. This was not observed in patients treated with CEA. Although this increased angulation did not lead to changes in cerebropetal bloodflow, it is possible that such angulations might result in chronic changes, such as re-stenosis. This however remains to be tested in future studies.

Chapter 5 provides the results of our in vitro bend and torsion study of five carotid stent designs. Given that considerable motion of the carotid artery is present during head movements, we hypothesized that a flexible stent with low torsion might be favorable to avoid stress imparted to the stent and carotid artery. We

evaluated the flexibility of different expanded carotid stents before and after deployment in a porcine carotid artery. Thereafter we measured torsion of the bare expanded stents.
Flexibility was determined using a three-point bend test recording the bending load (BL, in grams) required to flex the stent 25°. Increased BL implies decreased flexibility. Torsion was measured by recording the rotation load (RL, in grams) required to rotate the stents 30° along its axis. Increased RL implies increased torsion.
In the bare expanded state, the median BL was 6 g (1-22). The BL increased to 38 g (20-41) after deployment in a carotid artery, with the Carotid SE (21 g) and Wallstent (36 g) showing significantly lower BL ($p<0.0001$ and $p= 0.0016$, respectively). Overall, the RL was 11 g (1-76). Significantly higher RL was required to rotate the Wallstent (73 g) and Precise (20 g) stents (both, $p<0.0001$).
All stents were capable of bending and rotating along their axis within the range of motion caused by head movements. The flexibility of the currently used stents decreases after deployment in a carotid artery irrespective of its flexibility in the bare state.

In the third part, animal and in vitro studies are presented describing a future branch graft system. In **Chapter 6** intermediate results are reported of the development of a conventional, custom made branch graft system with side branches for treatment of aneurysms with essential branch arteries.
In a porcine model (n=4) supra- and juxtarenal aortic aneurysms were created by suturing a saccular Dacron patch into an anterior aortotomy. Angiography was performed to determine the exact location of the renal arteries. Accordingly, fenestrations were created in an appropriately sized aortic stent-graft. Initial deployment of the aortic graft is partial, whereby the top stent is secured in a cap and distal stents are being restrained, thus ensuring longitudinal and rotational manoeuvrability during alignment of the branch arteries. Separate branch grafts with silicone flanges for connection with the main stent-graft are subsequently placed in the renal arteries followed by full deployment of the main stent-graft.
In all trials postoperative angiography revealed all aneurysms excluded from the circulation without signs of endoleak and with patent renal arteries. At autopsy, the main stent-graft and all side branches proved to be adequately placed with intact connections between main stent-graft and branch grafts. The procedure was performed within reasonable operating time, blood loss and amount of contrast agent used.
Concluding, in this model, endovascular repair of complex aneurysms using a

modular branch graft system is feasible in a reliable, predictable and limited time consuming fashion. If such a system would become commercially available, inclusion criteria for endovascular repair could potentially be extended to no-neck infrarenal aneurysms, aorto-iliac, as well as aortic arch and thoraco-abdominal aneurysms.

In **Chapter 7** an in vitro traction study is reported investigating proximal fixation of a fenestrated stent-graft and a modular branch graft, in comparison with an infrarenal stent-graft with suprarenal bare stent fixation and a conventional hand-sewn anastomosis. This study is of importance as current mid-term results of EVAR still shows migration with increasing incidence along with length of follow-up. Fenestrated and branched grafts might improve long-term fixation, with the advantage to deploy the stent-graft further into the non-aneurysmal section of the aorta.

In this study human aortas were obtained at autopsy and transsected 20 mm below the renal arteries to mimic an infrarenal aneurysm neck. In random order, the infrarenal (A); fenestrated (B) and branched (C) graft were deployed in the aorta similar to clinical practice. Using a hydraulic material testing machine, longitudinal traction was applied to the distal end of each stent-graft until migration occurred, thus defining the displacement force (DF). Subsequently a hand-sewn infrarenal anastomosis was tested in a similar manner.

The median DF for A was 4.67 N (3.82-6.37), the DF increased to 9.17 N (8.03-10.81, p=0.0005) for B, and 16.95 N (14.78-19.67, p=0.0005) for C. A median force of 89.16 N (83.40-105.23) applied to the conventional anastomosis resulted in tearing of the aorta along the suture line.

Fenestrated stent-grafts, especially with additional branch grafts provide improved proximal fixation compared to an infrarenal stent-graft with suprarenal bare stent fixation. However, none of the tested stent-grafts approached the optimal time proven fixation, the hand-sewn anastomosis. In future, branched stent-grafts might enlarge the pool of anatomically feasible aneurysms suitable for EVAR and also improve long-term success of EVAR in infrarenal aneurysms currently treated with standard stent-grafts in terms of migration.

OVERALL CONCLUSIONS

- From Cine MR imaging of AAA it becomes apparent that true pressure related pulsatile wall motion is negligible.

- After EVAR increased longitudinal translation of both aneurysm and stent-graft is observed, indicating downward pulling forces at the proximal fixation site.

- Increased bending was seen at the site of maximal angulation, which implies a risk of metal fatigue and fabric damage.

- CAS leads to angulation with head movements due to complete lack of stent flexibility. We speculate that the highly mobile features of the carotid artery combined with stent inflexibility may hamper long term results.

- Despite angulation, short term postoperative diminished cerebropetal bloodflow could not be demonstrated.

- Flexibility and torsion in currently used stents is limited.

- Endovascular repair of complex aneurysms using a modular branch graft system is feasible in a reliable, predictable and limited time consuming fashion.

- Fenestrated stent-grafts, especially with additional branch grafts provide improved proximal fixation.

- The results of our studies support the current opinion as expressed in several recent communications that in patients with an expected long term survival an open repair is to be preferred.

SAMENVATTING EN CONCLUSIES

De meest voorkomende ziekten van bloedvaten uiten zich door verwijding (aneurysma) of vernauwing (stenose) van het betreffende bloedvat. Het aneurysma kan op den duur zó wijd worden dat het barst en de stenose kan leiden tot belemmering van de doorstroming. De klassieke chirurgische oplossing voor beide problemen bestaat uit "open" operatieve correctie van het misvormde vaatdeel door vervanging met een anatomisch normaal substituut. Sinds enige jaren kan men zonder open operatie, via een bloedvat, meestal in de lies, zowel het aneurysma (met een stent-graft) als de stenose (met een stent) behandelen. Deze endovasculaire methode is voor de patiënt minder belastend, maar het is de vraag of de resultaten op de lange duur net zo goed zijn als die na een open operatieve correctie.
In dit proefschrift worden diverse aspecten beschreven van de endovasculaire behandeling van het abdominaal aneurysma (EVAR) en de endovasculaire behandeling van de carotis vernauwing (CAS). In de eerste twee gedeelten worden de dynamische eigenschappen van beide therapieën onderzocht. De factor beweging heeft naar onze mening een grote invloed op de resultaten na langere termijn van EVAR en CAS. Met het oog op de dynamische ontwikkelingen binnen de endovasculaire chirurgie beschrijven wij in het derde deel onze ervaringen met de ontwikkeling van een stent-graft ter behandeling van het complexe aneurysma met essentiële zijtak arteriën.

In **Hoofdstuk 1** zijn de wandbewegingen van het aneurysma van de abdominale aorta (AAA) gedurende de hartcyclus in beeld gebracht met hoge resolutie cine MRI. Wandbewegingen kunnen gerelateerd zijn aan de druk in het aneurysma en daardoor een maat zijn voor de effectiviteit van uitschakeling van het aneurysma na EVAR.
Bij 21 patiënten is de tweedimensionale pulsatiele wandbeweging (2D-PWM) bepaald door het oppervlakte verschil tussen de transversale doorsneden van het AAA in de pieksystolische- en de einddiastolische fasen te meten.
De mediane 2D-PWM is 0.25 cm^2 (intrakwartiel, 0.10-0.40) bij een mediane diastolische oppervlakte van 28 cm^2 (intrakwartiel, 22-31). Indien men er vanuit gaat dat het AAA een cirkel is impliceert dit een mediane diameter verandering van 0.3 mm (intrakwartiel, 0.1-0.4). Desondanks zijn lokale wand verplaatsingen tot 2 mm aanwezig in diverse richtingen.
De verandering in diameter beschreven in deze studie (1%) is minder dan die in onderzoek verricht met ultrageluid (ongeveer 4%). De eendimensionale

meettechniek gebruikt in de ultrageluid studies waarbij PWM niet onderscheiden kan worden van verplaatsing en/of vervorming van het aneurysma is hier mogelijk verantwoordelijk voor. Hieruit concluderen wij dat ware druk gerelateerde pulsatiele wandbewegingen verwaarloosbaar zijn. 2D-PWM is niet bruikbaar om te beoordelen of het aneurysma effectief is uitgeschakeld.

Hoofdstuk 2 belicht het effect van de pulsatiele bloedstroom op het aneurysma en de stent-graft. Het doel van deze studie is om mechanismen te identificeren die leiden tot falen van EVAR op de lange termijn.
Bij 7 patiënten met AAA zijn de bewegingen van aneurysma en stent-graft gedurende de hartcyclus, in transversale, sagittale en coronale doorsneden, voor en na EVAR in beeld gebracht met cine MRI. Twee onafhankelijke onderzoekers, onbekend met het doel van de studie hebben aneurysma- en stent-graft contouren in de einddiastolische- en pieksystolische fase aangegeven. De maximale verplaatsing in de pieksystolische afbeelding versus de einddiastolische afbeelding wordt aangeduid als "translatie". Wand bewegingen van het aneurysma vóór EVAR zijn vergeleken met wand bewegingen ná EVAR. Daarnaast is gekeken naar veranderingen in de vorm van aneurysma en stent-graft gedurende de hartcyclus. De translatie van het aneurysma in voor-achterwaartse richting daalde van mediaan 1.05 mm (<0.5-1.29) vóór EVAR tot binnen de pixel grootte (<0.5 mm) ná EVAR (p=0.04). De translatie van het aneurysma in cranio-caudale richting nam toe van mediaan 1.01 mm (<0.5-1.51) vóór tot 1.69 mm (1.1-1.99) ná EVAR (p=0.02). Bij 4 stent-grafts zijn buigbewegingen tijdens de hartcyclus waargenomen ter plaatse van het gebied met de meeste angulatie.
Hieruit wordt geconcludeerd dat translatie in de lengterichting na EVAR toeneemt. Dit wijst op een toegenomen neerwaarts trekkende kracht. De waargenomen voortdurende buigbewegingen van de stent-graft ter plekke van de maximale angulatie geeft een verhoogde kans op metaalmoeheid en schade aan de bekleding van de stent-graft. Deze studie toont aan dat cine MRI bruikbaar is om dynamische informatie te verkrijgen van de repetitieve verplaatsingen en vervormingen van aneurysma en stent-graft. Met het oog op toekomstige stent-graft ontwikkeling ondersteunt deze studie het gebruik van goede proximale fixatie, zo nodig suprarenaal. Daarnaast verdient een flexibel middendeel zonder metalen componenten ter plaatse van angulaties de voorkeur.

In **Hoofdstuk 3** wordt de mobiliteit van de carotis arterie bij hoofdbewegingen na CAS bestudeerd. CAS is potentieel veiliger, minder traumatisch en wellicht goedkoper dan de carotis desobstructie (CEA). Ondanks goede initiële resultaten kan het functioneren van de stent op de lange termijn belemmerd worden door de mobiele eigenschappen van de halsslagader.
In deze studie is bij 7 patiënten na CAS 3D ´time-of-flight´ MR angiografie verricht. In 5 verschillende hoofdposities (neutraal, naar links en naar rechts gedraaid, naar voren en naar achter gebogen) zijn zowel de ipsilaterale gestente halsslagader als de contralaterale carotis arterie in beeld gebracht. De beide vaten werden beoordeeld op aanwezigheid van angulaties. Daarnaast werd de mate van torsie gemeten in de arteria carotis communis (CCA) en -interna (ICA) bij de naar links en rechts gedraaide hoofdbewegingen.
In de carotis arterie met stent, zijn angulaties aanwezig ter plaatse van de proximale en distale stent-vaatwand overgang. De contralaterale carotis arterie toonde diffuse configuratie veranderingen zonder specifieke angulatie op één locatie. In de neutrale hoofdpositie is de maximale angulatie ter plaatse van de distale stent vaatwand overgang 34.3ˆ (32.3-55.6). Bij buiging van het hoofd naar voren neemt de angulatie toe tot 47.6° (42.6-85.2, p=0.028) en bij buiging van het hoofd naar achteren neemt de angulatie af tot 26.5° (25.0-48.7, p=0.027). Bij alle patiënten ongeacht de hoofdpositie vertoont het deel van de carotis arterie met stent geen enkele vormverandering. Bij draaiing van het hoofd naar links en rechts ondergaat de CCA respectievelijk 28.6° (13.6-53.7) en 24.9° (2.0-50.6) torsie. In de ICA is de torsie respectievelijk 18.1° (12.7-40.5) en 15.2° (2.9-69.4) bij draaiing van het hoofd naar links en naar rechts.
De conclusie is dat na CAS scherpe ICA angulaties aanwezig zijn ter plaatse van de distale stent-vaatwand overgang die toenemen bij buiging van het hoofd naar voren. Zowel de CCA als de ICA ondergaat torsie bij draaiing van het hoofd naar links en rechts. Op basis van deze studie en naar aanleiding van overeenkomstige observaties na stent plaatsing in mobiele arteriën in de onderste extremiteit veronderstellen wij dat de mobiele eigenschappen van de halsslagader de lange termijn resultaten van CAS negatief kan beïnvloeden. Bij de ontwikkeling van carotis stents dient men rekening te houden met flexibiliteit en torsie in vivo.

Door de resultaten van de morfologische studie beschreven in het voorgaande hoofdstuk is de vraag gerezen of de waargenomen angulaties ter plaatse van de distale stent-vaatwand overgang van invloed zijn op de bloedstroom naar de

hersenen. Het antwoord volgt in **Hoofdstuk 4.** Met MR fase-contrast kwantificering wordt de volumetrische stroom snelheid (VFR) gemeten in de ICA bij patiënten na CAS en CEA in diverse hoofdposities. De carotis morfologie is door middel van MR angiografie in beeld gebracht. De correlatie tussen de VFR en de bijbehorende distale stent-vaatwand angulatie is beoordeeld. De resultaten van de patiënten behandeld met CAS (n=6) werden vergeleken met de patiënten na CEA (n=6). Na CAS nam de mediane angulatie toe met 10.2° (intrakwartiel, 7.3°- 17.9°) bij het hoofd naar voren gebogen. Bij patiënten na CEA was deze toename slechts 0.2° (intrakwartiel, -1.0 tot 2.4°, p=0.016). In alle andere hoofdposities zijn geen significante verschillen gevonden tussen de angulatie veranderingen na CAS versus CEA. Daarnaast is de VFR verandering, in alle hoofdposities, niet significant verschillend tussen de CAS en de CEA groep.
Uit deze studie kan geconcludeerd worden dat ICA angulatie significant toeneemt na CAS bij de hoofdbeweging naar voren ten opzichte van CEA. De toegenomen angulatie resulteert echter niet in een meetbare verandering van de hersendoorbloeding. Op de lange termijn kunnen dergelijke angulaties leiden tot chronische vaatwand veranderingen zoals restenose. Dit zal in toekomstige studies aangetoond dan wel uitgesloten moeten worden.

In **Hoofdstuk 5** beschrijven wij de resultaten van in-vitro buig- en torsietesten van 5 typen carotis stents. Zoals uit voorgaande hoofdstukken opgemaakt kan worden buigt en draait de carotis arterie aanzienlijk bij bewegen van het hoofd. Wij menen dat een flexibele stent met weinig torsie de stress op stent en vaatwand reduceert en daarom de voorkeur heeft. We onderzochten de flexibiliteit van de ontplooide stents voor en na plaatsing in varkens carotis arteriën. Vervolgens hebben wij torsie gemeten van de ontplooide naakte stents.
Flexibiliteit is bepaald met behulp van een driepunt buigtest opstelling. Het gewicht (BL, in gram) is gemeten dat nodig is om de stent 25° te buigen. Een hoge BL staat voor lage flexibiliteit. Torsie is gemeten door het gewicht (RL, in gram) te meten om een stent 30° te draaien om zijn as. Een hogere RL staat voor een toegenomen torsie.
Van de ontplooide stents zelf was de mediane BL 6 g (1-22). De BL neemt toe tot 38 g (20-41) na ontplooiing in de carotis arterie. Bij het type Carotis SE (21 g) en de Wallstent (36 g) was de BL significant lager (p<0.0001 en p=0.0016). De BL van de stents zelf is niet significant gerelateerd aan de BL na ontplooiing in de carotis arterie (p=0.089). De mediane RL van alle stents is 11 g (1-76). De Wallstent (73

g) en de Precise (20 g) hebben een significant hogere RL versus de andere stents (beide $p<0.0001$).
Alle geteste stents kunnen de door hoofdbeweging veroorzaakte buiging en torsie uitvoeren. Er blijkt géén verband te bestaan tussen flexibiliteit van de naakte ontplooide stent en na ontplooiing in een carotis arterie.

Het derde deel van dit proefschrift begint met **Hoofdstuk 6** waarin wij onze resultaten rapporteren van een proefdiermodel waarin het complexe aneurysma met essentiële zijtak arteriën wordt behandeld met een stent-graft met zijtakken. In 4 varkens zijn supra- of juxtarenale aneurysmata gecreëerd door een zakvormige Dacron patch op een anterieure aortotomie te hechten. Een angiografie wordt voor de endovasculaire herstelprocedure vervaardigd ter bepaling van de positie van de aftakking van de nier arteriën. Op geleide daarvan worden fenestraties in de hoofdprothese aangebracht. Vervolgens wordt de hoofdprothese in de aorta geplaatst en gedeeltelijk ontplooid waarbij longitudinale en rotatie beweegbaarheid aanwezig blijft. De nier arterie wordt via de fenestratie in de hoofdprothese voorzien van een voerdraad waarover de zijtak stent-graft geplaatst wordt. De zijtak is voorzien van een siliconen mantel die een vloeistof dichte verbinding maakt tussen zijtak en hoofdprothese. Uiteindelijk volgt volledige ontplooiing van de hoofdprothese. In alle experimenten is uitschakeling van het aneurysma zonder tekenen van lekkage en met behoud van een goede doorstroming van de nier arteriën bevestigd met angiografie. Bij obductie werd vastgesteld dat de hoofdprothese en zijtakken zich op de juiste plaats bevonden met intacte verbindingen tussen hoofd- en zijtakken. Alle procedures zijn verricht binnen acceptabele operatie duur, bloedverlies en contrastmiddel gebruik.
In dit proefdiermodel is endovasculair herstel van complexe aneurysmata mogelijk op een betrouwbare, voorspelbare en relatief snelle manier. Indien dit systeem beschikbaar komt voor klinisch gebruik, kunnen de inclusie criteria voor endovasculair herstel mogelijk worden uitgebreid naar de behandeling van infrarenale aneurysmata zonder proximale nek, aortoiliacale-, aorta boog- en wellicht thoracoabdominale aneurysmata.

De stijgende incidentie van stent-graft migratie bij follow-up maakt studie naar verbeterde proximale fixatie van belang. In **Hoofdstuk 7** wordt proximale fixatie van een infrarenale stent-graft met suprarenale stent fixatie, een gefenestreerde stent-graft en een zijtak stent-graft vergeleken met de fixatie kracht van een

conventionele vaat anastomose. Hierbij wordt gebruik gemaakt van een in-vitro trekopstelling. Door gefenestreerde stent-grafts en zijtak stent-grafts kan proximale fixatie mogelijk verbeteren door het ontplooien van de stent-graft hogerop in de aorta. In deze studie is gebruik gemaakt van humane kadaver aorta´s waarbij de abdominale aorta tot 20mm onder de nier arteriën is uitgenomen. In willekeurige volgorde wordt de infrarenale- (A), gefenestreerde- (B) en zijtak- (C) stent-graft ontplooid in de aorta op identieke wijze conform de klinische praktijk. Met een hydraulische testmachine wordt een longitudinale trekkracht uitgeoefend op de stent-graft totdat deze migreert. De kracht die nodig is om de stent-graft te migreren is gedefinieerd als de verplaatsingskracht (DF). Als laatste wordt een conventionele vaat anastomose gemaakt waarbij longitudinale tractie wordt uitgeoefend tot migratie van de vaatprothese.

De mediane DF in groep A is 4.67 N (3.82-6.37). In groep B neemt DF toe tot 9.17 N (8.03-10.81, p=0.0005) en in groep C tot 16.95 N (14.78-19.67, p=0.0005). Bij de vaat anastomose migreert de vaatprothese door scheuren van de aortawand ter plaatse van de naad bij een mediane DF van 89.16 N (83.40-105.23).

De gefenestreerde stent-graft, en in het bijzonder een met additionele zijtakken verbetert de proximale fixatie in vergelijking met de infrarenale stent-graft met suprarenale stent fixatie. De handgelegde conventionele vaat anastomose blijft echter de beste fixatie.

SLOTCONCLUSIES

- Met cine MRI van het AAA kan worden vastgesteld dat ware drukgerelateerde pulsatiele wand bewegingen verwaarloosbaar zijn.

- Na EVAR is de longitudinale verplaatsing van zowel het aneurysma als de stent-graft toegenomen, duidend op neerwaarts trekkende krachten ter plaatse van de proximale stent-graft fixatie.

- Door buigbewegingen ter plaatse van angulatie kan metaal moeheid en schade aan de bekleding van de stent-graft optreden.

- In CAS leidt het gebrek aan flexibiliteit van de stent tot angulaties bij bewegingen van het hoofd. Wij vermoeden dat de hoog mobiele eigenschappen van de carotis arterie gecombineerd met een stijve stent de lange termijn resultaten van CAS negatief kan beïnvloeden.

- Ondanks angulatie in CAS kan vermindering van de hersendoorbloeding in de eerste maanden na de ingreep met de door ons gebruikte onderzoeksmethoden niet worden aangetoond.

- Flexibiliteit en torsie zijn in de thans in gebruik zijnde stents beperkt.

- Endovasculair herstel van complexe aneurysmata met een modulair zijtak stent-graft systeem is mogelijk op een betrouwbare, voorspelbare en relatief snelle manier.

- De gefenestreerde stent-graft, met name met additionele zijtakken, geeft een verbeterde proximale fixatie.

- De resultaten van onze studies ondersteunen de huidige opinie dat bij de behandeling van patiënten met beperkte co-morbiditeit en een goede levens-verwachting een open procedure de voorkeur verdient.

DANKWOORD

Professor Wisselink, beste Willem, er bestaan chirurgen en chirurgen. Dank dat ik zoveel van zo'n grote heb mogen leren. Iedere steek moet perfect zijn, 'whatever it takes'. Het is een buitengewoon grote eer jouw eerste promovendus te mogen zijn.

Professor Rauwerda, beste Jan, jij hebt mij gewezen op dit 'gouden' dynamische thema. Zeer veel dank daarvoor. Je enthousiasme voor de vaatchirurgie en nu ook voor de opleiding Heelkunde werkt aanstekelijk.

Dr. Marcus, beste Tim, wetenschapper pur sang. Wat heb ik een geluk gehad om met jou, medisch fysicus en MR expert, te mogen werken. Vol enthousiaste ideeën en altijd bereid tot overleg. Dank!

De commissie, Prof.dr. J.H. van Bockel, Prof.dr. L.F. Moll, Prof.dr. J.A. Reekers, Dr. H.L.F. Brom, Prof.dr. N. Westerhof en Prof.dr. V.W.M. van Hinsbergh, hartelijk dank voor het beoordelen van dit manuscript en de bereidheid zitting te nemen in de beoordelingscommissie.

Professor Haarman, mijn dank is groot voor de mogelijkheden die u mij heeft geboden in de afgelopen jaren. Ik ben u zeer erkentelijk voor mijn opleiding, mijn onderzoeksjaar en de ruimte die ik kreeg in het Heelkunde bestuur.

Opleiders, chirurgen in Alkmaar, de VU en Haarlem, dank voor mijn mooie turbulente assistenten jaren.

Willem Wisselink, Jan Rauwerda, Bram Rijbroek en Hans Brom, waarde vaat-chirurgen, van jullie heb ik mijn vak geleerd. Mijn dank is groot.

Teus Linsen, eigenwijze student, een groot deel van het werk aan dit proefschrift is van jou. Ik ben je zeer dankbaar voor je hulp. Jouw boekje komt ook vol!

Jan Albert Vos, neef, carotis man, wat mooi dat ik je weer ben tegengekomen. Je schrijft tot mijn verbazing als de beste.

Jeroen Diks en Vincent Jongkind, collega onderzoekers, dank voor jullie hulp. Houd de vaten trein op de rails.

Mede auteurs Dr. Vahl, Dr. van den Berg en Dr. Overtoom dank voor het becommentariëren van de manuscripten en het insturen van patiënten voor de MR onderzoeken.

Professor Manoliu, ook u dank ik voor het kritische commentaar en de ruimte die u creëerde voor mij om gebruik te maken van de MRI. De gesprekken met u over de te hanteren studie methoden zijn zeer verhelderend geweest.

Ger Vink, Klaas en Esther en alle andere medewerkers van het dierexperimenteel laboratorium jullie dank ik voor de indrukwekkende zorg, kennis en toewijding voor en tijdens de operaties van de varkens. Op jullie afdeling kan alles!

Alle mensen van de angiokamer en in het bijzonder Gerard de Ruyter. Dank voor jullie enthousiasme en hulp bij het uitvoeren van de varkensstudie. Ook bij jullie is vaak alles mogelijk.

Elly de Lange, steun en toeverlaat in de statistische wereld. Dank voor jouw praktische aanpak.

Klaas Boshuizen, de in vitro aneurysma flow en carotis test opstellingen zijn door jouw grote technische kennis zo betrouwbaar geworden.

Albert van der Veen en Ronald van Schijndel, ingenieuze ingenieurs, dank voor jullie hulp bij het verwerken van de MR beelden en bij de tractie proeven.

Ilse Kruit, hulde voor jouw inspanningen! Het is een verademing om met je te werken.

Waarde paranimfen,
van der Elst, dank voor jouw immer kritische commentaar op mijn manuscripten. Grote maat, wat is het toch jammer dat we niet meer samen opereren.

Ziekman, bedankt. Tijd voor een goed glas whisky. Tsjing Boem.

Mijn broers dank ik voor het becommentariëren en verfraaien van mijn leven. Klaas in het bijzonder voor zijn waardevolle aanvullingen op dit dankwoord.

Mijn lieve ouders dank ik, Anton voor zijn aanmoedigingen en heldere kijk op al mijn teksten en lieve Lieselot voor alles.

Tot slot de belangrijkste van allemaal, Daphne

De wrâld om ús hinne,
giet úteinlyk hielendal oan ús foarby.
Dan haw ik mar foar ien ding oandacht,
en dat is foar dy.

Amsterdam, 2005
Floris Vos